INTERACTIVE EFFECTS OF TEMPERATURE AND METAL TOXICITY ON *Scenedesmus quadricauda* AND *Chlamydomonas augustae*

YONG WAI KUAN

INSTITUTE FOR ADVANCED STUDIES
UNIVERSITY OF MALAYA
KUALA LUMPUR

2019

INTERACTIVE EFFECTS OF TEMPERATURE AND METAL TOXICITY ON *Scenedesmus quadricauda* AND *Chlamydomonas augustae*

YONG WAI KUAN

THESIS SUBMITTED IN FULFILMENT OF THE REQUIREMENTS FOR THE DEGREE OF DOCTOR OF PHILOSOPHY

INSTITUTE FOR ADVANCED STUDIES
UNIVERSITY OF MALAYA
KUALA LUMPUR

2019

UNIVERSITY OF MALAYA

ORIGINAL LITERARY WORK DECLARATION

Name of Candidate: Yong Wai Kuan

Matric No: HHQ 150004

Name of Degree: Doctor of Philosophy

Title of ~~Project Paper/Research Report/Dissertation/~~Thesis ("this Work"): Interactive Effects of Temperature and Metal Toxicity on *Scenedesmus quadricauda* and *Chlamydomonas augustae*

Field of Study: Marine Biotechnology

I do solemnly and sincerely declare that:

(1) I am the sole author/writer of this Work;
(2) This Work is original;
(3) Any use of any work in which copyright exists was done by way of fair dealing and for permitted purposes and any excerpt or extract from, or reference to or reproduction of any copyright work has been disclosed expressly and sufficiently and the title of the Work and its authorship have been acknowledged in this Work;
(4) I do not have any actual knowledge nor do I ought reasonably to know that the making of this work constitutes an infringement of any copyright work;
(5) I hereby assign all and every rights in the copyright to this Work to the University of Malaya ("UM"), who henceforth shall be owner of the copyright in this Work and that any reproduction or use in any form or by any means whatsoever is prohibited without the written consent of UM having been first had and obtained;
(6) I am fully aware that if in the course of making this Work I have infringed any copyright whether intentionally or otherwise, I may be subject to legal action or any other action as may be determined by UM.

Candidate's Signature Date:

Subscribed and solemnly declared before,

Witness's Signature Date:

Name:

Designation:

INTERACTIVE EFFECTS OF TEMPERATURE AND METAL TOXICITY ON *Scenedesmus quadricauda* AND *Chlamydomonas augustae*

ABSTRACT

Abiotic stresses have significant implications on the growth of aquatic organisms, including microalgae which are the primary producers of the food chain. Heavy metals (HMs) such as copper (Cu) and nickel (Ni) are essential trace nutrients involved in the electron transfer, redox reaction, signalling mechanisms, and oxidative stress response of microalgae. However, when present at high concentrations, HMs are known to induce toxic effects on chlorophyll synthesis, photosynthetic efficiency, growth, reactive oxygen species (ROS) generation, and cellular metabolism. Heavy metal speciation and distribution in the aquatic environment is dependent on water temperature, which is a key environmental factor that strongly regulates growth of photosynthetic organisms. To date, inhibitory mechanism of heavy metals on microalgae at metabolic level, and its integrative effects with rising water temperature, remain unclear. In this study, the interactive effects of temperature and metal toxicity on two freshwater green microalgae, *Scenedesmus quadricauda* and *Chlamydomonas augustae,* were elucidated from the physiological (growth, photosynthesis, ROS, metal uptake) and biochemical (metabolite) aspects. Cell density of both species decreased with increasing concentrations of Cu and Ni. Photosynthetic parameters of the two microalgae obtained from the pulse amplitude modulated (PAM) fluorometry demonstrated that the maximum relative electron transport rate ($rETR_m$), light harvesting efficiency (α), saturation irradiance of electron transport (E_k) and non-photochemical quenching (NPQ) were sensitive to both stressors. The increased level of ROS corresponded to the increasing concentrations of HMs. Both species were able to accumulate substantial amount of Cu and Ni in their biomass. Untargeted mass-spectrometry metabolite profiling was used to understand the changes in metabolic flux and biochemical pathways. In general, the two species underwent primary

metabolism restructuring for adaptation and restoration of homeostasis. The results show that amino acids, fatty acids and sugars were the key primary metabolites involved in the microalgal adaptation. Amino acids and proteins were involved in chelating metal ions and reducing free metal ions in the cells. Pathways related to the carbohydrate and energy metabolism were also involved in the response, suggesting a change in energy expenditure. Sulfur-containing metabolites and sulfur metabolism were also significantly dysregulated because excess metal ions would bind to various ligands. Overall, *S. quadricauda* was more resistant to heat and metal toxicity than *C. augustae*, suggesting that *S. quadricauda* is a better candidate for phycoremediation. By integrating results from the physiological and biochemical responses, this project provides insights into the underlying mechanisms of the interactive stress response in green microalgae from the aquatic environment. Global warming and aquatic toxicology have been closely associated with microalgal metabolism, species abundance and diversity. Understanding the interactive effects of multiple stressors is crucial to predict microalgal responses to environmental changes which might affect community tolerance and species distribution in the long run.

Keywords: Abiotic stress, metal toxicity, microalgae, metabolomics, photosynthesis

KESAN INTERAKTIF SUHU DAN KETOKSIKAN LOGAM PADA *Scenedesmus quadricauda* DAN *Chlamydomonas augustae*

ABSTRAK

Tekanan abiotik mempunyai implikasi yang ketara terhadap pertumbuhan organisma aquatik termasuk mikroalga yang merupakan penghasil utama rantai makanan. Logam berat (HMs) seperti tembaga (Cu) dan nikel (Ni) adalah nutrien surih penting yang terlibat dalam pemindahan elektron, tindak balas redoks, mekanisme isyarat, dan tindak balas tekanan oksidatif mikroalga. Namun demikian, pada kepekatan yang tinggi, HMs diketahui boleh meyebabkan kesan toksik pada sintesis klorofil, kecekapan fotosintesis, pertumbuhan, penjanaan spesies oksigen reaktif (ROS), dan metabolisme sel. Spesiasi dan pengedaran HMs dalam persekitaran akuatik adalah bergantung kepada suhu air yang merupakan faktor persekitaran utama yang mengawalatur pertumbuhan organisma berfotosintesis. Sehingga kini, mekanisme perencatan HMs pada mikroalga di peringkat metabolik, dan kesan integratifnya dengan kenaikan suhu air, masih tidak jelas. Dalam kajian ini, kesan interaktif suhu dan ketoksikan logam pada dua mikroalga hijau dari sumber air tawar, *Scenedesmus quadricauda* dan *Chlamydomonas augustae*, telah disiasat dari aspek fisiologi (pertumbuhan, fotosintesis, ROS, serap logam) dan biokimia (metabolit). Ketumpatan sel kedua-dua spesies menurun dengan peningkatan kepekatan Cu dan Ni. Parameter fotosintesis mikroalga yang diperolehi dari fluorometri *Pulse Amplitude Modulated* (PAM) menunjukkan bahawa kadar pengangkutan electron relatif maksimum ($rETR_m$), kecekapan penuaian cahaya (α), penjanaan tepu pengangkutan elektron (E_k) dan pelindapkejutan fotokimia (NPQ) adalah sensitif terhadap kedua-dua tekanan. Tahap peningkatan ROS berkorelasi dengan peningkatan kepekatan HMs. Kedua-dua spesies ini mampu mengumpul jumlah Cu dan Ni yang banyak dalam biomas mereka. Profil metabolit massa-spektrometri tidak terperinci digunakan untuk memahami perubahan dalam fluks metabolik dan laluan biokimia. Secara am, kedua-dua spesies

mengalami penstrukturan semula metabolisme utama untuk penyesuaian dan pemulihan homeostasis. Keputusan menunjukkan bahawa asid amino, asid lemak dan gula adalah metabolit utama yang terlibat dalam penyesuaian mikroalga. Asid amino dan protein terlibat dalam ion logam chelating dan mengurangkan ion logam bebas dalam sel. Laluan yang berkaitan dengan metabolisme karbohidrat dan tenaga juga terlibat dalam tindak balas dan mencadangkan perubahan dalam perbelanjaan tenaga. Metabolit yang mengandungi sulfur dan laluan metabolisme sulfur juga diselaraskan dengan ketara kerana ion logam berlebihan akan terikat kepada pelbagai ligan. Secara keseluruhan, *S. quadricauda* lebih tahan terhadap suhu dan ketoksikan logam daripada *C. augustae*, justeru mencadangkan bahawa *S. quadricauda* adalah calon yang lebih baik untuk fikoremediasi. Dengan mengintegrasi data dari tindak balas fisiologi dan biokimia, projek ini telah menunjukkan mekanisme asas tindak balas interaktif tekanan dalam mikroalga hijau dari persekitaran akuatik. Kepanasan global dam toksikologi akuatik berkait rapat dengan metabolisme mikroalga serta kelimpahan dan kepelbagaian spesies. Pemahaman mengenai kesan interaktif pelbagai tekanan adalah penting untuk meramal tindak balas mikroalga terhadap perubahan alam sekitar yang berkemungkinan menjejaskan toleransi komuniti dan pengedaran spesies dalam jangka masa panjang.

Katakunci: Tekanan abiotik, ketoksikan logam, mikroalga, metabolomik, fotosintesis

ACKNOWLEDGEMENTS

This thesis would not be made possible without the help and support of many people whom I met during my Ph.D. candidature. I feel a deep sense of gratitude to my supervisors Professor Dr. Lim Phaik Eem and Associate Professor Dr. Sim Kae Shin for their assistance and suggestion throughout the course of my Ph.D. Also, a big thank you to the members in the Institute of Ocean and Earth Sciences (IOES) for their support and care, especially Professor Dr. Phang Siew Moi, Dr. Poong Sze Wan, Dr. Bahram Barati, and other helpful team members. My heartfelt appreciation to Professor Dong Wei from the South China University of Technology and his wonderful laboratory members for their warm hospitality and professional guidance. This journey wasn't easy, but luckily, I have my fellow postgraduate friends who keep inspiring me and pushing me forward. Thank you for supporting and cheering me up through all the ups and downs.

This journey was made easier by my parents who always believe in me and encourage me to reach for the stars, my siblings who show unconditional love and support, and my significant other who has been incredibly patient and supportive in every way imaginable. Thank you so much for believing in me and wanted the best for me. Also, I wouldn't be able to strive without the help and moral support from all my good friends who are so kind and understanding. When I felt stressed and uninspired, thank you for bringing in light and hope.

Besides the technical skills, the past few years had taught me so many life lessons on personal development. A big lesson that I learned was perseverance. In times of difficulties, we should never give up. I'll be forever grateful for all the opportunities, challenges, and memorable moments along my Ph.D. journey.

TABLE OF CONTENTS

LIST OF FIGURES

LIST OF TABLES

LIST OF SYMBOLS AND ABBREVIATIONS

DCFH-DA	2',7'-dichlorofluorescein diacetate
ATP	Adenosine triphosphate
α	Alpha, photosynthetic efficiency
ANOVA	Analysis of variance
ASCA	Analysis of variance - simultaneous component
AFCs	Antifouling compounds
As	Arsenic
BBM	Bold's basal medium
Cd	Cadmium
Ca	Calcium
CO_2	Carbon dioxide
Chl-*a*	Chlorophyll *a*
Cr	Chromium
Co	Cobalt
Cu	Copper
° C	Degree Celsius
Φ_{PSII}	Effective quantum yield of PSII photochemistry
ETR	Electron transport rate
GCMS	Gas chromatography-mass spectrometry
HM(s)	Heavy metal(s)
HCs	Herbicides
h	Hour
H_2O_2	Hydrogen peroxide
Fe	Iron

KEGG	Kyoto Encyclopedia of Genes and Genomes
Pb	Lead
LCMS	Liquid chromatography-mass spectrometry
Mg	Magnesium
Mn	Manganese
MS	Mass spectrometry
m/z	Mass-to-charge ratio
F_v/F_m	Maximum quantum efficiency of photosystem II
$rETR_m$	Maximum relative electron transport rate
Hg	Mercury
µM	Micromolar
MP-AES	Microwave plasma – atomic emission spectroscopy
mL	Millilitre
mM	Millimolar
Min(s)	Minute(s)
nm	Nanometre
Ni	Nickel
HNO3	Nitric acid
NPQ	Non-photochemical quenching
qN	Non-photochemical quenching coefficient
x *g*	Number of times the gravitational force
ppb	Parts per billion
ppm	Parts per million
%	Percent
qP	Photochemical quenching coefficient
PAR	Photosynthetically active radiation

PSI	Photosystem I
PSII	Photosystem II
Q_A	Primary electron acceptor quinone
PAM	Pulse amplitude modulation
RLC	Rapid light curve
ROS	Reactive oxygen species
rETR	Relative electron transport rate
rpm	Revolution per minute
E_k	Saturation irradiance for electron transport
Q_B	Secondary electron acceptor quinone
Se	Selenium
sp.	Species
SD	Standard deviation
SOD	Superoxide dismutase
UVR	Ultraviolet radiation
UMACC	University of Malaya Algae Culture Collection
H_2O	Water
Zn	Zinc

LIST OF APPENDICES

CHAPTER 1: INTRODUCTION

1.1 General Introduction

Microalgae are ecologically important as a major primary productivity driver. As the primary producers and food sources for higher trophic organisms, microalgae play a crucial role in photosynthetic carbon fixation and maintaining the equilibrium of food webs in the aquatic ecosystems (Häder & Gao, 2015). The current shifts of global climate due to anthropogenic activities have been reported to pose numerous impacts on microalgae. Extreme fluctuations in atmospheric temperature, light intensity, ultraviolet (UV) radiations, carbon dioxide (CO_2) levels, and salinity can lead to alterations in growth, disruption of homeostasis, photosynthetic rate, respiration, enzymatic activity, protection to oxidative damage, and trophic transfer in microalgae (Yong et al., 2016). Various studies on microalgal responses to these environmental changes are ongoing to provide a deeper insight into the relationship between microalgal growth, metabolic adjustment and community structure (Papiol, 2017; Sampaio & Rosa, 2019). The algae communities in the Arctic region exhibited metabolic differences in response to acclimatization and adaptation to different physico-chemical environment (Lutz et al., 2015). Elevated CO_2 and temperature might affect the carbon transfer in freshwater phytoplankton & zooplankton communities (Li et al., 2019). Snow algae in Antarctica exhibited variations in metabolic and taxonomic composition based on seasonal and geographical diversity (Davey et al., 2019).

Over the last decades, heavy metal contamination in the aquatic ecosystems due to anthropogenic activities has become a major concern. Naturally, heavy metals (HMs) in the aquatic environment source from weathering of soils and rocks. However, due to increasing anthropogenic activities, rapid development of cargo industry, coal combustion, chemical manufacturing, mining activities, wastewater discharge from sewage treatment plants, the amount of HMs in water is increasing in an alarming rate

(Ismail et al., 2016). Various reports from all around the world have shown that water quality contaminated by HMs have worsen over the years (Chen et al., 2018; Harvey et al., 2016; Khodami et al., 2017).

Some HMs are essential micronutrients for living organisms. In photosynthetic organisms, HMs such as copper (Cu) and nickel (Ni) are involved in the electron transfer, redox reaction, signalling mechanisms, and oxidative stress response (Castruita et al., 2011; Kropat et al., 2015). Copper plays an essential role in enzymatic reactions and photosystem II (PSII) - mediated electron transport chain (Adrees et al., 2015). Nickel is an essential 'ultramicronutrient' in various organisms. It is a cofactor for nickel-dependent enzymes such as urease, hydrogenase, carbon monoxide dehydrogenase, superoxide dismutase (SOD), and glyoxalase (Kováčik et al., 2018; Pathammavong, 2016). However, when present in excess amount, HMs are detrimental to the human health, environment and the ecosystem (Järup, 2003). At the cellular level, growth, morphology and physiology of organisms were affected by heavy metal contamination (Stankovic et al., 2014). From the ecological aspect, studies have reported that excess amount of metal in the aquatic systems posed negative impacts on biodiversity because they are generally stable elements that are unable to be metabolized biologically and could accumulate across the trophic levels (De Laender et al., 2013; Suresh Kumar et al., 2015).

Microalgae, the primary producers in aquatic ecosystems, are highly susceptible to heavy metal contamination. When present at high concentrations, HMs are known to induce toxic effects on microalgae via multiple mechanisms: (i) inhibiting functional groups of enzymes and transport systems; (ii) displacement and/or replacement of essential metal elements from molecules; (iii) generation of reactive oxygen species (ROS); and subsequently (iv) disruption of cellular and organellar membrane (Adrees et al., 2015). Excess metal ions in microalgae impair photosynthesis by inhibiting

photosynthetic electron transport rate, interfere with pigment and lipid biosynthesis, chloroplast ultrastructure, hence leading to a decrease in the photosynthetic efficiency (Suresh Kumar et al., 2014).

Copper is known to reduce chlorophyll synthesis and inhibit photosynthetic efficiency (Lombardi & Maldonado, 2011). Other effects of Cu toxicity include growth inhibition, ROS generation, and genetic mutation (Jamers et al., 2006). Copper also reduced the maximum quantum efficiency of photosystem II (F_v/F_m ratio), increased production of ROS, and induced severe physiological damage in *Closterium ehrenbergii* (Wang et al., 2017).

Nickel is an essential 'ultramicronutrient' used by phytoplankton in low concentrations for enzymatic activities. At higher concentrations, Ni induced biochemical, physiological and structural changes on microalgae (Debelius et al., 2011). In the green microalgae *Ankistrodesmus falcatus*, excess Ni reduced the concentrations of Chl-*a*, *b* and carotenoids; decreased the content of macromolecules, disrupted the antioxidant enzymatic responses through inhibiting SOD activity, and increasing catalase (CAT) and glutathione peroxidase (GPx) activities (Martínez-Ruiz & Martínez-Jerónimo, 2015). Excess Ni also induces oxidative stress by generating high levels of ROS (Kováčik et al., 2018). Nickel oxide nanoparticles inhibited cell division, altered relative cell size and granularity, affected photosynthetic apparatus and increased ROS levels in *Chlorella vulgaris* (Oukarroum et al., 2017).

In response to the extracellular pollutants, microalgae have developed adaptive strategies to maintain metal homeostasis inside the cells. Primary metabolites (sugars, amino acids, organic acids, and inorganic acids) are involved in the survival and adaptation mechanisms. Metabolites such as proline and histidine are directly involved in the stress response through metal ion chelation (Singh et al., 2015). Other amino acid

derivatives, organic acids and peptides are also involved in reducing the formation of free radicals and maintaining homeostasis (Jamers et al., 2013b; Wang et al., 2015; Zhang et al., 2015). Simultaneously, some fatty acids and sugars are involved in the second-line mechanisms such as energy partitioning and secondary metabolism (Zhang et al., 2014). Based on studies on protein expression and gene expression, the defence mechanisms against metal toxicity in microalgae involved general stress response pathways (Jamers et al., 2006; Nagalakshmi & Prasad, 2001). In addition to internal metabolic rewiring, microalgae remove HMs by two major mechanisms. The first mechanism is initial passive removal at cellular surface while the second mechanism is the active process which involves transporting the metal cations across cellular membrane into the cytoplasm and subsequently binding to intracellular compounds (Monteiro et al., 2012; Suresh Kumar et al., 2015). Metabolomics-based ecotoxicology study is one of the approaches to understand the mechanisms underlying the stress response (Obata & Fernie, 2012).

Metal removal efficiency varies greatly among different microalgae species depending on cell size, taxonomic group or metal solution-cell partition coefficients at equilibrium (K_d). For example, metal uptake of the strains ranged from 0.5 mg/g in *Closterium lunula* to 389 mg/g in *Spirulina* (Suresh Kumar et al., 2015). The strain-dependent metal ion biosorption capacity depends of the cell wall composition (polysaccharides and proteins) present in algae cell walls which vary among different species (Kaplan, 2013). Other factors that affect HM uptake into the cells include temperature, initial metal ion concentration, biomass, pH, and competition between ions present in the culture (Zeraatkar et al., 2016).

Global warming is one of the contributing factors to the decline of annual global phytoplankton biomass over the past century (Boyce et al., 2010). Thermal fluctuations affect fluidity and functioning of photosystem II on the thylakoid membrane, which

subsequently influence photosynthetic rate and aggravate photoinhibition. Temperature also influences lipid composition and membrane fluidity of microalgae cells (Lukeš et al., 2014). In general, elevated temperature altered intracellular photosynthetic performance and metabolic network of microalgae (Barati et al., 2018; Fanesi et al., 2016; Lee et al., 2017). This can lead to reduced biomass production, reaction rates and kinetic properties of enzymes (Zidarova & Pouneva, 2006).

Global warming and aquatic toxicology have been closely associated with microalgal metabolism, species abundance and diversity (Winder & Sommer, 2012). Reports showed that increased water temperatures will affect metal speciation, activity, ion biosorption capacity and formation of ligand complexes (Batley et al., 2004). A marine diatom, *Thalassiosira nordenskioeldii* exhibited temperature-dependent sensitivity to cadmium stress (Wang & Wang, 2008). High temperature was reported to increase toxicity of nano zinc oxides on *Skeletonema costatum* (Wong & Leung, 2014). Increase of temperature also resulted in higher inhibition by silver nanoparticles on the photosynthetic performance of *Chlorella vulgaris* and *Dunaliella tertiolecta* (Oukarroum et al., 2012a). The interactive effects are probably due to several factors: (i) the increased number of active sites in metal ion uptake; (ii) increased tendency of active sites to absorb metal ion; (iii) reduction in mass transfer resistance in diffusion layer by a reduction of thickness of diffusion boundary layer; and (iv) change of complex ion formation constant with temperature (Zeraatkar et al., 2016).

Understanding the interactive effects of multiple stressors is crucial to predict microalgal responses to environmental changes (Todgham & Stillman, 2013). Many studies have focused on a single environmental variable to determine biological response. It is increasingly evident that the inferences drawn from single-stressor studies might not be accurate in the multivariate environment, as the combined impacts of stress conditions

on organisms are complex and non-linear. Multiple stress factors may be additive, synergistic, or antagonistic to the physiological performance of microalgae species, and influence a complex interaction of various intracellular mechanisms ranging from gene expression, protein, and metabolic adjustments (Häder & Gao, 2015; Yong et al., 2016).

In this study, two freshwater green microalgae, *Scenedesmus quadricauda* and *Chlamydomonas augustae* were exposed to various concentrations of Cu and Ni at sub-optimal temperature to investigate the interactive effects of metal toxicity and temperature on microalgal metabolism. Chlorophytes have been recommended as model organisms in phytotoxicity assessment (OECD, 2011). Specifically, species belonging to the genera *Scenedesmus* and *Chlamydomonas* were frequently selected as the test organisms to investigate abiotic stress response due to their fast doubling rate, oleaginous property, and potential use for phycoremediation (Kluender et al., 2009; Nalewajko et al., 1997; Xia et al., 2016). Copper and Ni were chosen for this study due to their high availability in wastewater, toxicity, persistence and biomagnifying property in food chains. The stress responses were assessed from the growth, photosynthesis, ROS generation and metabolomics aspects to understand the effects at both the physiological and biochemical levels. By integrating results from the physiological and biochemical responses, this study aims to gain insights into the underlying mechanisms of the interactive stress response in green microalgae from the aquatic environment. The data will provide further understanding on microalgae adaptation to climate change and their application for bioremediation.

1.2 Problem Statement

Many reports drew inferences from a single environmental variable in understanding the response of microalgae to abiotic stresses. It has become increasingly evident that the natural environment is multivariate and the interaction of biotic and abiotic variables

plays remarkable effects on microalgae and their distribution in the ecosystem. This study aims to discuss the interactive effects of two abiotic stresses and provide valuable information into how different variables can interplay on the biochemical network of microalgae.

1.3 Research Questions

1. How do different temperature and metal toxicity levels influence growth and photosynthetic efficiency of microalgae?
2. What are the different mechanisms developed by microalgae to cope with heavy metal toxicity and heat stress?
3. What are the commonalities and differences of the stress responses? Do the mechanisms of temperature and metal toxicity tolerance converge on the same pathways or specific to each stress factor?

1.4 Hypotheses

$H0_a$ = Both *S. quadricauda* and *C. augustae* can adapt to warming and metal toxicity.

$H0_b$ = Both *S. quadricauda* and *C. augustae* cannot adapt to warming and metal toxicity.

$H1_a$ = There is no significant difference in the physiological responses (growth, photosynthetic efficiency, ROS levels and metal uptake) of *S. quadricauda* and *C. augustae* to warming, metal toxicity, and the interactive effects of the combined factors.

$H1_b$ = There are significant differences in the physiological responses (growth, photosynthetic efficiency, ROS levels and metal uptake) of *S. quadricauda* and *C. augustae* to warming, metal toxicity, and the interactive effects of the combined factors.

$H2_a$ = There is no significant difference in the metabolic responses of *S. quadricauda* and *C. augustae* to warming, metal toxicity, and the interactive effects of the combined factors.

$H2_b$ = There are significant differences in the metabolic responses of *S. quadricauda* and *C. augustae* to warming, metal toxicity, and the interactive effects of the combined factors.

1.5 Research Objectives

1. To reveal biochemical network affected by integrated environmental factors (temperature, Cu and Ni toxicity).
2. To identify unique mechanisms related to survival and adaptability among *S. quadricauda* and *C. augustae*.
3. To identify significant metabolites as key biomarkers in response to temperature, Cu and Ni toxicity.
4. To contribute data in mapping the complete reaction network in databases.

CHAPTER 2: LITERATURE REVIEW

2.1 Heavy metal (HMs) contamination

Heavy metals (HMs) are a group of non-biodegradable, persistent and ubiquitous environmental chemicals. In plant sciences and ecotoxicology studies, HMs are often defined as metals with a specific density of more than 5 g cm^{-3} (Järup et al., 2003). However, this definition has been disagreed by several studies because the physical properties such as atomic weight, density or chemical properties are not accurate in describing HMs and their toxicity profile (Duffus, 2002). Appenroth (2010) suggested to define "heavy metals" as all transition elements (except lanthanum and actinium), rare earth elements subdivided in the series of lanthanides and actinides, and a heterogenous group of elements including amphoteric oxides and metalloids.

Heavy metals can be generally divided into two categories in terms of their biological activities: the non-essential and essential HMs. Non-essential metals such as Hg, Ag and Pb are highly toxic to the biological systems. Essential metals such as Cu, Ni, Zn and Mn are micronutrients involved in biological functions particularly in redox reactions, enzymatic activity, biosynthesis and function of nucleic acids, chlorophyll, energy metabolism, stress adaptation, and secondary metabolites (Nagajyoti et al., 2010).

Table 2.1 summarises several important HMs and their functions in the biological systems. Copper is involved in the electron transfer, redox reaction, signalling mechanisms, and oxidative stress response of microalgae (Castruita et al., 2011; Kropat et al., 2015). Nickel is a 'ultra-micronutrient' essential to photosynthetic organisms, particularly as a cofactor for nickel-dependent enzymes such as urease, hydrogenase, and glyoxalase (Muyssen et al., 2004; Seregin & Kozhevnikova, 2006). Metals such as Zn maintain structural integrity of DNA and RNA by stabilizing their polyanionic structures. Calcium ions react with the carbonyl terminals in proteins to stabilize the structure (Singh

& Verma, 2018). Metals such as Zn and Fe are also indirectly involved in maintaining the homeostasis and preventing oxidative stress by acting as essential cofactors for SOD which converts superoxide to hydrogen peroxide (Palmer & Guerinot, 2009). Selenium is involved in the demethylation and removal of Hg from biological systems, formation and functioning of glutathione, and offers protection against UV radiation (Jakimska et al., 2011).

Table 2.1: Biological roles of selected metals in photosynthetic organisms

Element	Biological roles	Reference
Ca	• Stabilize protein structure	Singh & Verma (2018)
Co	• Core element of vitamin B12 and other co-enzymes	Nagajyoti et al. (2010)
Cu	• Primary electron donor in photosystem I • Cofactor for oxidase, mono- and di-oxygenase	Castruita et al. (2011)
Fe	• Cofactor for cytochrome, Fe-S proteins, SOD	Palmer & Guerinot (2009)
Mg	• Constituent for chlorophyll biosynthesis	Wettstein et al. (1995)
Mn	• Cofactor for malic dehydrogenase and oxalosuccinic decarboxylase, SOD • Required for water-splitting at photosystem II	Nagajyoti et al. (2010)
Ni	• Cofactor for nickel-dependent enzymes such as urease, hydrogenase, and glyoxalase	Muyssen et al. (2004)

Table 2.1, continued

Element	Biological roles	Reference
Se	• Demethylation and removal of HMs from biological systems, antioxidative reaction • Protection against UV radiation	Jakimska et al. (2011)
Zn	• Maintain integrity of ribosome • Provide structural role in transcription factor • Cofactor for RNA polymerase, alcohol dehydrogenase, carbonic anhydrase, SOD	Palmer & Guerinot (2009)

Naturally, HMs originate from weathering process and volcanic eruptions. Natural occurrences such as volcanogenic particles, forest wild fires, wind-blown dust and vegetation accounted for considerable worldwide emissions of Cd, Cu, Cr, Ni, Pb, and other metals in the range of 10^3 tons per year as summarized by Pacyna et al. (1995). Igneous and sedimentary rocks contain substantial amount of Cu, Ni, As, Cd, Cr, Pb, and Zn with concentrations ranging from ppb to ppm (Nagajyoti et al., 2010).

Although HMs are naturally occurring in the environment, there has been an increasing global public concern related to contamination and toxicity of HMs due to mining, smelting, industrial and domestic use of metals and metal-containing products over the past decades (Islam et al., 2015). Reported anthropogenic sources of HMs in the environment include the agricultural, industrial, chemical and manufacturing activities as summarized in Table 2.2.

Table 2.2: Various anthropogenic sources of selected heavy metals

(Adapted from Bradl, 2005; Nagajyoti et al., 2010; Pacyna et al., 1995)

Metal	Source
As	Pesticides, insecticides, herbicides, fungicides, mining, coal combustion
Cd	Manufacturing of batteries, pigments for dyes and paints, metal coatings, stabilizers, alloys, coal combustion, mining
Cu	Conductor for heat and electricity, pigments for dyes and paints, manufacturing of alloys, mining
Fe	Wrought and cast iron, manufacturing of steel and alloys, construction, transportation
Hg	Mining, amalgamation, fungicides, catalysts in chemical industries, dental fillings, scientific and medical instruments, mercury vapour lamps
Mn	Manufacturing of ferromanganese steels, manufacturing of batteries, welding, pigments for dyes and paints, components for electrical devices, catalysts in chemical industries
Ni	Electroplating, manufacturing of batteries, pigments for dyes and paints, components for electrical devices, catalysts in chemical industries
Pb	Manufacturing of batteries, welding, pigments for dyes and paints, components for electrical devices, catalysts in chemical industries, mining
Zn	Anti-corrosion coating, manufacturing of batteries, soldiering and welding, coal combustion

For example, Cu is an important material in manufacturing conductor for heat and electricity, pigments for dyes and paints, and alloys; Ni is heavily used in electroplating and battery manufacturing industries; Pb is widely used in the manufacturing of dyes and

pigments, batteries, and other electronic devices (Bradl et al., 2005). Large amounts of HMs present in the environment today were attributed to the use of inorganic and organic fertilizers. For instance, inorganic and phosphate fertilizers are generally rich with Ni, Pb and Zn. Copper, in particular, was widely used as fungicides and algicides (Husak et al., 2015).

Although the usage and disposal of HMs are highly regulated by various environmental policies, the levels of HMs in the environment continue to rise due to factors such as the increasing demand for each element, violation of rules, and the non-degradability and persistent properties of metals. These metals are released into the environment as landfill leachate, drainage and run-off, subsequently contaminating soil, groundwater and the ocean (Monteiro et al., 2012). According to the World Water Report released by the United Nations in 2018, more countries are experiencing high levels of water stress which threatens economic development and food security. Rivers, streams, lakes and soils are contaminated by HMs, pesticides, herbicides, and other chemical discharges (FAO and UN-Water, 2018; WWAP, 2018). There is a huge demand for clean fresh water for daily consumption and an efficient way for wastewater remediation.

Malaysia, as a developing country, is also experiencing HM pollution in soil, sediment and surface water. According to the study by Ismail et al. (2016), HM concentrations in surface water along the Straits of Malacca were at an alarming level due to wastewater discharge from the industrial areas in northern and southern Peninsular Malaysia. Bayan Lepas area in Penang, one of the important industrial areas in the country, was shown to be strongly polluted by Cd and Cu (Khodami et al., 2017). A water and sediment analysis of the Port Klang coastal area showed that the concentrations of As, Cd, Cr, Hg, Pb, and Zn were significantly higher than the background values and considered hazardous (Sany et al., 2013). High concentrations of Ni, Cu, Zn, Cd, and Pb discharged from industrial

effluents, sewage and mining sites were found in the surface waters in Selangor River basin (Sakai et al., 2017). Other sources of HM contamination in Malaysia include motor vehicle emissions, biomass combustion, coal-fired power plants, illegal disposal, and leachate from unsanitary landfills which heavily contaminate groundwater (Sakai & Yoneda, 2018). Extensive agricultural activities in Cameron Highlands posed potential health risks to the local communities because the concentrations of HMs had exceeded the National Standard for Drinking Water Quality (Razali et al., 2018). Heavy metal exposure might induce potential health risk such as respiratory tract illness, rhinitis and cancer. The level of HMs in the Klang district might pose carcinogenic health risks as the Lifetime Cancer Risk value were relatively higher than the standards by the United States Environmental Protection Agency (Praveena et al., 2018).

Heavy metal contamination from industrial waste disposal and anthropogenic activities has become a major concern due to its detrimental effects to the environment and ecosystem (Singh et al., 2011). Organisms living in the aquatic environment, especially primary producers such as microalgae are highly sensitive to toxicants.

2.2 Global warming

An unprecedented rate of temperature rise has been observed since the industrial revolution. According to the prediction by the Intergovernmental Panel on Climate Change (IPCC), global temperature is likely to increase by 1.5°C between the year 2030 and 2052. Atmospheric warming and other factors such as changes in river flow had significantly increased water temperature around the world (Vliet et al., 2013). The strongest ocean warming was predicted to occur in subtropical and tropical regions with an increase in mean sea surface temperature between 0.6 and 2ºC (IPCC, 2013). Various climate models had associated warming with climate change such as extreme rainfall intensities and humidity in most regions (Lehmann et al., 2015). According to the analysis

by Lehmann et al. (2015), Southeast Asia showed an exceptionally high increase in record-breaking precipitation anomalies between 1981-2010, an observation consistent with the pattern of rising temperature. In the long run, an increase of 1.5 to 2°C due to human activities will pose numerous hazards for humans, freshwater systems and vegetation (Döll et al., 2018). Some studies have shown that the increase of water temperature is attributed to the increase in anthropogenic heat input from wastewater (Kinouchi et al., 2007). Substantial riverine thermal pollution was associated with the heat emission from the cooling systems from thermoelectric power plants (Raptis et al., 2016).

Aquatic organisms are highly sensitive to thermal fluctuations. Temperature is a fundamental variable for water quality and has profound impact on human and natural systems, including the rise in sea level, biodiversity loss, and increases in extreme weather (Allen et al., 2018). Most biological and chemical activities are a function of temperature. Some of the key biochemical and metabolic pathways that are highly sensitive to temperature are aerobic capacity, enzymatic activities, antioxidant activity, photosynthesis, yield production and quality (Hasanuzzaman et al., 2013). The increase in sea surface temperature resulted in a reduction in global production of ocean phytoplankton in the past decades (Boyce et al., 2010). Warming can also alter species interactions and food-web structure by increasing biological metabolism and energetic demand. This might lead to reduced fisheries catches and subsequent food crisis (Kyewalyanga, 2015). Global warming also leads to more frequent heatwaves in the ocean, further affecting the physiology of marine organisms, shifting community dynamics and species richness in the freshwater ecosystem (Frölicher et al., 2018; Gruner et al., 2017; Velthuis et al., 2017).

2.3 Aquatic toxicology and global warming

The natural aquatic systems are dynamic and constantly subjected to changing conditions such as temperature, pH, alkalinity, conductivity, chemical composition, and other parameters (Domingos et al., 2014). Among the different ecological conditions, global warming and aquatic toxicology have been closely associated with biological metabolism, species abundance and diversity (Winder & Sommer, 2012).

Temperature is a primordial factor for growth and may influence the rate of adaptation to toxicants by altering the uptake, accumulation, and degradation of pollutants in different environmental compartment (e.g. sediment, water, biota) (Zeraatkar et al., 2016). Hence, temperature was investigated as one of the key parameters in this study. Formation of metal ligand complexes is temperature-dependent. Warming might alter metal biogeochemistry, metal sources, metal complexation, and redox cycling in the marine ecosystems (Hoffmann et al., 2012). High temperatures in tropical and subtropical regions might elevate diffusion rate and speed up chemical reactions, hence favouring HM toxicity (Abdel-Tawwab & Wafeek, 2014; Reynolds & Casterlin, 1980). According to Hutchins et al. (1996), Q_{10} for metal uptake ranges between 3 to 5, occasionally up to 7 to 12 (between 3- to 5-fold and 7- to 12-fold increase in uptake rate with every 10°C increase in environmental temperature). Temperature differences at different depth may alter solubility, speciation and diffusion rate of metal ions in the water (Cairns et al., 1975; Suresh Kumar et al., 2015).

Changes in ambient temperature could alter susceptibility of organisms to various contaminants especially when they are found in the urban or industrialized areas. For example, nonlinear and synergistic effects of iron and temperature were observed on phytoplankton abundance, physiology and nutrient availability (Rose et al., 2009). Temperature enhanced the community tolerance to Cu in the bacterial communities in

photosynthetic biofilms, but not on community structure or physiological profile (Boivin et al., 2005). Freshwater mussels exposed to urban pollutants in municipal wastewaters displayed a higher sensitivity to temperature change such as reduced lipid content, increased xenobiotic biotransformation and increased oxidative stress (André et al., 2017). The increase in temperature might favour higher uptake into the cells due to the temperature-dependent changes such as metal speciation effects, chemical reaction and diffusion rates, depending on the species and other environmental conditions (Abdel-Tawwab & Wafeek, 2014; Cairns et al., 1975). The toxic effects of pollutants can be biomagnified through the food chain, shifting population dynamics and distribution in the long run.

The interaction between thermal changes and pollutants is complex and might be synergistic, additive or antagonistic to the biological responses. Understanding the interactive effects of multiple stressors is crucial to predict the tolerance limits, survival, and primary productivity of organisms to environmental changes (Todgham & Stillman, 2013).

2.4 Response of microalgae to the changing climate

2.4.1 Microalgae

Microalgae are photosynthetic organisms found in different habitats ranging from sea ice, sea waters, snow, inland waters to soil (Sharma & Rai, 2011). As the primary producers in the ecosystems, microalgae contribute largely in food web dynamics by being the food source for herbivorous rotifers, cladocerans, insect larvae, copepods and other protozoa (Yun et al., 2016). Microalgae also plays an important ecological role in biogeochemical cycles (particularly the carbon cycle), nutrient cycling, and carbon sequestration through photosynthesis (Kyewalyanga, 2015).

While some microalgae are extremophiles that can thrive in extreme environments, microalgal growth is generally dependent on various environmental conditions. Factors such as temperature, pH, UV radiation, light and nutrient availability can adversely affect the growth, physiology, photosynthetic rate, metabolic rate and biochemical composition of the microalgae (Yong et al., 2016). Climate change might modify the primary productivity of microalgae and alter the species composition, size structure, resulting in the far-reaching consequences on the structure, seasonal dynamic and taxonomic composition on aquatic ecosystems (Winder & Sommer, 2012). For example, an increase in temperature leads to smaller sized cells, reduced photosynthetic carbon fixation, reduced $CO_{2\ [atm]}$ drawdown, and lead to further climate consequences (Brierley et al., 2009). These environmental variables are generally referred to as "stressors" in the ecological context to describe variables that exceed their normal range and affect the individual taxa, community structure or ecosystem (Piggott et al., 2015).

In addition to being the primary producers in food chains, microalgae are frequently used as bioindicators for water quality biomonitoring due to their ecological importance, wide distribution and sensitivity to environmental changes (Wu et al., 2017). Microalgae are also useful biomaterials for biotechnological applications and commercial interests due to their fast doubling rate, adaptive capability to numerous conditions, high lipid content, the production of secondary metabolites (Spolaore et al., 2006). Various studies had shown that microalgae can be exploited for commercial purposes as the vehicles for carbon sequestration for industrial processes and phycoremediation (Ansari et al., 2017; Nalewajko et al., 1997). Microalgae cultivation is a sustainable alternative for phototrophic carbon fixation to produce high value-added biomass for environmental and economical applications.

2.4.2 Heavy metal contamination and its impact on microalgae

Microalgae are frequently applied for environmental risk assessment, biomonitoring and toxicity tests. Metal ecotoxicology studies (the effects of increased metal concentrations on the biota and the environment) on algae are crucial because (i) the impacts of pollutants on algal populations might reflect the effects on the local coastal environment; (ii) the metal accumulation on algae might be biomagnified across the trophic levels; (iii) the data obtained from the ecotoxicological study can be applied to determine critical levels of pollutants in the environment (Leal et al., 2016).

Different species showed different range of tolerance to HM toxicity. According to the study by Dao and Beardall (2016a), the growth rate and generation time of *Scenedesmus acutus* and *Chlorella* sp. were affected by Pb where the IC_{50} values were 1.95 x 10^{-9} M and 0.4 x 10^{-9} M respectively. Growth of *C. sorokiniana* and *S. acuminatus* was strongly inhibited by Cu concentrations ranging from 100 - 400 µM (Hamed et al., 2017). High concentrations of Cd (in the range of 10^{-7} to 10^{-5} M) also reduced the growth rate of *T. nordenskioeldii*, a marine diatom (Wang & Wang, 2008). Growth inhibition was observed in *Chlamydomonas tremulans* and *C. clinobasis* when free Cu concentration exceeded 0.1 µM (Knauer et al., 1997).

Sensitivity to metal toxicity is dependent on the type of metal and the exposure period. The growth of *S. quadricauda* was reduced most extensively by Cu compared to Mn, Cd and Pb (Fargašová et al., 1999). Copper was the most toxic metal to *Synechococcus* compared to Ni and Zn with an EC_{50} growth rate inhibition value of 4 µg L^{-1} (Debelius et al., 2011). Liu et al. (2017) showed that high concentrations of Cr, Mn, Zn, and Cu inhibited growth of *Chlorella* sp. significantly. Zhang et al. (2015) reported that excess Pb significantly induced growth inhibition in *Chlorella* sp. after a two-week exposure. In a long-term metal exposure study on green alga *Pseudokirchneriella subcapitata*, growth

rate was significantly inhibited by Cd, Cr, Cu, and Zn. However, cells were able to resume growth after being resuspended in fresh medium (Machado et al., 2015). Generally, HM toxicity on microalgae is strongly dependent on the concentrations of free metal ions.

Essential metals are structurally integrated in the photosynthetic apparatus or in the metalloenzymes necessary for photosynthesis (Dao & Beardall, 2016b). Excess metal ions may reduce photosynthetic rate of microalgae by interfering fluorescence kinetics and altering the structure of photosynthetic apparatus. For instance, Cu and Zn are essential cofactors in enzymatic reactions. However, when present in excess (i.e. in the range of micromolar), Cu^{2+} and Zn^{2+} substituted the Mg^{2+} ion in chlorophyll molecules in the light harvesting complex II (LHC II) of *S. quadricauda* (Küpper et al., 2002). The substituted chlorophylls (commonly known as Cu-Chl or Zn-Chl) are highly stable. As a result, the chlorophylls underwent a shift in the light absorption spectra, hence lowering the photosynthetic efficiency (Küpper et al., 1998). In addition to disrupting the photosynthetic pigment content, toxic HMs interfere with the light and dark reactions, chloroplast membrane structure, light-harvesting and oxygen-evolving complexes, photosystems and electron transport chains (Appenroth, 2010). Non-essential metals such as Pb induced a significant change in antenna size and heterogeneity of PSII (Dao & Beardall, 2016b). Apart from being directly involved in the photosynthesis machinery, excess metal ions also interact with enzymes with thiol (-SH) groups, aggravating photoinhibition and oxidative stress (Suresh Kumar et al., 2014). Figure 2.1 shows a schematic diagram of the possible sites that HMs can interfere with the photosynthetic machinery in algae, such as the water-splitting system and the electron transport chain.

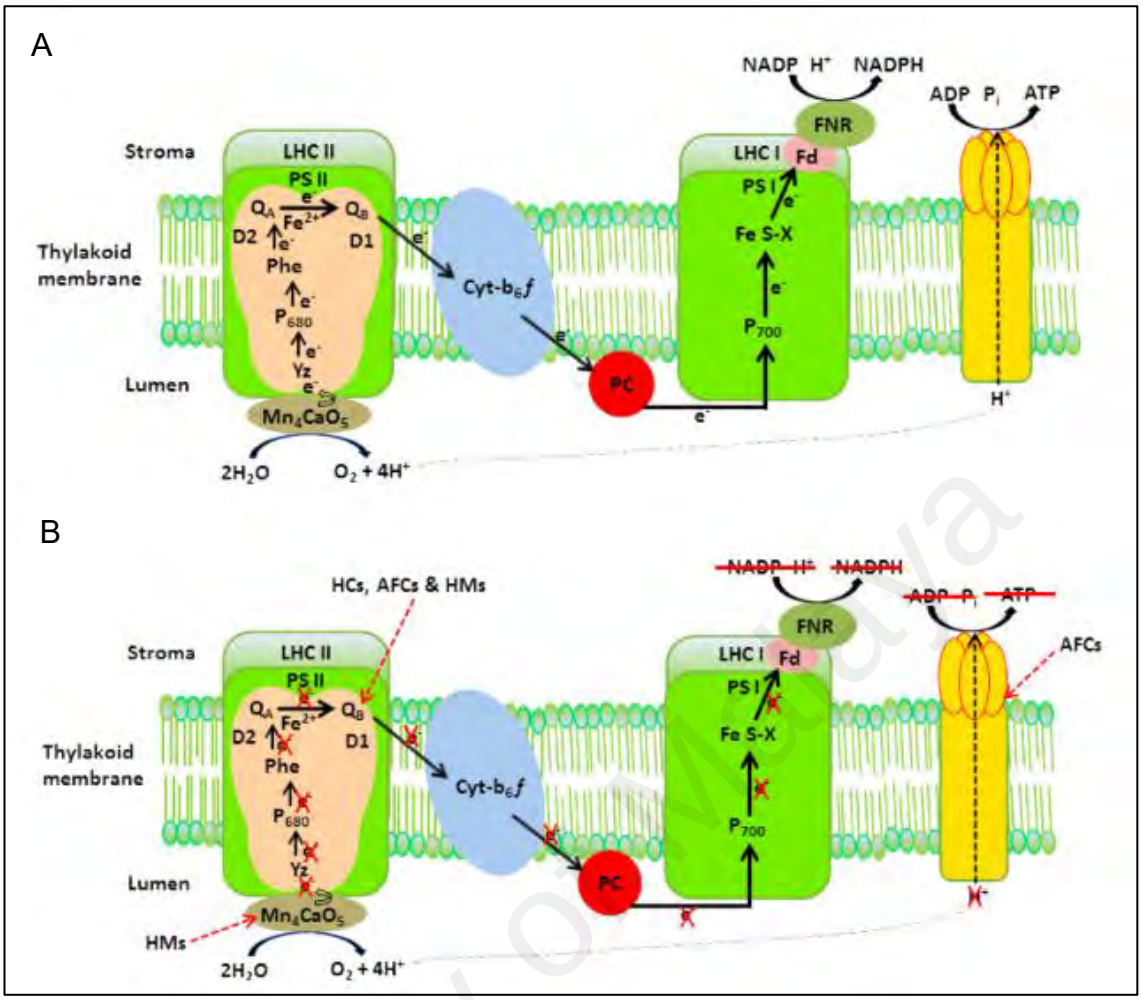

Figure 2.1: The inhibitory effects of heavy metals (HMs), herbicides (HCs) and antifouling compounds (AFCs) on the light reaction and photosynthetic apparatus. (A) the light reactions of photosynthesis under normal conditions. (B) HMs might affect the electron transport chain (indicated by black arrows) in the water-splitting process, photosystem II (PSII), primary and secondary electron acceptor quinone (Q_A and Q_B), photosystem I (PSI), and ATP synthase. [1]

[1] Figure reprinted from Suresh Kumar, K., Dahms, H.-U., Lee, J.-S., Kim, H. C., Lee, W. C., & Shin, K.-H. (2014). Algal photosynthetic responses to toxic metals and herbicides assessed by chlorophyll *a* fluorescence. Ecotoxicology and Environmental Safety, 104, 51–71. http://doi.org/10.1016/j.ecoenv.2014.01.042, with permission from Elsevier. See Appendix E for a copy of the copyright transfer agreement.

Chlorophyll *a* (Chl-*a*) fluorescence measurement is a rapid, sensitive and non-intrusive method to monitor photosynthetic performance of microalgae in response to toxic metals

(Suresh Kumar et al., 2014). Table 2.3 summarizes the various parameters used to describe the photosynthetic performance of microalgae the such as maximum quantum efficiency (F_v/F_m), relative electron transport rate (rETR), photo-adaptive index (E_k), and non-photochemical quenching (NPQ).

Table 2.3: Various parameters commonly used to describe photosynthetic efficiency (Adapted from Dao & Beardall, 2016a; Maxwell et al., 2000; Suresh Kumar et al., 2014)

Parameter	Description
F_v/F_m	• Maximum quantum yield • Reflects the potential quantum efficiency of PSII • Used as an indicator of plant photosynthetic performance • A simple and rapid way to monitor stress
NPQ	• Non-photochemical quenching • Reflects the ability of a cell to dissipate excess light energy harvested during photosynthesis as heat • Used as an indicator of photoprotection
rETR	• Relative electron transport rate • Measures the rate of linear electron transport through PSII • Used as an indicator of environmental stress
Φ_{PSII}	• Effective quantum yield of PSII photochemistry • Measures the proportion of light absorbed by chlorophyll in PSII

Table 2.3, continued

Parameter	Description
E_k	• Photo-adaptive index or saturation irradiance for electron transport • Indicates the rate of photosynthesis and photoadaptation
Alpha (α)	• Light harvesting efficiency • Indicates the rate of photosynthesis and photoadaptation
qP	• Coefficient of photochemical quenching
qN	• Coefficient of nonphotochemical quenching

The maximum quantum yield, F_v/F_m had been used as a sensitive indicator of plant photosynthetic performance in response to toxic metals. A study in *Chlorella* sp. and *S. acutus* showed that Pb reduced the F_v/F_m, $rETR_m$ and α values by impairing the functions of PSII reaction centre and electron transport chain (Dao & Beardall, 2016a). This phenomenon was further elaborated by relating the parameters to reduced antenna size ratio of $PSII_\alpha/PSII_\beta$ and absorption flux per fully active reaction centre (Dao & Beardall, 2016b). The F_v/F_m value of a dinoflagellate, *Prorocentrum minimum* decreased remarkably after exposure to 0.5 mg/L $CuSO_4$ for 48 h (Guo et al., 2016). Copper inhibited the oxidizing side of PSII and decreased the Chl-*a* proportion in *Phaeodactylum tricornutum* (Cid et al., 1995). Nickel oxide nanoparticles caused a reduction in Φ_{PSII}, rETR and qP in the freshwater alga *P. subcapitata* (Sousa et al., 2018).

Non-photochemical quenching, NPQ indicates the relative increase in the non-photochemical deactivation processes such as the fluorescence emission, heat dissipation and energy spillover from PSII to PSI. Changes in NPQ is frequently linked to photosynthetic pigment alteration and abiotic stress. *Chlorolobion braunii*, a tropical

freshwater phytoplankton dissipated light energy through non-photochemical process upon inhibition by Cd and Cu (Echeveste et al., 2017). Nowicka et al. (2016) reported that the acclimation to HM-induced stress occurred within minutes in *C. reinhardtii* through exhibiting effective NPQ mechanisms in response to Cu, Cr and Cd. Similar observation was also reported in *S. incrassatulus* in which the NPQ value increased with the increasing Cu^{2+} concentrations, accompanied by an inhibition on PSII electron transport from Q_A, Q_B and the plastoquinone pool (Perales-Vela et al., 2007).

The impacts of HMs on photosynthesis are often associated with changes in other parameters such as gene expression, enzymatic reaction and intracellular redox states. Jamers et al. (2006) reported that the genes involved in photosynthesis such as Chl-*a*/*b* binding protein LhcII-1 and Chl-*a*/*b* binding protein LI818r were differentially expressed in *C. reinhardtii* after Cu exposure. The exposure of *P. subcapitata* to Cd, Cr, Cu and Zn led to a reduction in Chl-*a* content and $\Phi_{PSII,}$ coupled with modifications in membrane integrity and mitochondrial membrane potential (Machado et al., 2015).

Oxidative damage is often regarded as the main mechanisms involved in metal-mediated cell toxicity (Dao & Beardall, 2016a). Transition metals such as Cu and Fe can catalyse oxygen reduction and produce free radicals that can oxidize biological molecules resulting in major cellular changes. Figure 2.2 is a schematic representation of the mechanisms of heavy-metal induced oxidative stress in cellular response.

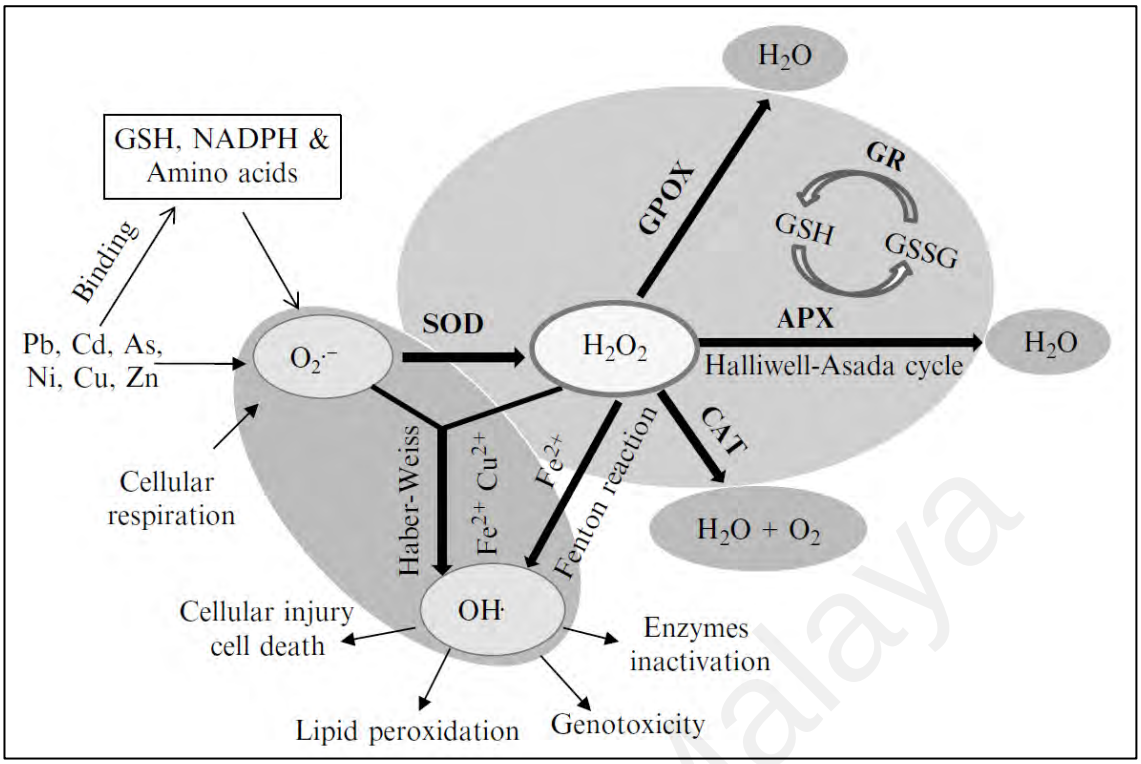

Figure 2.2: Schematic mechanisms of heavy-metal-induced oxidative stress. Heavy metals bind to molecules and induce ROS generation through direct and indirect mechanisms. The subsequent cascade reactions lead to enzyme inactivation, genotoxicity, lipid peroxidation, cellular injury or cell death. [2]

[2] Figure reprinted from Shahid, M., Pourrut, B., Shahid, M., Pourrut, B., Dumat, C., Nadeem, M., … Pinelli, E. (2014). Heavy-metal-induced reactive oxygen species: Phytotoxicity and physicochemical changes in plants. In D. Whitacre (Ed.), Reviews of environmental contamination and toxicology (Vol. 232, pp. 1–44). Springer, Cham. http://doi.org/10.1007/978-3-319-06746-9_1, with permission from Springer Nature. See Appendix F for a copy of the copyright transfer agreement.

Under normal condition, metal ions are essential cofactors for antioxidant enzymes such as SOD and its isoforms. The presence of excess metal ions might result in overproduction of reduced form of oxygen and associated biochemical damage (Nagajyoti et al., 2010). According to Aust et al. (1985), metals can be directly or indirectly involved in the generation of free radicals and ROS through four different ways, which are the direct transfer of electron in reduction, disturbance of metabolic pathways,

inactivation or down-regulation of the enzymes of the antioxidative defence system and depletion of antioxidants with small molecular weight. Through oxidative modifications and displacement of essential cations from specific enzyme binding sites, metal ions can also modify free amino acids and proteins. Amino acids such as histidine, arginine, lysine, proline, methionine and cysteine are the most common oxidative sites in proteins (Shahid et al., 2014).

To date, there is extensive literature on the effects of HMs on ROS production in different organisms. Szivák et al. (2009) tested the ROS levels in *C. reinhardtii* to redox active metals (Fe, Cu, Ag, Cr, Cr) and non-redox active metals (Pb, Cd, Zn). The results showed that low free ion concentrations of both redox and non-redox active metals (10^{-6} to 10^{-9} M) enhanced ROS production as an earlier response to metal stress. Lead also enhanced the ROS in green microalgae, possibly through disruption of equilibrium between ROS production and scavenging systems (Dao & Beardall, 2016a). Formation of ROS was regarded as one of the main mechanisms for Ni toxicity in aquatic environments by affecting the signalling transduction pathways related to cell cycle and apoptosis (Brix et al., 2017). The formation of ROS is dependent on the type of HMs. Redox-active metals (e.g. Cu and Fe) initiate the Haber-Weiss reaction and catalyse the formation of hydroxyl radicals, whereas non-redox active metals (e.g. Cd, Pb, Hg) disrupt the metabolic equilibrium by inactivating the antioxidant pool (Tripathi & Gaur, 2004). Different metals were shown to produce varied species of reaction oxygen. For example, Cu was reported to produce H_2O_2, O_2^- and $^{\bullet}NO$ whereas Ni induced production of H_2O_2 and O_2^- (Shahid et al., 2014).

Heavy-metal-induced production of ROS can result in a widespread damage to plants such as enzyme inhibition, protein oxidation, lipid peroxidation, DNA damage and cell signalling. To combat oxidative damage, microalgae have evolved a complex network of

defence mechanism. This includes complexation of HMs with organic acids, sequestration into vacuoles, activation of metallothioneins and phytochelatins, and activation of antioxidant enzymes such as SOD, catalase (CAT), and ascorbate peroxidase (APX) (Shahid et al., 2014). In green alga *Acutodesmus obliquus*, Pb increased the formation of H_2O_2 and lipid peroxidation and the deleterious effects were counteracted by enzymatic (SOD, CAT and APX) and non-enzymatic (ascorbate and glutathione) antioxidant systems (Piotrowska-Niczyporuk et al., 2015). *Chlamydomonas reinhardtii* acclimated to oxidative stress induced by Ag, Cd, Cr, Cu and Hg ions through up-regulation of the transcription of ROS detoxifying enzymes (Nowicka et al., 2016).

Microalgae have evolved a complex network of defence mechanism to combat oxidative damage. Metal toxicity and tolerance is highly dependent on the species' antioxidant capacity and redox homeostasis. Knauert & Knauer (2008) showed that ROS played a primary role in Cu toxicity to two freshwater green algal species, *P. subcapitata* and *C. vulgaris* and the defence system was species-specific. In general, the first step of antioxidant activity usually involves the selection at the algal cell walls which are the first protective barrier against HMs uptake. This is attributed to the different types of binding groups and ligands on algal cell walls such as the sulfuryl, hydroxyl, phosphate, amine or sulfate groups. Some of the factors which influence the HM ion biosorption are initial metal ion concentration, biomass, pH, temperature, and presence of other ions (Zeraatkar et al., 2016). Adsorption of metal ions was reported to be one of the key tolerance mechanisms in some species such as *Oocystis nephrocytioides* (Soldo et al., 2005).

To survive and adapt against environmental perturbations and abiotic stresses, microalgae employ a series of responses by regulating levels of primary metabolites, secondary metabolites, photosynthetic intermediates, metal-transport protein, ion fluxes and osmolytes in the cells (Arbona et al., 2013). Heavy metals elicit changes in the

complex metabolic network inside photosynthetic organisms. The internal distribution of metal ions is highly dependent on the intracellular transport and detoxification mechanisms involving metabolites, enzymes and genetic modifications. The proposed metabolic modification in plants in response to HM toxicity can be categorised into three types: (i) changes in pigment production; (ii) up- or down-regulation of metabolites such as glutathione and ascorbic acid; and (iii) restructuring of metabolic pool to channel energy consumption to survival and adaptation instead of growth (Nagajyoti et al., 2010).

Metabolites are highly sensitive to stressors and their composition always indicate the underlying changes in the metabolic network, energy supply, and consumption of storage molecules (Kluender et al., 2009). The expression of various metabolites such as amino acids, sugars, small molecular organic acids, were affected and regulated to counteract the toxic effects of HMs (Zhang et al., 2014). The detected metabolites are usually amino acids, sugars, small molecular organic acids, polar, apolar metabolites such as fatty acids and sterol (Xue et al., 2015).

Molecules such as metallothioneins and phytochelatins are key metal-binding ligands in the homeostasis. Phytochelatins are small polypeptides that are activated by metal ions such as Cd, Pb, Zn and Cu for binding and transporting HMs to cell vacuoles (Shahid et al., 2014). Phytochelatins synthesized by microalgae in response to Cd, Cu, As and Pb might be transformed into biosensor components to detect environmental pollution (Miazek et al., 2015). Glutathione (GSH) is a sulfur-containing tripeptide that protects cells from HMs by quenching ROS. The differential levels of GSH accompanied by changes in antioxidant enzyme activity was involved in the response of *C. reinhardtii* to Cu (Jiang et al., 2016). Glutathione metabolism and the activities of related enzymes such as γ-glutamylcysteine synthetase, GSH S-transferase, GSH-peroxidase and GSSG-

reductase were highly involved in the HM response of *S. bijugatus* (Nagalashkmi & Prasad, 2001).

Nitrogen metabolism is involved in cellular response to HM toxicity by regulating the expression of polyamines, amino acids and derivatives. Polyamines such as putrecine, spermidine and spermine participate in membrane stabilization and prevent generation of ROS (Oukarroum, 2016). A remarkable decrease in organic osmolytes and metabolites such as sucrose, alanine, leucine, isoleucine, glycerophosphocholine and betaine were observed in *C. vulgaris* in response to Cu and Cd toxicity (Zhang et al., 2014). The levels of proteins and monosaccharides in green alga decreased with the increasing concentrations of Pb (Piotrowska-Niczyporuk et al., 2015). In marine microalgae, cellular uptake and detoxification of Cu were reported to be via reduction of Cu (II) to the less toxic Cu (I), as well as synthesis of polyphosphate bodies and phytochelatins (Adams et al., 2016). Malondialdehyde (MDA) is often up-regulated as a product of the lipid peroxidation process induced by HMs (Jiang et al., 2016). Upon exposure to Ag, the number of lipid bodies in *C. reinhardtii* increased as a response to lipid membrane damage to restore new membrane lipids (Pillai et al., 2014). Metals, metalloids and metallic nanoparticles caused a shift in lipid content and change in fatty acid profile (Miazek et al., 2015). In the study conducted by Koppel et al. (2017), the intracellular lipid concentration of polar marine microalga *Cryothecomonas armigera* was greatly reduced by Cu, Ni, Pb, Zn, and Cd. This phenomenon was concurrent to growth inhibition and may be a result of cellular repair mechanisms. Protein modifications were also observed in the detoxifying response of microalgae. Heavy metal ions can bind to thiol groups of proteins and replacing functional HMs in key proteins for ATP synthesis (Pillai et al., 2014). Kováčik et al. (2017) reported an increase in the level of ascorbic acid, non-protein thiols and phenols under high dose of Cd in *S. acutiformis*. Sequestration by vacuoles also helps to maintain metal homeostasis and detoxifies HMs (Kaplan et al.,

2013). A time-dependent study conducted by Kluender et al. (2009) showed that the energy metabolism and carbohydrate synthesis of *S. vacuolatus* was impaired under phytotoxic conditions. Aliphatic organic acids in Krebs cycle such as citrate, fumarate and lactate were affected under Ni treatment in *S. quadricauda* (Kováčik et al., 2016).

In addition to primary metabolites, secondary metabolites are also heavily involved in the stress response. Considerable changes in flavonoids, polyphenols and proline were observed in *C. sorokiniana* and *S. acuminatus* under Zn toxicity. This observation was accompanied by enhanced antioxidant enzyme activities to combat the pronounced oxidative stress induced by HMs (Hamed et al., 2017).

Metabolomics is a technique for biomarker discovery and pathway mapping to describe a particular phenotype (Johnson et al., 2016). This analysis has been suggested as a useful tool to identify physiological markers and metabolic pathways in green algae (Arbona et al., 2013). In the context for metal toxicity studies, metabolomics provides "real-time" understanding on the physiology and identify the low molecular weight molecules involved in the detoxification mechanisms (Booth et al., 2011). Understanding the metabolic profile of microalgae under different conditions will provide valuable insights into systems biology, microalgal biotechnology and the potential targets for genetic engineering (Veyel et al., 2014).

2.4.2.1 Copper toxicity on microalgae

Copper is an essential element in transcriptional regulator proteins, chaperones, protein transporters and receptors, oxidoreductases, electron transfer proteins, free radical scavenging enzymes, oxidase, and monooxygenase (Festa et al., 2011). More than 30 enzymes require Cu for normal functioning and catalysing redox reactions. Copper is also crucial in CO_2 assimilation and ATP synthesis (Yruela et al., 2005). In cyanobacteria and eukaryotic green alga, the homeostasis of Cu in photosynthetic organisms are regulated for cytochrome c oxidase and photosynthetic electron carrier plastocyanin (Burkhead et al., 2009). Cu deficiency strongly inhibited the PS I and II electron transport activities and enzymatic reaction rates (Adrees et al., 2015).

Over the last decades, Cu contamination in the aquatic ecosystems due to anthropogenic activities has become a major concern in many regions (Chen et al., 2018; Harvey et al., 2016; Khodami et al., 2017). The excessive use of Cu-based pesticides to control agricultural diseases and pests had increased Cu accumulation in the surface soil and groundwater (Adrees et al., 2015). This scenario is expected to worsen over the years as the global demand for Cu is projected to increase by 275 – 350 % in the year 2050 (Elshkaki et al., 2016).

Various organisms had showed a great sensitivity to excess Cu. High Cu concentrations affected plant morphology, growth, biomass and yield (Adrees et al., 2015). High Cu directly increased the levels of ROS such as hydroxyl radicals (O_2^{2-}), hydrogen peroxide (H_2O_2), singlet oxygen ($^1O_2$), and perhydroxyl radical ($H_2O\cdot$). The increased ROS initiate a series of chain reaction in proteins, lipids, and DNA, causing oxidative damage and impairing cell functions. Redox cycling between Cu^+ and Cu^{2+} might also catalyse the synthesis of free radicals which damage macromolecules and disrupt the homeostasis in the cells (Burkhead et al., 2009). The increase in oxidative

stress is usually counteracted by an increased production of antioxidant enzymes such as catalase, SOD, ascorbate peroxidase (APX), peroxidase (POD) and glutathione reductase (GR) (Adrees et al., 2015). The oxidative stress response usually depends upon species of the organism, exposure duration and concentration of Cu toxicity.

Among the many effects of excess Cu, the impacts on photosynthetic apparatus and pigment levels were among the most important observations in autotrophs. Copper toxicity on chlorophyll biosynthesis was reported in many plants and algae, where a significant decrease in total chlorophyll (Chl-*a*+*b*) and carotenoid contents were observed in crop plants and phytoplankton. Copper interferes with chlorophyll organization and induces structural damage to the photosynthetic apparatus at the thylakoid levels (Adrees et al., 2015).

Organisms utilize several mechanisms to maintain the homeostasis of Cu inside the cells. The first defence strategy is to control the amount of Cu uptake, accumulation, chelation of Cu ions and adsorption on the cell walls. Once inside the cells, the excess metal can be chelated by metabolites such as citrate, proline or histidine. Alternatively, Cu can be sequestered, metabolized and stored in vacuole, apoplast and cell walls (Adrees et al., 2015).

2.4.2.2 Nickel toxicity on microalgae

Nickel is a cofactor in enzymes such as urease, hydrogenase, and SOD (Egleston et al., 2008). The growth of *Trichodesmium*, a cyanobacterium, can be limited by Ni availability in the culture media. Nickel increased SOD activities and nitrogen fixation rates, suggesting that NiSOD might be involved in protecting enzymes from superoxide inhibition during photosynthesis (Ho, 2013).

The global demand for Ni has risen over the years due to its wide application in the metallurgical, chemical, agricultural and manufacturing industries. More than two-thirds of the world's Ni lateritic deposits are located in the tropics especially in the South East Asia region (Binet et al., 2018; Mudd & Jowitt, 2014). The increasing anthropogenic release of Ni into the environment has been identified as a key pollutant in tropical waters and may be toxic to various organisms in the aquatic ecosystems (Cempel & Nikel, 2006).

Microalgae are highly or moderately sensitive to Ni (Binet et al., 2018). When present in excess amount, Ni induces various biochemical, physiological and structural changes in the organisms. Nickel in micromolar concentrations was sufficient to affect concentrations of photosynthetic pigments, antioxidant enzyme activities and macromolecule content in green microalgae (Martínez-Ruiz & Martínez-Jerónimo, 2015). Nickel oxide nanoparticles decreased cell viability, altered relative cell size and granularity, inhibited photosynthesis, and increased ROS levels in *C. vulgaris* (Oukarroum et al., 2017). The response to Ni toxicity varies between species and isolates. For example, the Ni removal efficiency of *C. vulgaris* was around 33-41% whereas *C. miniata* removed nearly 99% of the Ni in wastewaters (Wong et al., 2000). Nickel reduced the germination rate, protein and chlorophyll contents, growth rate and velocity of movement in flagellates in the green alga *Haematococcus lacustris* (Xyländer & Braune, 1994). Brix et al. (2017) identified several potential molecular initiating events explaining the toxicity of Ni on aquatic organisms: imbalance of Ca^{2+} homeostasis, disruption of Fe homeostasis, and ROS-induced oxidative damage.

To counteract excess Ni, the carbohydrate and protein levels in microalgae were regulated to reduce metal bioavailability and toxicity in *Prorocentrum donghaiense* (Huang et al., 2018). Other adaptation strategies to counteract Ni include synthesis of N-

containing compounds, growth regulators, antioxidant enzymes and S-containing compounds (Sachan & Lal, 2017).

2.4.3 Effects of warming on microalgae

Temperature is a key environmental factor that strongly regulates growth of photosynthetic organisms. In the context of microalgal physiology, global warming is one of the contributing factors to the decline of annual global phytoplankton biomass over the past century (Boyce et al., 2010). The effects of sea surface temperature on the declining trends of chlorophyll content were remarkable in tropical and subtropical regions. Global warming and changing temperature regimes were shown to affect the primary productivity, macromolecular composition and carbon allocation in microalgal cells (Wagner et al., 2016).

In general, microalgae can adapt and survive in a broad range of temperature due to their eurythermal adaptivity (Lee et al., 2017). However, elevated temperature beyond the tolerated range will affect the growth rate and alter the biochemical pathways of microalgae. Growth rate, population count, Chl-*a* content and biomass of *S. quadricauda* significantly decreased at 39°C (Zargar et al., 2006). Elevated temperature in the environment impaired photosynthetic rate, affected viability of PSII and fluidity of the thylakoid membrane, lowered biomass production in *Choricystis minor* (Zidarova & Pouneva, 2006). The same study also reported that high temperature reduced biomass production, reaction rates and kinetic properties of enzymes.

Photosynthetic energy partitioning is a function of temperature. Thermal fluctuations affect fluidity and functioning of PSII on the thylakoid membrane, which subsequently influence the photosynthetic rate and aggravate photoinhibition (Smirnoff, 1995). The adaptation of a species to temperature is dependent on its efficiency to utilize the absorbed light energy to non-photochemical quenching or alternative electron pathways (Fanesi et

al., 2016). Lee et al. (2017) reported that the photosynthetic efficiency and pigment content of *Chlorella* isolated from the tropical freshwater region was sensitive to temperature higher than 38°C. A decrease in F_v/F_m and $rETR_m$ was observed in marine *Chlorella* exposed to high temperatures (Barati et al., 2018).

Generally, heat stress affects the stability and activity of proteins, enzymes and nucleic acids in the cells. The overall effects in heat stress can lead to reduced biomass production, reaction rates and kinetic properties of enzymes (Zidarova & Pouneva, 2006). Lipid composition and membrane fluidity of microalgae cells were reported to be temperature-dependent (Lukeš et al., 2014). A trend of desaturation was observed in the fatty acid profile of Antarctic *Chlamydomonas* sp. ICE-L at 15ºC in which the expression level of mRNAs for fatty acid desaturases changed following elevation of temperature (An et al., 2013). Heat also causes several metabolic changes associated with dysregulation in the electron transport chains and ROS production (Arbona et al., 2013).

Acclimation of snow alga *C.* cf. *nivalis* to a wide range of temperatures might be due to the structural flexibility in the D1 protein of thylakoid membrane which consists largely of negatively charged phosphatidylglycerol (Lukeš et al., 2014). Interspecies variability for sensitivity to heat was also observed in *Chlorella* species where the Antarctic strain showed higher expression of HSP70B heat shock proteins (Chankova et al., 2013). A hypothetical model proposed that the heat shock response in *Chlamydomonas* is a highly complex network which includes protein homeostasis of enzymes, molecular chaperones and transcripts, photosynthesis, ROS scavengers, membrane lipid remodelling and cell cycle (Schroda et al., 2015). Metabolic network also has been shown to be markedly regulated by sub-optimal temperatures in order to regulate cellular osmotic pressure, maintain redox homeostasis, and balance energy distribution (Cao et al., 2016; Schroda et al., 2015).

The impact of temperature on microalgae extends beyond the cellular level into the species, community and biogeochemical levels (Behrenfeld et al., 2016; Wagner et al., 2016). Global warming results in stronger stratification in the water column, thereby reducing the depth of the upper mixing layer and bringing more photosynthetic marine microalgae closer to the surface of the sea, a situation where more microalgae could be subjected to stresses of drastic light and UV fluctuations (Steinacher et al., 2009). Weaker mixing and stronger stratification subsequently suppress the upward nutrient flux. The nutrient-depletion scenario on the surface water will affect phytoplankton growth (Winder & Sommer, 2012). Under high water temperature, the growth rate of cyanobacteria was higher than that of green microalgae due to their ability to migrate vertically in the water column and resist grazers. The competitive advantage of cyanobacteria might lead to changes in the algal-grazer relationship and community structure (Lürling et al., 2013). Furthermore, the increased water temperature can impact on the resource allocation of the phytoplankton species, implicating a change in biogeochemical cycling of nitrogen and phosphate (Toseland et al., 2013).

2.4.4 Interactive effects of heavy metal contamination and warming on microalgae

Some reports showed that increased algal culture temperatures will increase metal ion biosorption capacity. Marine diatom, *T. nordenskioeldii* exhibited temperature-dependent sensitivity to cadmium stress (Wang & Wang, 2008). High temperature was reported to increase toxicity of nano zinc oxides on *S. costatum* (Wong & Leung, 2014). Increase of temperature also resulted in higher inhibition by silver nanoparticles on photosynthetic performance of *C. vulgaris* and *D. tertiolecta* (Oukarroum et al., 2012a). These interactive effects are probably because (i) increased number of active sites in metal ion uptake; (ii) increased tendency of active sites to absorb metal ion; (iii) reduction in mass transfer resistance in diffusion layer by a reduction of thickness of diffusion boundary layer; (iv)

change of complex ion formation constant with temperature (Zeraatkar et al., 2016). In the natural aquatic ecosystems, microalgae are distributed at different depths of water column due to thermal stratification.

At the cellular level, high temperature and metal toxicity interactively affected the growth rate, photosynthesis, overall metabolism, transcriptional responses, metal ion distribution, and detoxification mechanisms of microalgae (Leung et al., 2017; Wang & Wang, 2008). Among the different cellular responses, photosynthesis was reported to be one of the key processes markedly affected by the combined stresses. For example, high temperature and Cu toxicity reduced photosynthetic index of *C. vulgaris* due to lower efficiency of photosynthetic electron transport and structural change of the photosynthetic apparatus (Oukarroum et al., 2012b). Enhanced PSII photoinhibition was reported in *C. pyrenoidosa* exposed to sub-lethal Cu concentrations and sub-optimal temperature (Vavilin et al., 1998).

The interactive effects between metal ions and temperature are complex and hard to predict because each of the factors alter the physiology of microalgae considerably. The response is also greatly influenced by origins and behaviour of the species, culture conditions and, physicochemical activities of the environment. For example, iron and temperature increase reacted synergistically and increased plankton assemblages in the polar regions (Rose et al., 2009).

The interaction between thermal changes and pollutants might be synergistic, additive or antagonistic to the biological responses. In ecology studies, the term “synergism” is used to define the cumulative effect of multiple stressors that are more prevalent than the additive sum of effects by each individual stressor, whereas the term “antagonism” is used to define a cumulative effect that is less than “additive” (Piggott et al., 2015). To date, there is an extensive literature on the independent effects of Cu and temperature on

growth and metabolic responses of microalgae (El-Sheekh et al., 2017; Hamed et al., 2017; Olsson et al., 2015; Sibi et al., 2014). However, the interactive effects of Cu toxicity and temperature were scarcely reported and are somewhat not inconsistent (Monteiro et al., 2012; Suresh Kumar et al., 2015). Similarly, the interactive effects of Ni and warming on green microalgae were not understood. Understanding the physicochemical dynamics of multi-stressors on organisms is critical. In addition, a comprehensive description on the mechanisms underlying metal toxicity and temperature on microalgae is yet to be elaborated. In this context, research is still needed to better understand the mechanisms that drive the influence of temperature on the vulnerability of microalgae to metal toxicity.

2.5 Microalgae for phytotoxicity testing and phycoremediation

Algae were used to monitor water toxicity and early detection of pollution as recommended by the United Nations in their nature-based water quality monitoring initiatives (WWAP, 2018). Among the many species of microalgae, chlorophytes have been recommended as model organisms in phytotoxicity assessment (OECD, 2002). Specifically, species belonging to the genera *Scenedesmus* and *Chlamydomonas* were frequently selected as the test organisms to investigate abiotic stress response due to their fast doubling rate, oleaginous property, and potential use for phycoremediation (Kluender et al., 2009; Xia et al., 2016).

Microalgae had been proposed as a potential candidate for phycoremediation to remove metals and pollutants from wastewater (Monteiro et al., 2012). The use of algal biomass as an alternative for wastewater remediation was proposed because it was more cost-effective, environmental-friendly and low-maintenance compared to the physicochemical methods (e.g. chemical precipitation, filtration, adsorption, coagulation or physical ion exchange) which are generally inconvenient and costly.

Heavy metal tolerance capacity and removal efficiency of microalgae vary between genus, species, biomass of the cells and concentration of the metal. Microalgae with smaller cell size, having higher surface area and more binding sites for metals, are generally recommended (Yan & Pan, 2002). Among the many species of microalgae, *Chlamydomonas*, *Chlorella*, *Scenedesmus* and *Spirulina* spp. were reported to have high efficiency and potential in heavy metal remediation (Suresh Kumar et al., 2015). *Chlorella vulgaris* was able to accumulate up to 91% of total cellular Ni^{2+} upon exposure to 40 µg mL^{-1} Ni solutions (Wong et al., 2000). The metal uptake capacity of microalgae can occur through bioaccumulation by living cells or biosorption by non-living algal biomass. The benefit of employing living microalgae over the latter for phycoremediation is having a continually self-replenishing system that can run continuously over an extended period of time (Suresh Kumar et al., 2015).

The strain-dependent metal ion biosorption capacity depends on the cell wall composition (polysaccharides and proteins) present in algal cell wall which varies among different species. The anionic and cationic sites on the functional groups (e.g. carboxyl, hydroxyl, phosphate, amino and sulfhydryl) contribute to different uptake capacity of microalgae (Monteiro et al., 2012; Suresh Kumar et al., 2015). The metal ion binding capacity during the biosorption processes by microalgae involve ion exchange, complexation, electrostatic attraction and microprecipitation mechanisms (Vetrivel et al., 2017).

Owing to their biosorption and bio-conversion properties, microalgae can be cultivated in agro-industrial, municipal, pharmaceutical and textile wastewater. In general, microalgae can absorb complex toxic compounds and convert them to simple non-toxic compounds. The biomass obtained from wastewater treatment might be further utilized for biofuel generation or other biotechnological applications (Wang et al., 2016).

Removal of metals from the mine water samples could be a combination of adsorption and ion-exchange physicochemical mechanisms based on the charged groups present in the cell wall of the algal biomass (Vetrivel et al., 2017). Various methods have been reported to recover HMs from alga strains after treatment from wastewater (Singh et al., 2016).

Microalgae as biosorbents appear to be more promising than macroalgae because of more efficient cultivation methods, higher production yield with faster growth, greater biosorption efficiency, and higher specific biosorption area. The heavy metal biosorption capacity of algae proved to be effective because of the algal cell wall, which is composed of a fibre-like structure and an amorphous embedding matrix of various polysaccharides (Vetrivel et al., 2017).

2.5.1 *Scenedesmus*

Scenedesmus is a genus of green algae found in diverse ecosystems with various water quality (Phinyo et al., 2017). *Scenedesmus quadricauda* are present in the aquatic ecosystems in colonies of 4-celled (or 2-, 8-, 16- celled) coenobium with spiny projections in many species. *Scenedesmus* can change their cellular organization and form coenobium consisting of 1, 2, 4, 8 and 16 cells depending on a number of factors such as the presence of grazers and nutrient availability (Gavis et al., 1979; Giraldo-Zuluaga et al., 2016).

Various species in the *Scenedesmus* genus had been used as common bioindicators of abiotic stressors. Li et al. (2016) investigated the response of microalgae to increased CO_2 and warming using *S. acuminatus*. Their results showed that the two abiotic stressors acted synergistically and affected cell productivity and characteristics of extracellular polymeric substances. Cultures of *S. quadricauda* exposed to UV-A and UV-C showed increase in soluble proteins, oxidative stress and metabolites such as benzoic acid derivatives and cinnamic derivatives (Kováčik et al., 2010). The *Scenedesmus* genus is

also frequently selected as the test organisms to detect the presence and effects of nutrients or toxins resulting from anthropogenic inputs to aquatic systems (Fawaz et al., 2018). The EC_{50} values for *S. quadricauda* on growth inhibition was reported to be 0.27 and 0.58 mg/L for Cu^{2+} and Ni^{2+} respectively (Fargašová et al., 1999).

Phycoremediation remedies using green algae was widely reported in the past decades. Wong et al. (2015) proposed that *S. quadricauda* was a viable candidate for wastewater treatment as the culture removed high quantities of orthophosphate, ammonia nitrogen and phosphate from the wastewater while synthesizing high lipid content. The *S. quadricauda* was reported to degrade inorganic compounds and pesticides such as metalaxyl, pyrimethanil, and fenhexamid (Baglieri et al., 2016).

2.5.2 *Chlamydomonas*

Microalgae in the *Chlamydomonas* genus are generally characterised as unicellular chlorophytes with two anterior flagella, a distinct cell wall and the presence of one or two pyrenoids in the cytoplasm (Harris et al., 2001). Various species of *Chlamydomonas* are widely distributed in the aquatic ecosystems, soil, glacier, industrial wastewater and sewage ponds (Merchant et al., 2006).

The *Chlamydomonas* genus is often regarded as the model organism for genetic, biochemical and ecological studies because of its simple life cycle, easy cultivation method and the widely available data about its functional systems (Harris et al., 2001). Different species of *Chlamydomonas* were used to study photosynthetic machinery, genetic regulation and metabolic response under various environmental conditions. Schroda et al. (2015) used *C. reinhardtii* to investigate metabolic imbalances, DNA expression, signal transduction and photosynthetic light reactions under heat stress.

Various studies reported the potential use of *Chlamydomonas* in heavy metal pollution studies and phytotoxicity testing. It can be used to study trace nutrient interactions, nutrition-dependent metabolic changes, relationship between photo-oxidative stress and metal homeostasis (Merchant et al., 2006). An integrated approach combining studies at the biochemical, physiological and growth levels was used to investigate the effects of Cu toxicity on *C. reinhardtii* (Jamers et al., 2013a). Stewart et al. (2015) explained the temporal dynamics of Pb speciation in the species.

CHAPTER 3: METHODOLOGY

3.1 Microalgae strain and culture conditions

Two freshwater chlorophytes, *S. quadricauda* (Turpin) Brébisson, (UMACC041) and *C. augustae* (UMACC246) were obtained from the University of Malaya Algae Culture Collection (UMACC) (Table 3.1).

Table 3.1: Origins of microalgae species

Species	Source	Region	Reference
Scenedesmus quadricauda (Turpin) Brébisson (UMACC041)	Fish tank, University of Malaya	Tropical	Ng et al., 2014
Chlamydomonas augustae (UMACC246)	Soil, paddy field, Indonesia	Tropical	Teoh et al., 2013

The stock cultures were cultivated in Bold's Basal Medium (BBM) (Phang & Chu, 1999) (Table 3.2) and maintained in a shaking incubator (80 rpm) at the temperature of 25 ± 1°C. The illumination settings were ~40 µmol photons m^{-2} s^{-1} for *S. quadricauda* and ~60 µmol photons m^{-2} s^{-1} for *C. augustae* with 12:12h light: dark cycle.

Table 3.2: Composition of Bold's Basal Medium (BBM)

Stock	Chemical	per 400 mL	per L
1	$NaNO_3$ (Friendemann Schmidt, USA)	10.0 g	
2	$MgSO_4 \cdot 7H_2O$ (Friendemann Schmidt, USA)	3.0 g	
3	NaCl (Friendemann Schmidt, USA)	1.0 g	
4	K_2HPO_4 (Friendemann Schmidt, USA)	4.0 g	
5	KH_2PO_4 (Friendemann Schmidt, USA)	6.0 g	
6	$CaCl_2$ (Friendemann Schmidt, USA)	1.0 g	
7	**Trace elements solutions**		
	$ZnSO_4 \cdot 7H_2O$ (Friendemann Schmidt, USA)		8.82 g
	$MnCl_2$ (Acros Organics, USA)		1.44 g
	MoO_3 (Acros Organics, USA)		0.71 g

Table 3.2, continued

Stocks	Stocks	per 400 mL	per L
	$CuSO_4 \cdot 5H_2O$ (Friendemann Schmidt, USA)		1.57 g
	$Co(NO_3)_2 \cdot 6H_2O$ (Friendemann Schmidt, USA)		0.49 g
8	H_3BO_3 (Friendemann Schmidt, USA)		11.4 g
9	EDTA·Na_2 (Friendemann Schmidt, USA)		50.0 g
	KOH (Friendemann Schmidt, USA)		31.0 g
10	$FeSO_4 \cdot 7H_2O$ (Friendemann Schmidt, USA)		4.98 g
	Concentrated H_2SO_4 (Merck, USA)		1.0 mL

* To prepare 1.0 L BBM, 10.0 mL was added from each stock solution numbered 1-6 and 1.0 mL was added from each stock solution numbered 7 – 10. The pH was adjusted to 6.80.

3.2 Preparation of growth media supplemented with excess Cu and Ni

The Cu stock solution (100 mM) was prepared from copper (II) sulfate pentahydrate ($CuSO_4 \cdot 5H_2O$, Friendemann Schmidt, USA) and added to BBM at various concentrations (300, 600, 1000 µM for *S. quadricauda*; and 50, 150, 250 µM for *C. augustae*). The Ni stock solution (7.72 mM or 1 g L^{-1}) was prepared from nickel chloride hexahydrate ($NiCl_2 \cdot 6H_2O$, Sigma, USA) and added to BBM at various concentrations (0.42, 4.21, 42.07 µM). The media supplemented with metal solutions were left to equilibrate for 24 h at room temperature (RT) prior to algal inoculation. All glasswares were soaked with 10% nitric acid (HNO_3, Merck, USA) overnight, washed thrice with distilled water, autoclaved and dried before use.

Free metal ions in their soluble and divalent forms are known to be the main toxic species to phytoplankton (Sunda, 1975). The initial Cu^{2+} and Ni^{2+} concentrations and activities at control and sub-optimal temperatures were calculated using the Visual MINTEQ 3.1 chemical equilibrium calculation software. For the ease of presentation, all Cu and Ni concentrations were expressed as the nominal concentrations of $CuSO_4 \cdot 5H_2O$ or $NiCl_2 \cdot 6H_2O$ added into BBM.

3.3 Factorial experimental design

Cultures in the exponential growth phase were cultivated in 500 mL Erlenmeyer flasks with 300 mL BBM. The growth curves for both species are shown in Appendix A. The initial cell density for the experiments was approximately 4 x 10^4 cells mL^{-1} for *S. quadricauda* and 1 x 10^5 cells mL^{-1} for *C. augustae*. Cell densities of all samples were determined using an improved Neubauer haemocytometer. The experiments for *S. quadricauda* were carried out in triplicates. Four replicates were used in the experiments for *C. augustae.* Cultures in BBM without extra supplemented Cu or Ni cultivated at 25°C were used as controls. The control temperature was 25°C for both strains. For *S. quadricauda*, the sub-optimal temperature used in this study was 35°C according to a previous study by Zargar et al. (2006) which showed that the species could tolerate temperature up to 36°C. For *C. augustae*, the sub-optimal temperature used in this study was 30°C according to a previous study by Teoh et al. (2013) which showed that the specific growth rate of this strain declined sharply at temperatures beyond 30°C. For the ease of presentation, each sample was named with a corresponding abbreviation as shown in Table 3.2.

The experimental design and integrative approach are explained as follows:

Treatment time: In Experiment 1, the cultures of *S. quadricauda* were exposed to control and sub-optimal temperatures for 3 and 6 days to investigate the time-dependent effects of warming and Cu toxicity. In Experiment 2, 3 and 4, the cultures were exposed to control and sub-optimal conditions for 24 h. Copper toxicity tests on microalgae are typically acute and short-term (Leal et al., 2016).

Integrative study: The methodology used for Experiment 1 differed from Experiment 2, 3 and 4. Metal content in biomass was not quantified in Experiment 1. In addition to that, the metabolomics study in Experiment 1 only utilized gas chromatography-mass

spectrometry (GCMS) whereas the metabolomics studies in Experiment 2, 3 and 4 utilized both GCMS and LCMS (liquid chromatography-mass spectrometry) for metabolic profiling. The machines were unavailable and dysfunctional during the period when Experiment 1 was carried out. Nevertheless, all four experiments provided valuable insights in answering the research questions in this study.

Table 3.2: Exposure of *S. quadricauda* and *C. augustae* to different concentrations of Cu and Ni solutions

Experiment	Species	Metal	Concentration (µM)	Abbreviations
1: Interactive effects of warming and Cu toxicity on *S. quadricauda*	*S. quadricauda*, UMACC 041	Cu	Control 300 600 1000	*Scene*-0Cu *Scene*-3000Cu *Scene*-6000Cu *Scene*-1000Cu
2: Interactive effects of warming and Cu toxicity on *C. augustae*	*C. augustae*, UMACC 246	Cu	Control 50 150 250	*Chlamy*-0Cu *Chlamy*-50Cu *Chlamy*-150Cu *Chlamy*-250Cu
3: Interactive effects of warming and Ni toxicity on *S. quadricauda*	*S. quadricauda*, UMACC 041	Ni	Control 0.42 4.21 42.07	*Scene*-0Ni *Scene*-0.42Ni *Scene*-4.21Ni *Scene*-42Ni
4: Interactive effects of warming and Ni toxicity on *C. augustae*	*C. augustae*, UMACC 246	Ni	Control 0.42 4.21 42.07	*Chlamy*-0Ni *Chlamy*-0.42Ni *Chlamy*-4.21Ni *Chlamy*-42Ni

3.4 Measurement of photosynthetic performance

To measure the photosynthetic properties of the microalgae in response to warming and metal toxicity, non-invasive Chl-*a* parameters were measured by a Water-Pulse-Amplitude-Modulated (PAM) fluorometer (Walz GmbH, Germany) (Barati et al., 2018). Briefly, the cultures were dark-adapted for 15 mins before the generation of rapid light curves (RLCs). The actinic light levels used were 0, 48, 105, 158, 233, 358, 530, 812 and 1216 µmol photons m^{-2} s^{-1}, each for a duration of 10 s. Maximum quantum yield of PSII (F_v/F_m) was obtained directly from the software (WinControl, Walz, Germany). Other photosynthetic parameters such as photosynthetic efficiency (α), maximum rate of relative electron transport ($rETR_{max}$), saturation irradiance for electron transport (E_k), non-photochemical quenching (NPQ), photochemical quenching coefficient (qP), and non-photochemical quenching coefficient (qN) were calculated using Microsoft Excel 2016 and SPSS software version 22 (IBM, USA) according to Lee et al. (2017) and Walz (2000). The *in vivo* absorption spectra in Experiment 1 were detected within the range of 400 – 700 nm using a microplate spectrophotometer (Thermo MultiSkan, USA).

3.5 Analysis of ROS level

A cell-permeable fluorescent probe, 2',7'-dichlorofluorescein diacetate (DCFH-DA, Sigma, USA) was used to determine ROS levels in the samples. The stock solution of DCFH-DA was prepared in dimethyl sulfoxide (DMSO) at a concentration of 10 mM and stored at -80°C. At the end of the experimental period, algal cells were mixed with fluorescent dye to a final concentration of 50 µM and incubated in a dry bath at 37°C for 10 mins in the dark. For Experiment 1 & 2, the fluorescence intensity of the DCF compound was measured at an excitation wavelength of 488 nm and emission wavelength of 525 nm using a microplate reader (Thermo MultiSkan, USA). For Experiment 3 & 4, the fluorescence intensity of the DCF compound was measured using a CytoFLEX Flow

Cytometer (Beckman Coulter, USA). The data were expressed as the mean fluorescence intensity at the FITC-A channel.

3.6 Metal content in biomass

Metal content in the biomass was analysed by the Agilent 4100 microwave plasma – atomic emission spectroscopy (MP-AES, USA). Fifty millilitres of each sample were collected on the GF/C filter papers followed by acid digestion. Four millilitres of HNO_3 and 0.5 mL H_2O_2 (Merck, USA) were added to each harvested biomass and incubated for 24 h. Each sample was diluted 20 or 50 times with Milli-Q water prior to analysis by MP-AES. The standard curves were generated with Cu (0 - 5.0 ppm) and Ni (0 – 1.0 ppm) standard solutions (Agilent Technologies, USA) (Appendix D). Data were expressed as the metal content of the biomass in the unit of picogram per cell (pg $cell^{-1}$).

3.7 Statistical analysis

The significant differences between control and treated samples were calculated by one-way analysis of variance (ANOVA) and two-way ANOVA with Tukey post-hoc test using SPSS software version 22 (IBM, USA). Pearson correlations between factors and responses were also performed with the SPSS software. Data for cell density, ROS levels and metal content were expressed as mean ± standard deviation (SD).

3.8 Metabolic profiling

3.8.1 Metabolic profiling for Experiment 1

3.8.1.1 Sample pre-treatment

At the end of the experiment, 150 mL of each sample were centrifuged at 2000 x g for 10 mins to collect the cell pellet, immediately flash-frozen with liquid nitrogen, and stored at -20°C prior to extraction. A mixture of methanol:chloroform:H_2O (10:3:1, v/v) containing 25 µg mL^{-1} FMOC-glycine (Sigma, USA) as an internal standard was used to extract metabolites. The samples were sonicated for 10 mins in ice water bath. After

centrifugation, the samples were dried in a vacuum concentrator, followed by derivatization with 20 µL of methoxyamine hydrochloride in pyridine (20 µg mL^{-1}) (Sigma, USA) for 90 mins at 37°C and 100 µL N-Methyl-N-(trimethylsilyl) trifluoroacetamide (MSTFA, Sigma, USA) for 30 mins at 37°C (Fiehn et al., 2000).

3.8.1.2 Instrument analysis

Samples were immediately injected into the Agilent 7890A gas chromatography with 5975C mass spectrometry detector (GCMS, USA) for metabolite analysis. The separation was performed on a CP-Sil 8 CB column (30 m x 250 µm x 0.25 µm, Agilent, USA). Helium was used as carrier gas and the flow rate was 1 mL min^{-1}. The injection volume was 1 µL in splitless mode. Injection and transfer line temperatures were 250 and 280°C respectively. The scan range for MS was set as 35-600 m/z. The oven temperature was held at 70°C for 1 min, then increased to 300°C at 10°C min^{-1} and held for 5 mins. Total run time was 29 mins.

3.8.1.3 Data processing, statistical and pathway analyses

For data processing, Agilent raw data (.d) files were first converted to .mzXML cross-platform open file format using the freely-available MSConvert tool in Proteowizard software (http://proteowizard.sourceforge.net/). The .mzXML files were uploaded to XCMS Online (http://xcmsonline.scripps.edu) for feature detection and retention time (RT) alignment (Gowda et al., 2014). Principal component analysis (PCA) and orthogonal partial least squares-discriminant analysis (OPLS-DA) models were performed with MetaboAnalyst (http://www.metaboanalyst.ca/) to explore the difference between different treatment groups. For the multilevel datasets, Analysis of Variance - Simultaneous Component Analysis (ASCA) was performed with MetaboAnalyst to split the original datasets into different subsets describing the variation between temperatures, concentrations and their interactions (Xia et al., 2015). The dataset was first normalized

by cell density, log transformation and Pareto Scaling (Dai et al., 2016). Manly's unrestricted permutation test was applied to test the significance of the effects associated with factors. The permuted values were compared with the original variations and the significant features (metabolites) were identified based on the leverage (its relative contribution) and the squared prediction errors (SPE) associated with each partition. Significant features were selected by Leverage/SPE analysis and annotated by searching against the National Institute of Standards and Technology (NIST) 11 library.

3.8.2 Metabolic profiling for Experiment 2, 3 and 4

3.8.2.1 Sample pre-treatment

To further understand the effects of warming and metal toxicity on microalgae, two metabolomics platforms, gas chromatography-mass spectrometry (GCMS) and liquid chromatography-mass spectrometry (LCMS) were employed to include compounds with different molecular weight, polarity, and volatility. The sample preparation method was modified from Zhang et al. (2017). Briefly, cell pellets collected from 150 mL of each sample were flash-frozen with liquid nitrogen and stored at -20°C prior to extraction. The mixture of methanol: H_2O (4:1, v/v) containing 25 µg mL^{-1} FMOC-glycine as an internal standard was used to extract metabolites. The samples were sonicated for 10 mins in ice water bath to enhance the extraction efficiency. After sonication, the samples were centrifuged for 10 mins at 13,000 x*g* at 4°C. The supernatant was collected and split into two fractions: one for GCMS analysis and one for LCMS analysis. The fractions for GCMS were dried in a vacuum concentrator (Thermo, USA), followed by derivatization according to Fiehn et al. (2000). Each sample was first derivatised with 100 µL of methoxyamine hydrochloride in pyridine (5 mg mL^{-1}) (Sigma, USA) for 90 mins at 37°C, followed by 100 µL N-Methyl-N-(trimethylsilyl) trifluoroacetamide (MSTFA, Sigma, USA) for 30 mins at 37°C. The fractions for LCMS analysis were used without any further treatment.

3.8.2.2 Instrument analysis

Agilent 7890A gas chromatography with 5975C mass spectrometry detector (Agilent, USA) was used for GCMS analysis. A BPX-5 column (30 m x 0.25 mm x 0.25 µm, SGE, Australia) or CP-Sil 8 CB column (30 m x 0.25 mm x 0.25 µm, Agilent, USA) was used in this study. The carrier gas was helium at a flow rate of 1 mL min^{-1}. Five microlitres of each sample was injected in splitless mode. The injector, ion source and transfer line temperatures were set at 250, 230 and 280°C respectively. The oven temperature was held at 90°C for 1 min, increased to 130°C at 20°C min^{-1}, increased to 280°C at 6°C min^{-1}, then increased to 300°C at 25°C min^{-1} and held for 6 mins. The scan range for MS was set as 50-800 m/z.

Agilent Infinity 1290 binary ultrahigh performance liquid chromatography (UHPLC) system coupled to a 6550-electrospray ionisation quadrupole time-of-flight mass spectrometer (LC-ESI-QTOF, Agilent, USA) was used for LCMS analysis. The acquisition parameters were as follows: fragmentor voltage, 175V; sheath gas temperature, 350°C; sheath gas flow, 11 L min^{-1}; nebulizer pressure, 40 psi; nozzle voltage, 1000 V; drying gas temperature, 200°C; drying gas flow, 12 L min^{-1}. The MS data was collected in centroid mode within the mass range of 40-1100 m/z. Five microliters of each sample were injected onto the column at a flow rate of 0.4 mL min^{-1}. The C18 column (Zorbax 2.1 x 100 mm, 1.8 µm, Agilent, USA) was held at 50 ºC. For positive mode, solvent A in mobile phase composed of 0.1% formic acid (Sigma, USA) in Milli-Q water and solvent B composed of 0.1% formic acid in acetonitrile (Merck, USA). For negative mode, solvent A composed of Milli-Q water with 5 mM ammonium acetate (Sigma, USA) and solvent B composed of acetonitrile and Milli-Q water (95:5, v/v) with 5 mM ammonium acetate. The gradient of mobile phase for both positive and negative modes was as follows: 5% B increased to 45% in 9 mins, to 100% in 6 mins and kept for 3 mins, decreased to 5% in 2 mins and kept for 5 mins.

3.8.2.3 Data processing, statistical and pathway analyses

Agilent raw data (.d) files were first converted to .mzXML file format using the MSConvert tool in the ProteoWizard software (https://proteowizard.sourceforge.net/). Following that, the .mzXML files were uploaded to MZmine 2 software (https://mzmine.github.io/) for feature detection, deconvolution, and alignment. The workflow and respective parameters for data processing with MZmine is shown in Table 3.3.

The aligned features were uploaded to MetaboAnalyst (https://www.metaboanalyst.ca/) and normalized by cell density, log transformation and Pareto Scaling. Analysis of Variance - Simultaneous Component Analysis (ASCA) was performed to describe the variation between temperatures, Ni concentrations and their interactions. Significant features ($p < 0.05$) were selected and annotated based on the mummichog algorithm in the 'MS Peaks to Pathways' module in MetaboAnalyst (Chong et al., 2018; Li et al., 2013). The algorithm was also connected to the KEGG global metabolic network to explore the pathways, compounds and matched peaks involved in the stress response. Following that, the 'Pathway Analysis' module in MetaboAnalyst was utilized to identify the most impactful pathways involved in the stress response (Xia et al., 2012). The metabolic pathways are represented as circles according to their scores from enrichment (vertical axis) and topology analyses (pathway impact, horizontal axis) using MetaboAnalyst 2.0. The colours indicate more significant changes of metabolites in the corresponding pathway. The size of the circle corresponds to the pathway impact score and is correlated with the centrality of the involved metabolites.

Table 3.3: Methods and parameters used for data processing with MZmine

Step	Parameter	Value
Mass detection	Mass detector	Centroid
	Noise level	1E3
Chromatogram builder	Min time span (min)	0.05
	Min height	1E3
	m/z tolerance	0.005 m/z or 10 ppm for LCMS 0.1 m/z or 10 ppm for GCMS
Chromatogram deconvolution	Algorithm	Local minimum search
	Chromatographic threshold	1.0 %
	Search minimum in RT range (min)	0.1
	Minimum absolute height	1E4
	Minimum relative height	1.0 %
	Min ratio of peak top/edge	1
	Peak duration range (min)	0.1-5
Isotope peak grouper	m/z tolerance	0.005 m/z or 10 ppm for LCMS 0.1 m/z or 10 ppm for GCMS
	RT tolerance	0.5 absolute min
	Maximum charge	3
	Representative isotope	Most intense
Join aligner	m/z tolerance	0.005 m/z or 10 ppm for LCMS 0.1 m/z or 10 ppm for GCMS
	Weight for m/z	10
	RT tolerance	1.5 absolute min
	Weight for RT	10
Gap-filling	Same RT and m/z range filling	0.005 m/z or 10 ppm for LCMS 0.1 m/z or 10 ppm for GCMS

3.9 Summary of research approach

Figure 3.1 summarizes the research approach used in this study. Two tropical chlorophytes, *S. quadricauda* (UMACC 041) and *C. augustae* (UMACC 246), were obtained from the University of Malaya Algae Culture Collection (UMACC). The cultures were exposed to two abiotic stresses: temperature or metal toxicity. In Experiment 1, *S. quadricauda* was exposed to 2 temperature conditions (control: 25°C; sub-optimal: 35°C), and Cu with the concentrations of 300, 600 and 1000 µM. In Experiment 2, *C. augustae* was exposed to 25 and 30°C, and Cu with the concentrations of 50, 150 and 250 µM. In Experiment 3, *S. quadricauda* was exposed to 25 and 35°C, and Ni with the concentrations of 0.42, 4.2 and 42 µM. In Experiment 4, *C. augustae* was exposed to 25 and 30°C, and Ni with the concentrations of 0.42, 4.2 and 42 µM. Cultures in BBM without extra supplemented Cu or Ni were used as controls. Following the exposure of the two microalgae to warming and metals, the physiological and biochemical responses of the microalgae were investigated by multiple assays. Growth was measured based on cell count using an improved Neubauer haemocytometer. Photosynthetic rate was determined using a Water-PAM fluorometer. The levels of ROS were measured using a cell-permeable fluorescent probe, DCFH-DA. To investigate the amount of metal uptake by the biomass, the cells were acid-digested and analysed by MP-AES. To understand the changes in metabolic profile, the cultures were subjected to chemical extraction, followed by analysis by GCMS or LCMS. The data were analysed using multivariate analysis, subsequently followed by metabolite annotation and pathway assignment.

Selected microalgae from the University of Malaya Algae Culture Collection

Scenedesmus quadricauda, UMACC 041

Chlamydomonas augustae, UMACC 246

↓

Exposure of microalgae to temperature and metal toxicity stress

		UMACC 041	UMACC 246
Temperature	Control (°C)	25	25
	Sub-optimal (°C)	35	30
Metal Toxicity	Copper (µM)	0, 300, 600, 1000	0, 50, 150, 250
	Nickel (µM)	0, 0.42, 4.21, 42.07	0, 0.42, 4.21, 42.07

↓

Integrative approach

Growth	**Photosynthetic rate**	**ROS level**
Cell count	Measurement of chlorophyll fluorescence determined using pulse amplitude modulated (PAM) fluorometry	ROS level determined using cell-permeable fluorescent probe, 2',7'-dichlorofluorescein diacetate (DCFH-DA)

Metal uptake by biomass

Harvest biomass by filtration

↓

Acid digestion

↓

Multi-element analysis by Agilent 4100 Microwave plasma-atomic emission spectrometry (MP-AES)

Metabolic profile

Metabolite extraction

↓

Analysis by GCMS and LCMS

↓

Data processing and multivariate analysis

↓

Metabolite annotation and pathway assignment

Figure 3.1: Flowchart of research approach used in this study

CHAPTER 4: RESULTS

4.1 Experiment 1: Interactive effects of warming and Cu toxicity on *S. quadricauda*

4.1.1 Free Cu^{2+} Concentration

Cu speciation was altered by temperature as shown in Table 4.1. The free Cu^{2+} concentration in the control media was 0.00263 µM at 25°C, and slightly higher at 35 ° C (0.00299 µM). At 300, 600 and 1000 µM, free Cu^{2+} concentration in the culture media was generally higher at 25°C compared to 35°C. The estimated chemical activities of the free Cu^{2+} (pCu = - log Cu^{2+} activity) at higher Cu concentrations were relatively higher at 35°C compared to 25°C.

Table 4.1: Free cupric ion (Cu^{2+}) concentration and the logarithm of Cu^{2+} activity at 25 and 35°C

Nominal [Cu] (µM)	**Nominal [Cu] (ppm)**	**Temperature (°C)**			
		25		**35**	
		[Cu^{2+}] (µM)	**Log Cu^{2+} activity**	**[Cu^{2+}] (µM)**	**Log Cu^{2+} activity**
Control	Control	0.00263	-8.846	0.00299	-8.795
300	75	112.17	-4.220	94.060	-4.301
600	150	262.48	-3.854	205.69	-3.964
1000	250	440.15	-3.634	323.07	-3.773

4.1.2 Cell density

Table 4.2 shows the Pearson correlation coefficients between factors and responses. Cell density was positively correlated with treatment period. The F_v/F_m values were negatively correlated with temperature, Cu concentration, and free Cu^{2+} concentration. Both NPQ and qN were negatively correlated with temperature, whereas $rETR_m$ and E_k were negatively correlated with treatment period. qP was negatively correlated with treatment period yet positively correlated with free Cu^{2+} concentration. ROS was negatively correlated with treatment period and positively correlated with Cu concentration, free Cu^{2+}, and Cu^{2+} activity.

Table 4.2: Pearson correlation coefficients between various factors (day, temperature, Cu concentration, free Cu ions and activity) and responses

Response	**Factor**				
	Day	**Temperature**	**Cu**	**[Cu^{2+}]**	**Log Cu^{2+} activity**
Cell density	0.857**	0.103	0.046	0.043	0.054
F_v/F_m	-0.188	-0.331*	-0.428**	-0.366*	-0.253
NPQ	0.039	-0.375**	-0.110	-0.086	-0.099
qP	-0.523**	-0.258	0.261	0.305*	0.216
qN	-0.069	-0.404**	0.098	0.128	0.070
Alpha (α)	0.172	0.239	-0.119	-0.130	0.088
$rETR_m$	-0.436**	0.003	-0.238	-0.252	-0.072
E_k	-0.446**	-0.051	-0.197	-0.208	-0.086
ROS	-0.497**	-0.015	0.434**	0.451**	0.321*

* $p<0.05$, ** $p<0.01$

The effect of temperature and Cu concentration on the cell density of *S. quadricauda* are shown in Figure 4.1. On day 3 and 25°C, cell density of *Scene*-1000Cu was lower

than *Scene*-0Cu (1.61 x 10^5 cells mL^{-1}). Overall, cell densities at 35°C were higher than those of 25°C and remained similar across all Cu concentrations at day 3.

The cell density of the cultures increased 2-3 folds on day 6 compared to day 3. At 25°C, the cell density was the highest in *Scene*-600Cu (6.57 x 10^5 cells mL^{-1}) compared to the control (4.15 x 10^5 cells mL^{-1}). At 35°C, cell densities were lower at 300 and 600 µM Cu, but higher at 1000 µM Cu compared to the control. Statistical analysis showed that the effect of temperature on the cell density was significant on day 3 ($p < 0.05$), whereas high Cu concentrations and the combined factors did not affect cell density significantly ($p > 0.05$) (Table 4.3 and 4.4).

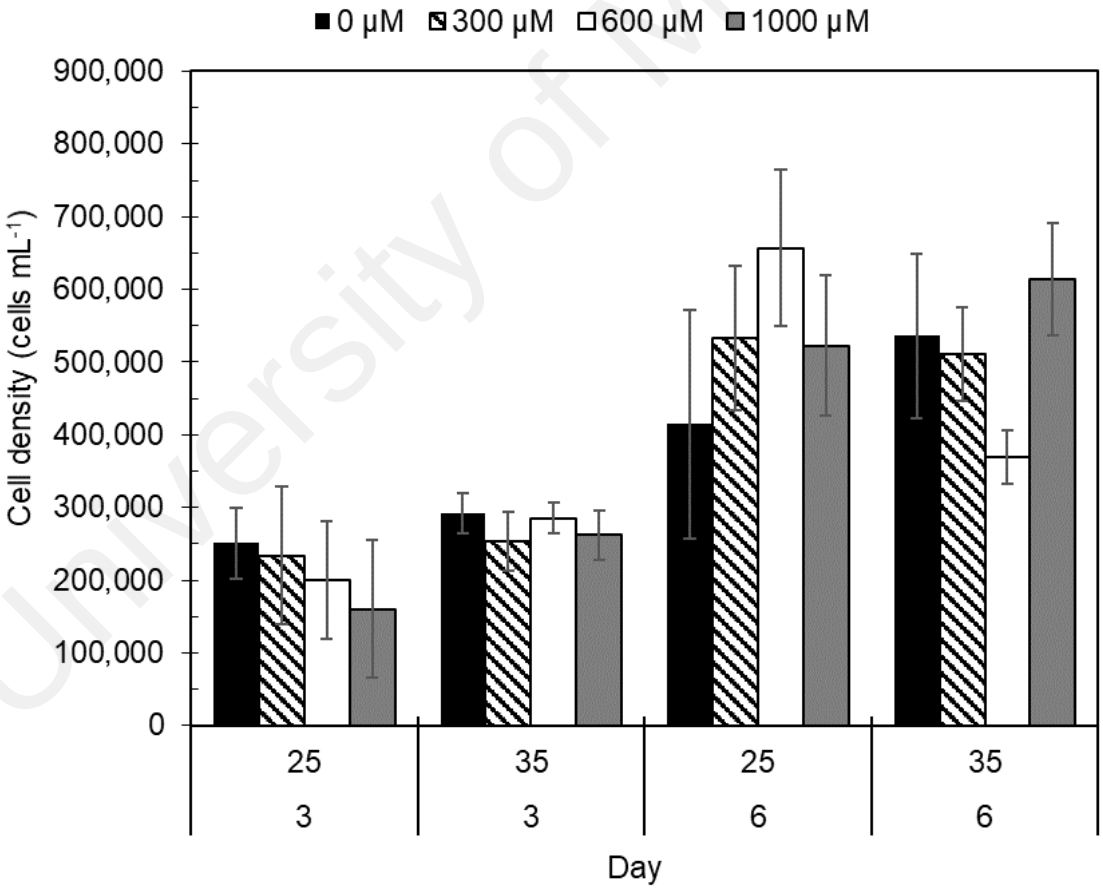

Figure 4.1: Cell density of *S. quadricauda* in response to warming and high Cu concentrations on day 3 and 6. Data are presented as mean ± standard deviation.

Table 4.3: Summary of two-way ANOVA testing the combined effect of Cu concentrations and temperature (25 and 35°C) on the physiological and photosynthetic parameters of *S. quadricauda* after 3 days of exposure

Parameter	Source of variation	SS	*df*	F	Sig.
Cell density	Temperature	2.29×10^{10}	1	5.961	0.027
	Cu	1.09×10^{10}	3	0.948	0.441
	Temperature * Cu	6.47×10^{9}	3	0.56	0.649
	Error	6.16×10^{10}	16		
F_v/F_m	Temperature	0.007	1	4.415	0.052
	Cu	0.090	3	19.888	0.000
	Temperature * Cu	0.055	3	12.119	0.000
	Error	0.024	16		
NPQ	Temperature	5.226×10^{-5}	1	0.002	0.965
	Cu	0.016	3	0.213	0.886
	Temperature * Cu	0.096	3	1.246	0.328
	Error	0.387	15		
qP	Temperature	0.018	1	5.393	0.035
	Cu	0.019	3	1.879	0.177
	Temperature * Cu	0.019	3	1.862	0.179
	Error	0.051	15		
qN	Temperature	0.001	1	0.298	0.593
	Cu	0.016	3	1.330	0.302
	Temperature * Cu	0.020	3	1.683	0.213
	Error	0.060	15		
Alpha (α)	Temperature	0.000	1	2.586	0.127
	Cu	0.000	3	1.651	0.217
	Temperature * Cu	0.000	3	0.603	0.622
	Error	0.001	16		
$rETR_m$	Temperature	1.08×10^{3}	1	5.564	0.031
	Cu	4.78×10^{3}	3	8.233	0.002
	Temperature * Cu	2.00×10^{3}	3	3.445	0.042
	Error	3.09×10^{3}	16		
E_k	Temperature	2.26×10^{4}	1	7.285	0.016
	Cu	5.50×10^{4}	3	5.898	0.007
	Temperature * Cu	3.42×10^{4}	3	3.665	0.035
	Error	4.97×10^{4}	16		
ROS	Temperature	0.415	1	1.026	0.321
	Cu	495.602	3	407.831	0.000
	Temperature * Cu	320.419	3	263.673	0.000
	Error	9.722	24		

SS = sum of squares; *df* = degree of freedom

Table 4.4: Summary of two-way ANOVA testing the combined effect of Cu concentrations and temperature (25 and 35°C) on the physiological and photosynthetic parameters of *S. quadricauda* after 6 days of exposure

Parameter	Source of variation	SS	*df*	F	Sig.
Cell density	Temperature	4.86×10^{8}	1	0.049	0.828
	Cu	4.09×10^{10}	3	1.365	0.289
	Temperature * Cu	7.07×10^{10}	3	2.363	0.11
	Error	1.60×10^{11}	16		
F_v/F_m	Temperature	0.002	1	1.478	0.242
	Cu	0.001	3	0.300	0.825
	Temperature * Cu	0.005	3	1.051	0.397
	Error	0.024	16		
NPQ	Temperature	0.335	1	30.552	0.000
	Cu	0.129	3	3.928	0.030
	Temperature * Cu	0.085	3	2.594	0.091
	Error	0.164	15		
qP	Temperature	0.000	1	0.497	0.492
	Cu	0.002	3	0.906	0.461
	Temperature * Cu	0.007	3	3.300	0.049
	Error	0.010	15		
qN	Temperature	0.039	1	34.424	0.000
	Cu	0.008	3	2.409	0.108
	Temperature * Cu	0.005	3	1.520	0.250
	Error	0.017	15		
Alpha (α)	Temperature	6.017×10^{-5}	1	0.594	0.452
	Cu	0.000	3	0.769	0.528
	Temperature * Cu	0.000	3	0.731	0.548
	Error	0.002	16		
$rETR_m$	Temperature	1.11×10^{3}	1	17.365	0.001
	Cu	1.96×10^{2}	3	1.019	0.410
	Temperature * Cu	4.65×10^{2}	3	2.419	0.104
	Error	1.03×10^{3}	16		
E_k	Temperature	1.27×10^{4}	1	6.870	0.019
	Cu	3.68×10^{3}	3	0.665	0.586
	Temperature * Cu	1.11×10^{4}	3	2.002	0.154
	Error	2.95×10^{4}	16		
ROS	Temperature	1.156	1	501.863	0.000
	Cu	2.548	3	368.774	0.000
	Temperature * Cu	1.386	3	200.652	0.000
	Error	0.055	24		

SS = sum of squares; *df* = degree of freedom

4.1.3 *In vivo* absorption spectra

The *in vivo* absorption spectra (normalized to 680 nm) of *S. quadricauda* cultured under different temperatures and Cu concentrations are shown in Figure 4.2. On day 3, addition of Cu caused a reduction in amplitude of the absorbance value in the blue region of the chlorophyll peaks both at 25 and 35°C. Changes in the amplitude between 500-650 nm were observed across different Cu concentrations, temperatures and on both treatment periods.

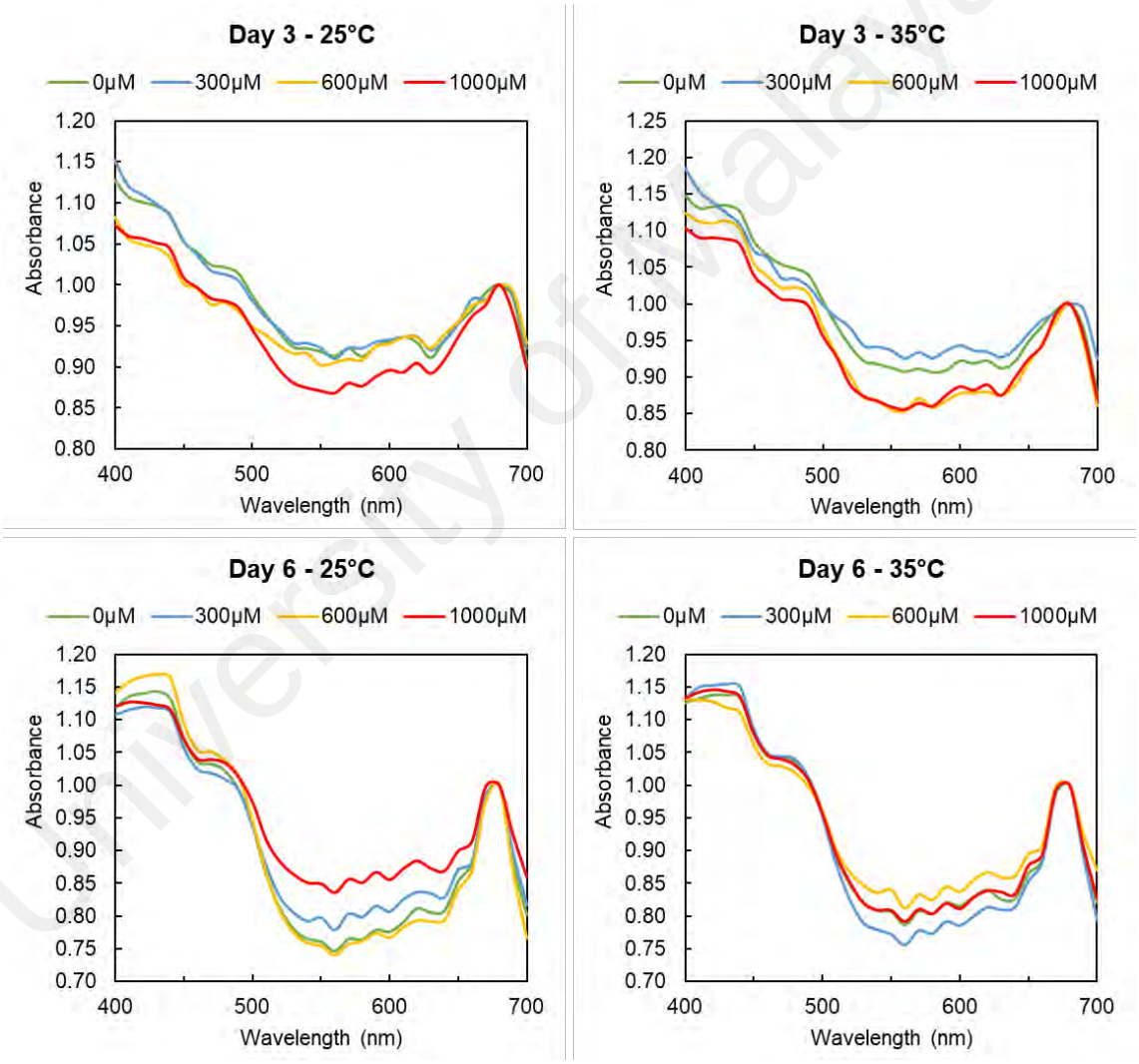

Figure 4.2: *In vivo* absorption spectra of *S. quadricauda* at different Cu concentrations, temperatures and treatment period. The spectra were normalized to the absorbance value at 680 nm, corresponding to the absorbance peak of Chl-*a*.

4.1.4 Photosynthetic performance

On day 3, the maximum quantum yield of PSII (F_v/F_m) decreased 30% from 0.807 at the control to 0.56 at *Scene*-1000Cu at 25°C (Figure 4.3A). High Cu concentrations and the combined factors significantly affected F_v/F_m ($p < 0.01$), whereas no significant change in F_v/F_m was induced by the higher temperature. On day 6, *S. quadricauda* was able to maintain a relatively stable F_v/F_m across different Cu concentrations.

In terms of the light harvesting efficiency (α) and relative maximum electron transport rate ($rETR_{max}$), no significant change was observed across different temperatures and Cu concentrations (data not shown). The saturation irradiance for electron transport, E_k, was observed to decline on day 3 at both temperatures with increasing Cu concentrations (Figure 4.3B). E_k values were higher at 25°C than those at 35°C, except for *Scene*-1000Cu. On day 6, the values decreased at 35°C but increased at 25°C. Temperature, high Cu concentrations, and the combined factors significantly affected E_k on day 3 ($p < 0.05$) (Table 4.3), in contrast to day 6 in which only the effect of temperature was significant ($p < 0.05$) (Table 4.4).

On day 3, NPQ increased from 0.856 to 0.926 with increasing Cu concentrations at 25°C (Table 4.5). The values were generally higher than those at 35°C, which were 0.783 to 0.971 for *Scene*-300Cu and 0.836 for *Scene*-1000Cu. On day 6, NPQ values decreased with increasing Cu concentrations. The values were lower at 35°C compared to 25°C. Temperature and Cu, as independent factors, affected NPQ significantly ($p < 0.05$), but the effect of combined factors was not significant ($p > 0.05$) (Table 4.4). The qN values were significantly lower at 35°C compared to 25°C on day 6 (Table 4.5). The qP values ranged between 0.3-0.4 across all treated temperatures, Cu concentrations and period, except that the values increased to 0.520 for *Scene*-1000Cu and 25°C on day 3 and decreased to 0.287 for *Scene*-1000Cu on day 6 (Table 4.5).

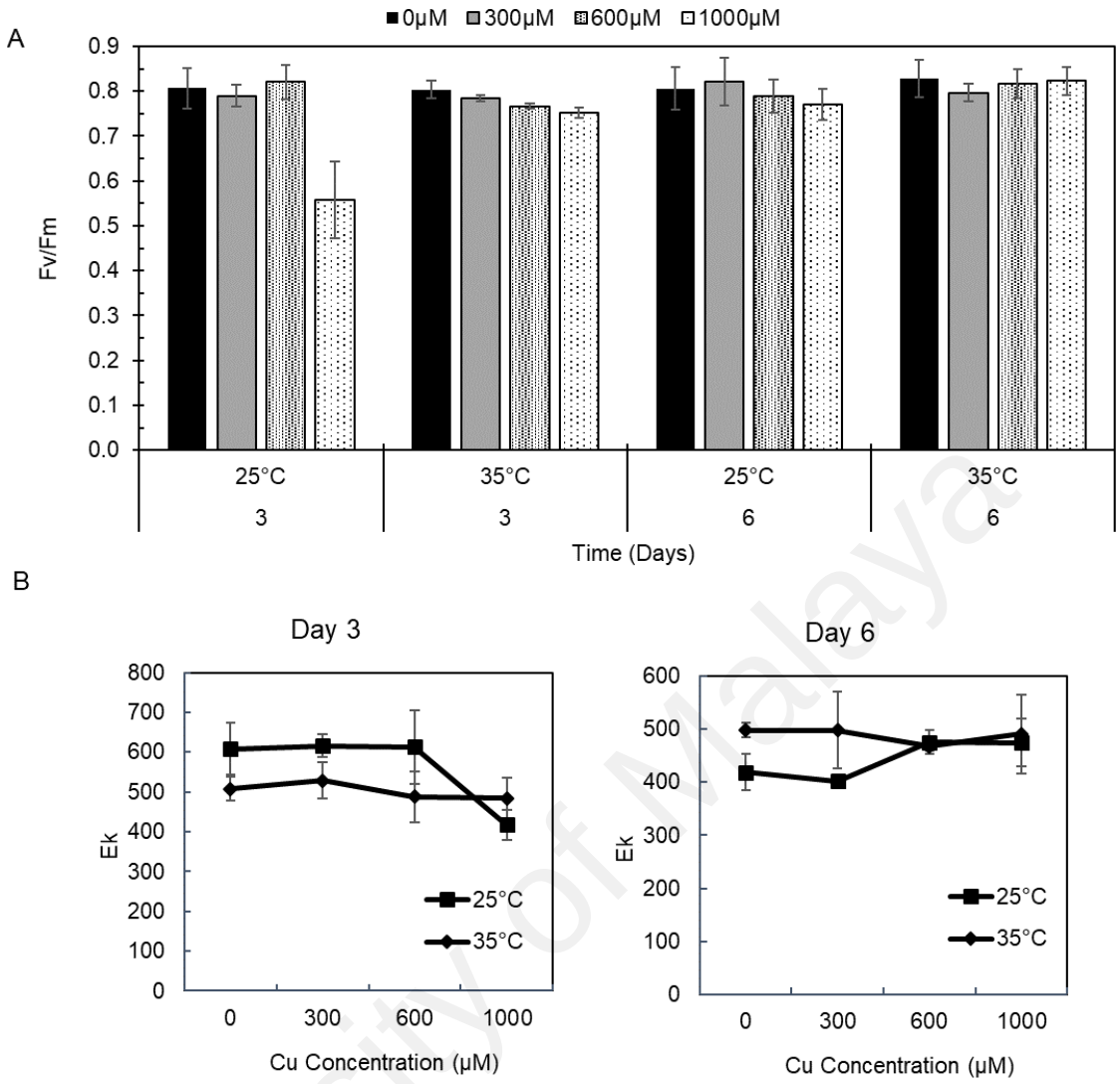

Figure 4.3: Interaction of Cu concentrations (control, 300, 600 and 1000 μM) and temperatures (25 and 35°C) on the (A) maximum quantum yield (F_v/F_m) of photosystem II and (B) saturation irradiance for electron transport (E_k) of *S. quadricauda*. Data are presented as mean ± standard deviation.

Table 4.5: Effects of temperature and high Cu concentrations on the quenching coefficients (qP, qN, and NPQ) of *S. quadricauda*

Nominal Cu Concentration (µM)	Day 3						Day 6					
	qP		qN		NPQ		qP		qN		NPQ	
	25°C	35°C	25°C	35°C	25°C	35°C	25°C	35°C	25°C	35°C	25°C	35°C
Control	0.388	0.347	0.538	0.491	0.856	0.783	0.313	0.329	0.625	0.495	1.178	0.761
300	0.404	0.385	0.508	0.578	0.753	0.971	0.287	0.351	0.578	0.505	1.019	0.751
600	0.389	0.375	0.547	0.550	0.923	0.855	0.353	0.329	0.550	0.468	0.877	0.674
1000	0.520	0.366	0.630	0.544	0.926	0.836	0.347	0.322	0.550	0.502	0.860	0.774

4.1.5 ROS levels

The exposure of algal cells to Cu induced an increase in the intracellular ROS levels (Figure 4.4). On day 3, the difference between control and higher Cu treatment was significant ($p < 0.01$) in *Scene*-1000Cu, which was 14-folds higher than the control. At 35°C for day 3, ROS levels in *Scene*-600Cu and *Scene*-1000Cu were significantly ($p < 0.01$) increased for 13-folds and 6-folds respectively. ROS levels at day 6 was significantly higher at high Cu concentration ($p < 0.01$) in *Scene*-600Cu for both 25 and 35°C, but lowest in *Scene*-1000Cu at 35°C. The combined factors significantly affected ROS fold-change on day 3 and 6 ($p < 0.01$) (Table 4.3 and 4.4).

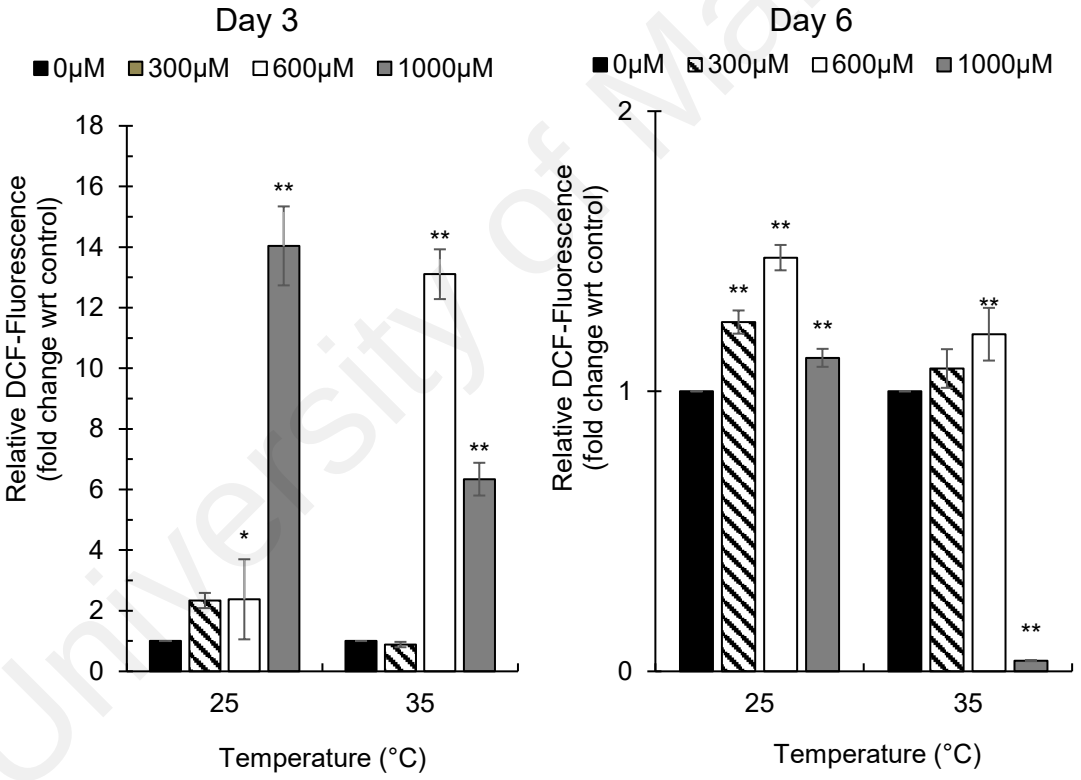

Figure 4.4: ROS levels measured by DCFH-DA and expressed as fold change of DCF fluorescence units with respect to control. Data are presented as mean ± standard deviation of the mean.

4.1.6 Metabolic profile

Principal component analysis (PCA) and orthogonal partial least squares-discriminant analysis (OPLS-DA) models were used to explore the difference between 25 and 35°C (Figure 4.5). Based on the PCA score plots, the greatest variance in the dataset was within-group variability (PC1, 85.5 % and 72.4% on day 3 and 6 respectively). Metabolome of high Cu concentrations contributed to the variation within each temperature groups, as observed in 1000 µM Cu at 25°C on day 3 and 600 µM Cu at 35°C on day 6. No clear separation was observed between the two temperatures on day 6 [(Day 3 - Predictive component: R^2X = 0.0792, R^2Y = 0.233, Q^2 = -0.651; Orthogonal component 1: R^2X = 0.754, R^2Y = 0.458, Q^2=1.05) (Day 6 - Predictive component: R^2X = 0.0575, R^2Y = 0.539, Q^2 = -1.05; Orthogonal component 1: R^2X = 0.654, R^2Y = 0.317, Q^2=0.724)].

ASCA was conducted to understand metabolic variations derived from different temperatures, Cu concentrations and their interaction. The model validation was confirmed by permutation test. Based on the statistical values, Cu concentration on day 3 was the only factor which contributed to significant differentiation among the samples (Day 3: p = 0.95, p < 0.05 and p = 0.05; Day 6: p = 0.55, p = 0.05 and p = 0.9 for temperature, Cu concentrations and interaction respectively). Major trends associated with each factor and their interactions are shown in Figure 4.6. Temperature accounted for 100% variation on day 3 and day 6. Cu concentrations accounted for 86.78% and 85.66% on day 3 and 6 respectively. Interaction between the two factors resulted in 88.52% of variation on day 3 and 40.8% on day 6.

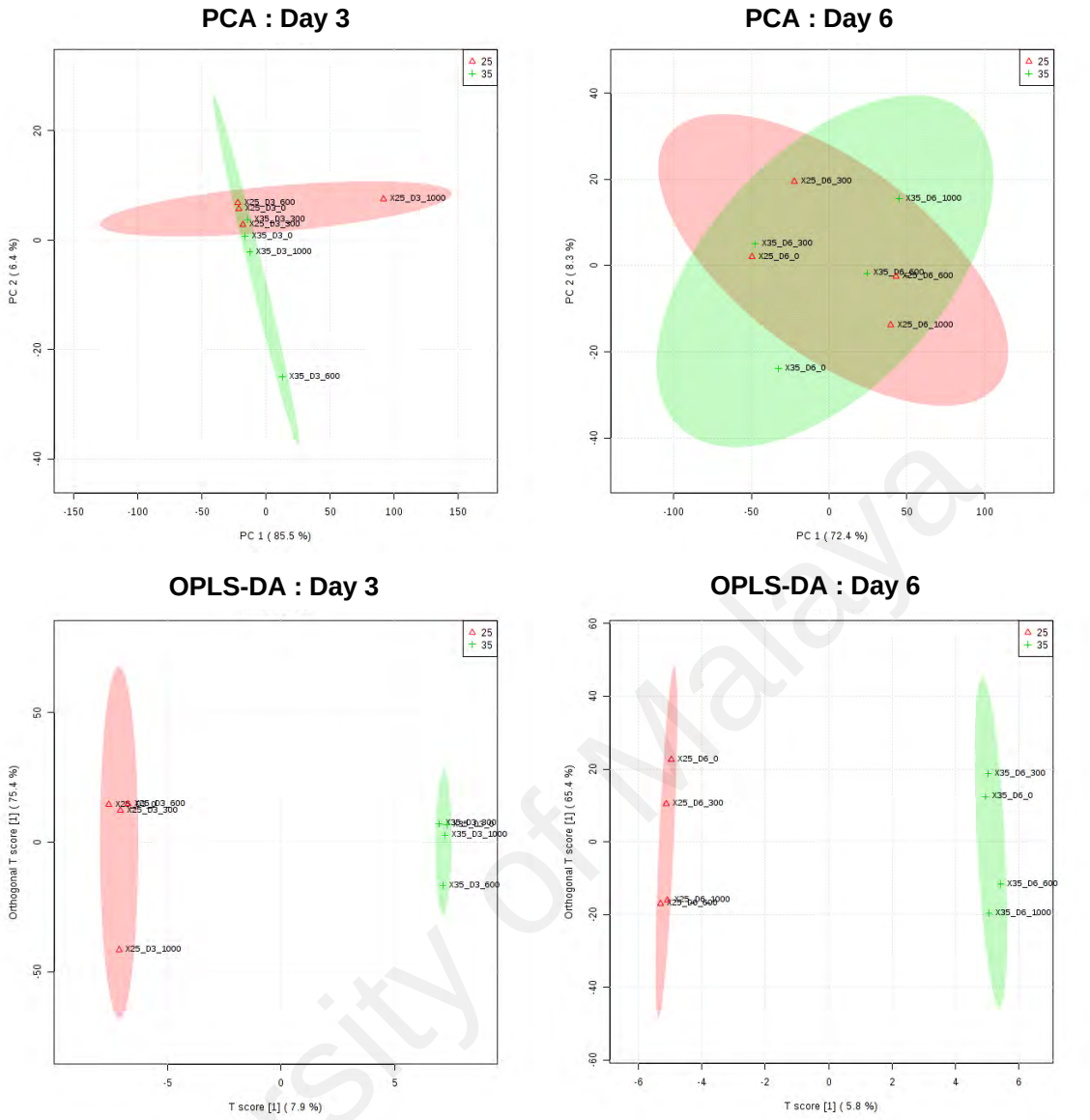

Figure 4.5: PCA and OPLS-DA score plots for 25 and 35°C treatment groups on day 3 and 6.

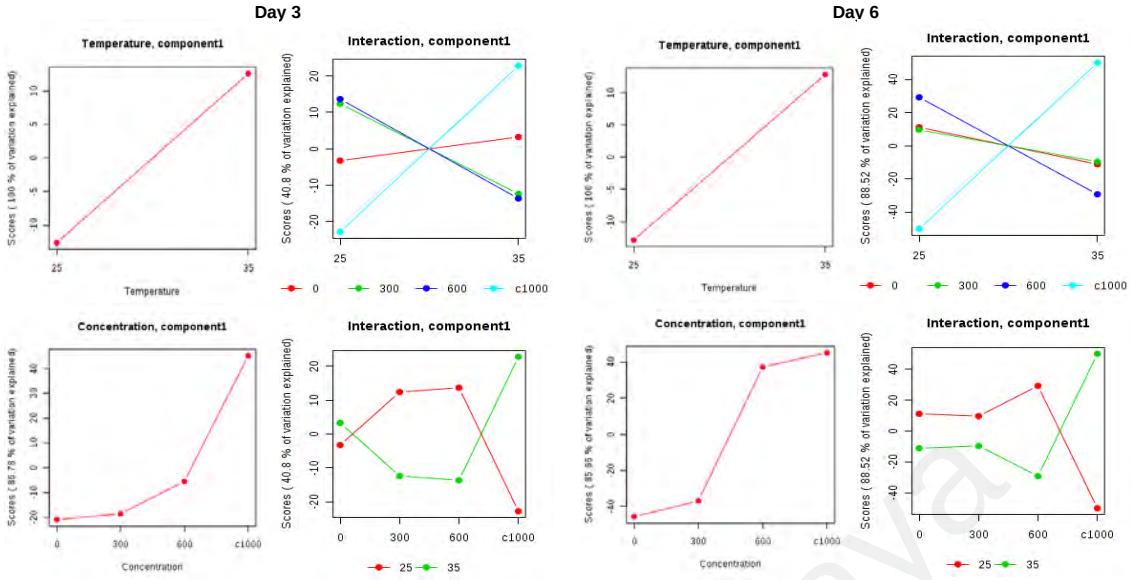

Figure 4.6: ASCA score plots for temperature, Cu concentrations and the interactions between the two factors based on components 1 and 2 of the corresponding sub models.

Significant features were selected based on leverage and SPE values (Table 4.6). Metabolites which were significant factors contributing to the interaction were mainly fatty acids such as hexadecanoic acid, propanoic acid, octadecanoic acid and oleic acid. Amino acids such as aminomalonic acid, proline and glycine were significantly down-regulated by the interactive factors (Figure 4.7). Likewise, significant perturbations caused by temperature factor also involved fatty acids and amino acids in the response. As seen in Figure 4.8A, hexadecanoic acid, glycine, myristic acid and propionic acid, tetradecanoic acid and oxalic acid were the contributing factors for variations in the metabolic profile. Meanwhile for the effect of Cu concentration, the annotated significant features include ethanedioic acid and proline. In addition to the fatty acid and amino acid, down-regulation of galactose, lactose and sucrose were observed at 25°C in *S. quadricauda* treated with 1000 µM Cu (Figure 4.8B).

Table 4.6: ANOVA-simultaneous component analysis (ASCA) with leverage/squared prediction error (SPE) scatter plots and the significant factors of the ASCA-variables submodel temperature (a), Cu concentration (b), and interaction between the two factors (ab)

Metabolite	Day	Factor	Leverage	SPE
Aminomalonic acid	3	ab	0.008039	0.706935
Galactose	3	b	0.002501	0.334408
Lactose	3	b	0.002051	0.415566
Ethanedioic acid	3	b	0.002009	1.42063
Glycine	3	ab	0.015302	0.165664
Glycine	3	a	0.002732	9.86E-32
Hexadecanoic acid	3	ab	0.007212	0.240746
Hexadecanoic acid	3	a	0.002441	9.86E-32
Proline	6	ab	0.011245	0.250503
Proline	6	a	0.008408	3.94E-31
Myristic acid	6	a	0.00774	3.94E-31
Octadecanoic acid	6	ab	0.009339	1.043766
Oleic acid	6	ab	0.017303	0.873285
Oxalic acid	6	a	0.006376	3.94E-31
Propanoic acid	3	ab	0.006855	1.099991
Propanoic acid	6	a	0.007111	3.94E-31
Tetradecanoic acid	6	a	0.006811	3.94E-31
Tetradecanoic acid	6	ab	0.010385	4.373624

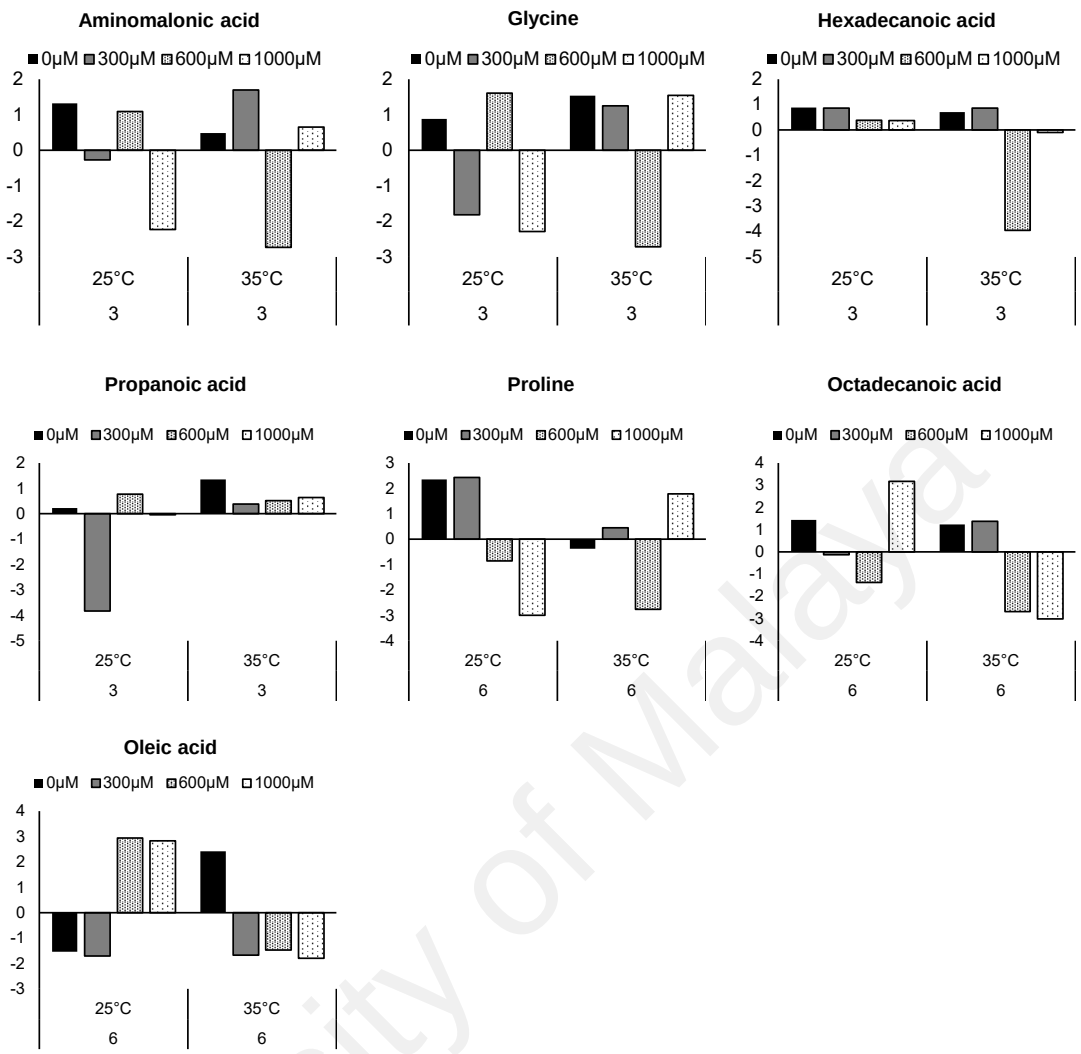

Figure 4.7: Representative patterns of variation in metabolite contents responding to the interactive effects of temperature and Cu concentrations.

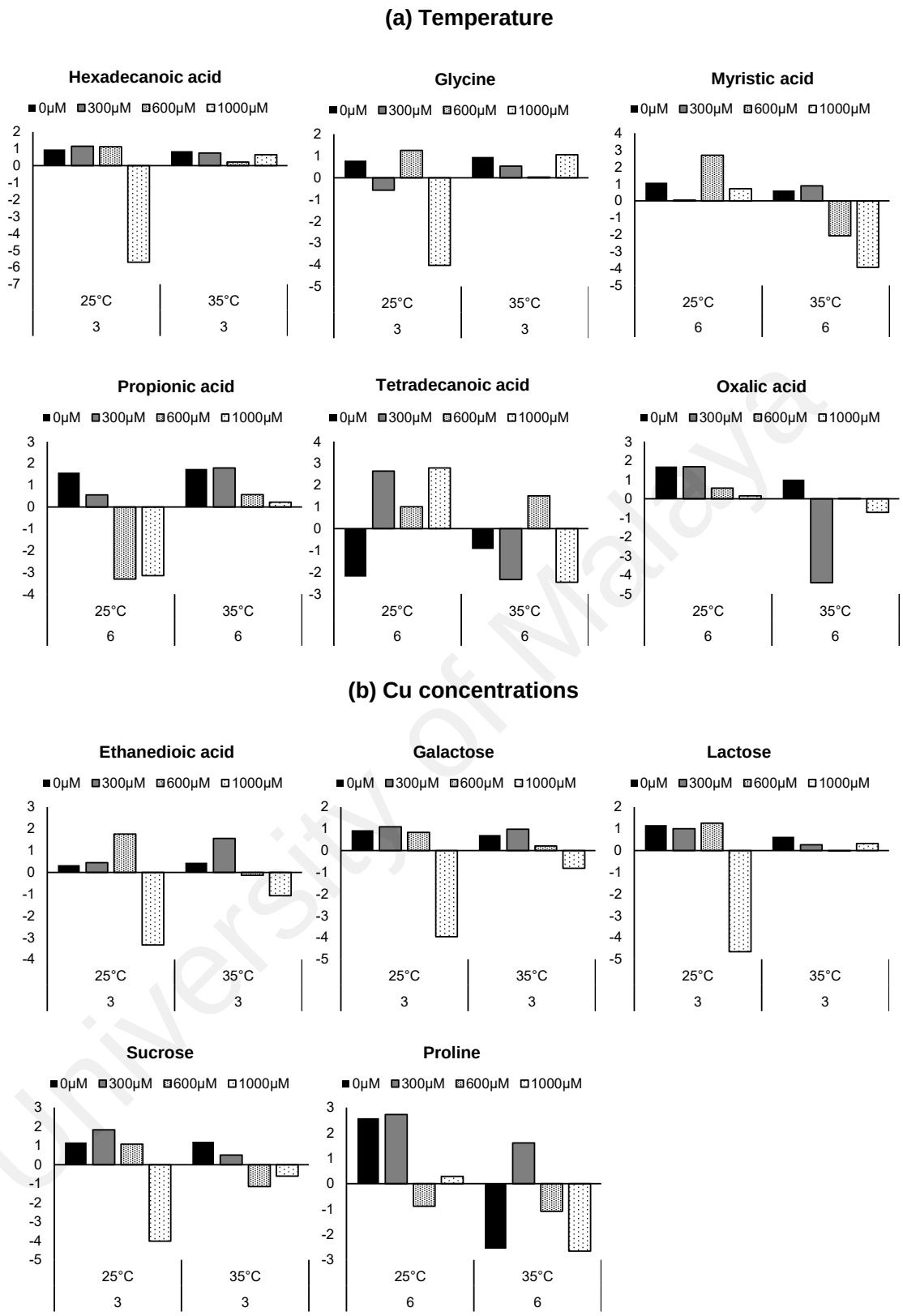

Figure 4.8: Representative patterns of variation in metabolite contents responding to (A) temperatures and (B) Cu concentrations respectively.

4.2 Experiment 2: Interactive effects of warming and Cu toxicity on *C. augustae*

4.2.1 Free Cu^{2+} Concentration

The concentration and activity of free Cu^{2+} ion in BBM at 25 & 30°C are shown in Table 4.7. The concentrations of Cu^{2+} were higher at 30°C in control and 50 µM $CuSO_4 \cdot 5H_2O$, but lower at 150 µM and 250 µM compared to 25°C. The estimated chemical activities of Cu^{2+} (pCu = -log Cu^{2+} activity) did not vary considerably between 25 and 30°C, though the values were slightly lower at 0 and 50 µM and higher at 150 and 250 µM at 30°C.

Table 4.7: Free cupric ion (Cu^{2+}) concentration and the logarithm of Cu^{2+} activity at 25 and 30°C

Nominal [Cu] (µM)	**Nominal [Cu] (ppm)**	**Temperature (°C)**			
		25		**30**	
		[Cu^{2+}] (µM)	**Log Cu^{2+} activity**	**[Cu^{2+}] (µM)**	**Log Cu^{2+} activity**
Control	Control	0.00263	-8.849	0.00282	-8.822
50	12.5	0.48	-6.592	0.51	-6.569
150	37.5	37.15	-4.703	34.59	-4.736
250	62.5	87.42	-4.332	80.65	-4.369

4.2.2 Cell density

Table 4.8 shows the Pearson correlation coefficients between factors and responses. Temperature was highly correlated with the increased production of ROS in the cells. Copper concentration, free ion concentration and activity were significantly correlated with cell density and metal content in the biomass, while affecting the photosynthetic parameters such as F_v/F_m, alpha, $rETR_m$ and E_k.

Table 4.8 Pearson correlation coefficients between various factors (temperature, Cu concentration, free Cu ions and activity) and responses

Response	Factor			
	Temperature	**Cu**	**[Cu^{2+}]**	**Log Cu^{2+} activity**
Cell density	-0.391*	-0.798**	-0.751**	-0.828**
F_v/F_m	-0.097	-0.720**	-0.694**	-0.681**
NPQ	-0.396*	-0.481**	-0.418*	-0.529**
qP	0.408*	0.590**	0.530**	0.618**
qN	-0.307	-0.372	-0.387*	-0.289
alpha	-0.173	-0.742**	-0.689**	-0.732**
$rETR_m$	-0.380*	-0.700**	-0.657**	-0.683**
E_k	-0.378*	-0.630**	-0.601**	-0.599**
ROS	0.909**	0.034	0.038	0.056
Metal content in biomass	0.188	0.789**	0.852**	0.608**

* $p<0.05$, ** $p<0.01$

The cell density of *C. augustae* decreased with increasing Cu concentrations at 25 and 30°C (Figure 4.9). At 25°C, the cells density for control was 2.63 x 10^5 cells mL^{-1} and decreased around 27% to 1.93 x 10^5 cells mL^{-1} in *Chlamy*-250Cu. At 30°C, the cells density for control was 2.62 x 10^5 cells mL^{-1} and decreased around 55% to 1.18 x 10^5 cells mL^{-1} in *Chlamy*-250Cu. In terms of temperature, the cell densities were generally higher at 25°C compared to 30°C. Warming enhanced the effect of Cu toxicity on growth inhibition, as the cell density of *Chlamy*-250Cu exposed to 30°C was 39% lower than *Chlamy*-250Cu exposed to 25°C. Statistical analysis showed that the effect of the individual and combined factors on cell density was significant (p = 0.000). Table 4.9 summarizes data obtained from two-way ANOVA testing the combined effect of

temperature and Cu concentrations on the physiological and photosynthetic parameters of *C. augustae*.

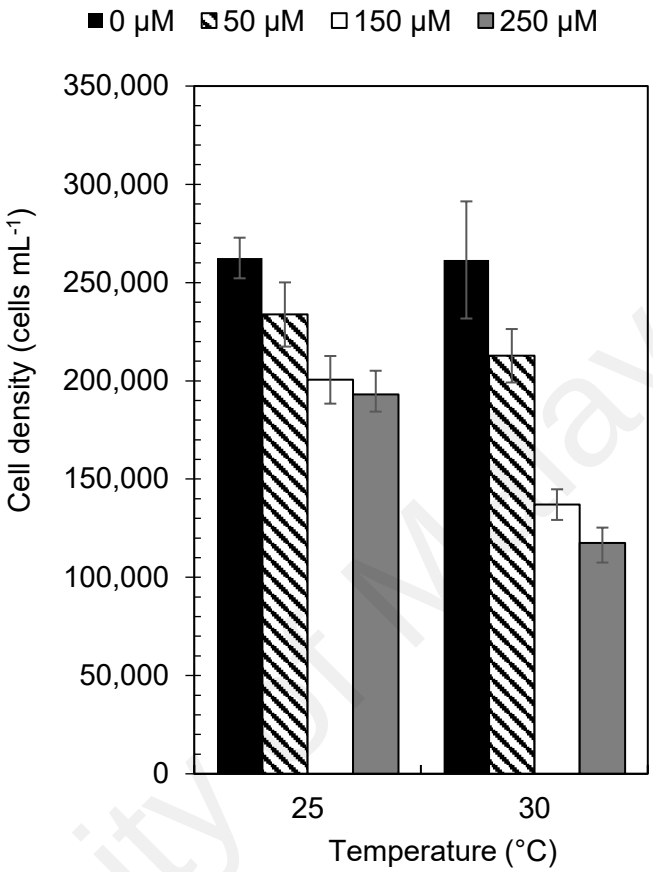

Figure 4.9: Cell density of *C. augustae* in response to warming and high Cu concentrations. Data are presented as mean ± standard deviation of the mean.

Table 4.9: Summary of two-way ANOVA testing the combined effect of Cu concentrations and temperature (25 and 30°C) on the physiological and photosynthetic parameters of *C. augustae*

Parameter	Source of variation	SS	*df*	F	Sig.
Cell density	Temperature	1.30×10^{10}	1	56.642	0.000
	Cu	5.87×10^{10}	3	85.570	0.000
	Temperature * Cu	7.39×10^{9}	3	10.764	0.000
	Error	5.49×10^{9}	24		
F_v/F_m	Temperature	0.008	1	5.211	0.023
	Cu	0.456	3	98.047	0.000
	Temperature * Cu	0.029	3	6.171	0.000
	Error	0.378	244		
NPQ	Temperature	0.015	1	5.198	0.034
	Cu	0.047	3	5.293	0.008
	Temperature * Cu	0.029	3	3.313	0.041
	Error	0.059	20		
qP	Temperature	0.042	1	7.526	0.013
	Cu	0.145	3	8.696	0.001
	Temperature * Cu	0.061	3	3.628	0.031
	Error	0.112	20		
qN	Temperature	0.000	1	0.895	0.355
	Cu	0.002	3	1.390	0.275
	Temperature * Cu	0.002	3	0.995	0.415
	Error	0.010	20		
Alpha (α)	Temperature	0.009	1	1.737	0.202
	Cu	0.178	3	11.983	0.000
	Temperature * Cu	0.027	3	1.790	0.182
	Error	0.099	20		
$rETR_m$	Temperature	7.00×10^{3}	1	9.808	0.005
	Cu	3.25×10^{4}	3	15.191	0.000
	Temperature * Cu	8.60×10^{3}	3	4.015	0.022
	Error	1.43×10^{4}	20		
E_k	Temperature	8.85×10^{3}	1	7.913	0.011
	Cu	3.49×10^{4}	3	10.413	0.000
	Temperature * Cu	1.69×10^{4}	3	5.028	0.009
	Error	2.24×10^{4}	20		
ROS	Temperature	2.85×10^{9}	1	741.927	0.000
	Cu	3.54×10^{7}	3	3.073	0.058
	Temperature * Cu	5.01×10^{8}	3	43.501	0.000
	Error	6.15×10^{7}	16		
Metal content in biomass	Temperature	1.18×10^{-4}	1	1.300	0.266
	Cu	5.60×10^{-4}	3	6.158	0.003
	Temperature * Cu	3.38×10^{-4}	3	3.711	0.027
	Error	9.10×10^{-5}	22		

SS = sum of squares; *df* = degree of freedom

4.2.3 Photosynthetic performance

Photosynthetic efficiency of *C. augustae* was sensitive to warming and excess Cu in the media as shown in Table 4.10. The maximum quantum yield of PSII (F_v/F_m) was significantly affected by Cu concentrations ($p = 0.000$) (Figure 4.10A). The F_v/F_m values of the control samples was 0.739 ± 0.003 and decreased in *Chlamy*-250Cu to 0.645 ± 0.063 and 0.614 ± 0.034 at 25 and 30°C respectively. Overall, the cells remained photosynthetically active after 24 h exposure as the F_v/F_m remained above 0.6.

Surprisingly, both factors and their interaction did not induce a significant effect on NPQ ($p > 0.05$). All NPQ values of the Cu-supplemented samples were lower than the control (0.489 ± 0.023) (Figure 4.10B). The combined factors significantly increased qP values across all treatment samples ($p = 0.031$). At 25°C, the qP value was 0.522 ± 0.035 in *Chlamy*-0Cu and increased to 0.798 ± 0.030 in *Chlamy*-250Cu. At 30°C, the qP value was 0.744 ± 0.027 in *Chlamy*-0Cu and increased to 0.797 ± 0.024 in *Chlamy*-250Cu. *Chlamy*-150Cu exhibited the highest value of qP across all treatment. Similar to the observation in NPQ values, no significant change was observed for qN values across different temperature and Cu concentrations (Table 4.10).

The light harvesting efficiency (alpha, α), $rETR_m$ and E_k values followed a similar decreasing trend with increasing Cu concentrations (Table 4.10, Figure 4.10C and D). At 25°C, the α values decreased from 0.738 ± 0.14 in control to 0.638 ± 0.114 and 0.480 ± 0.054 in *Chlamy*-150Cu and *Chlamy*-250Cu. Similarly, at 30°C, the α values decreased from 0.716 ± 0.039 in *Chlamy*-0Cu to 0.521 ± 0.009 and 0.543 ± 0.101 in *Chlamy*-150Cu and *Chlamy*-250Cu respectively. Neither temperature or the combined factor had significant impacts on alpha across all treatment. Increased doses of Cu had remarkably impacted on the efficiency of the electron transport rate (Figure 4.10C). The $rETR_m$ decreased nearly 70% in *Chlamy*-250Cu. Warming also significantly reduced the $rETR_m$

by approximately 50% in *Chlamy*-0Cu exposed to 30°C. The saturation irradiance for electron transport, E_k was significantly impacted by the individual and combined factors ($p < 0.05$) (Figure 4.10D). In general, the E_k values were lower at 30°C. At 25°C, the value was 246.49 ± 15.72 in *Chlamy*-0Cu and lowered to 107.39 ± 25.67 in *Chlamy*-250Cu. At 30°C, the value was 138.05 ± 29.13 in *Chlamy*-0Cu and lowered to 97.94 ± 15.51 in *Chlamy*-250Cu.

Table 4.10: Effects of temperature and various Cu concentrations on the photosynthetic performance of *C. augustae*

Temperature (°C)	**[Cu] (µM)**	**F_v/F_m**	**NPQ**	**qP**	**qN**	**$rETR_m$**	**alpha**	**E_k**
25	0	0.74	0.49	0.52	0.10	181.77	0.74	246.49
	50	0.73	0.41	0.65	0.10	137.27	0.68	197.64
	150	0.67	0.31	0.81	0.08	75.16	0.64	115.23
	250	0.64	0.33	0.80	0.07	50.63	0.48	107.39
30	0	0.75	0.34	0.74	0.08	98.00	0.72	138.05
	50	0.70	0.36	0.74	0.09	93.27	0.62	148.78
	150	0.68	0.31	0.80	0.09	72.29	0.52	138.30
	250	0.61	0.34	0.80	0.07	53.46	0.54	97.94

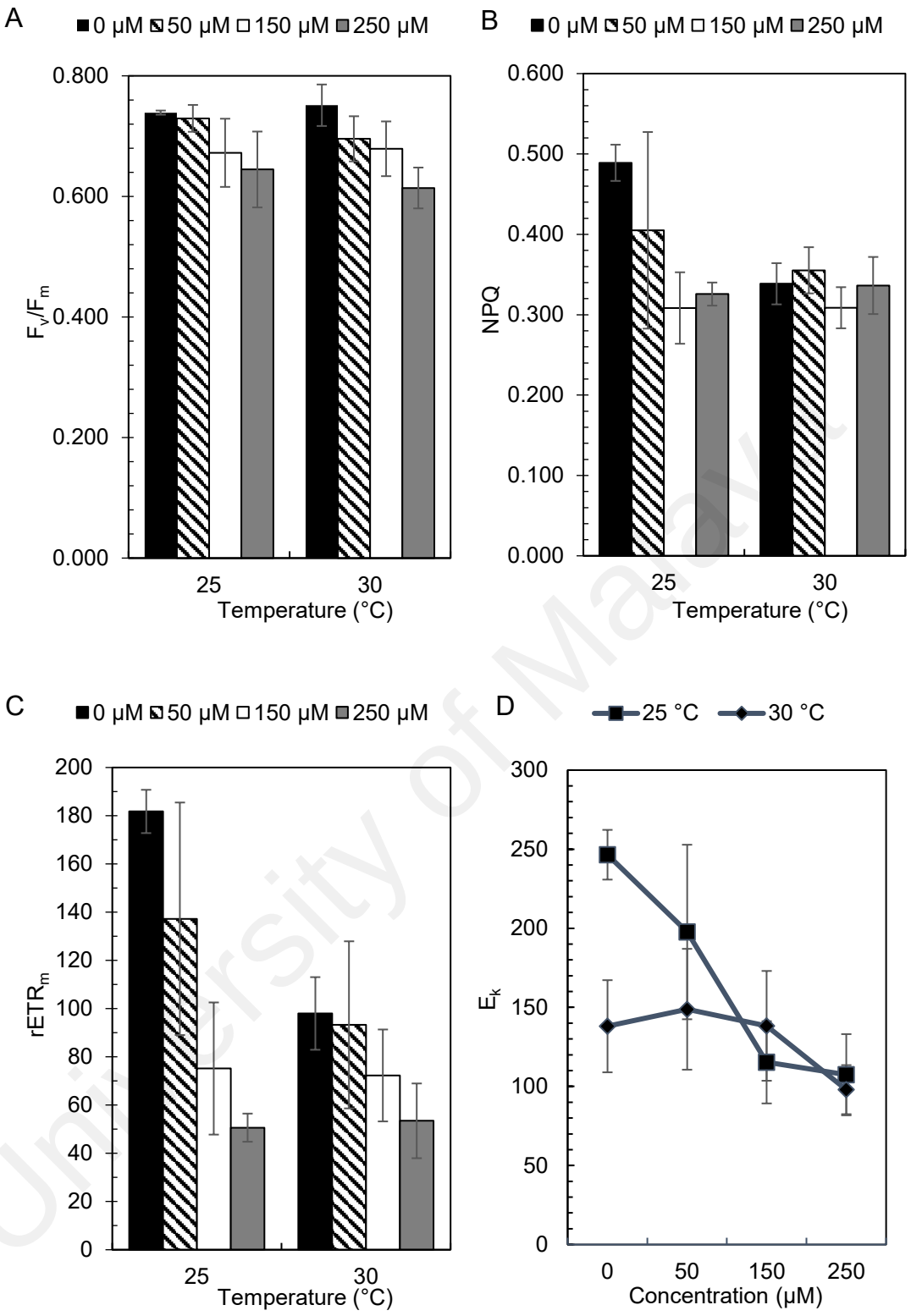

Figure 4.10: Photosynthetic performance (F_v/F_m, NPQ, $rETR_m$, and E_k) of *C. augustae* (mean ± SD) exposed to various Cu concentrations at 25 and 30°C.

4.2.4 ROS levels

The synergistic relationship between warming and Cu toxicity induced a remarkable increase in the production of ROS (Figure 4.11). The levels of ROS at 30°C were generally higher than the corresponding Cu-supplemented cultures at 25°C. This indicates that the oxidative stress level of the cells was significantly affected by sub-optimal temperature ($p < 0.000$). At 25°C, the DCF-fluorescence in *Chlamy*-150Cu and *Chlamy*-250Cu were 2-3 folds higher than that of *Chlamy*-0Cu. Based on the data from two-way ANOVA, temperature and the interaction of the combined factors impacted the ROS production significantly ($p = 0.000$), whereas Cu concentration did not affect the DCF-fluorescence significantly.

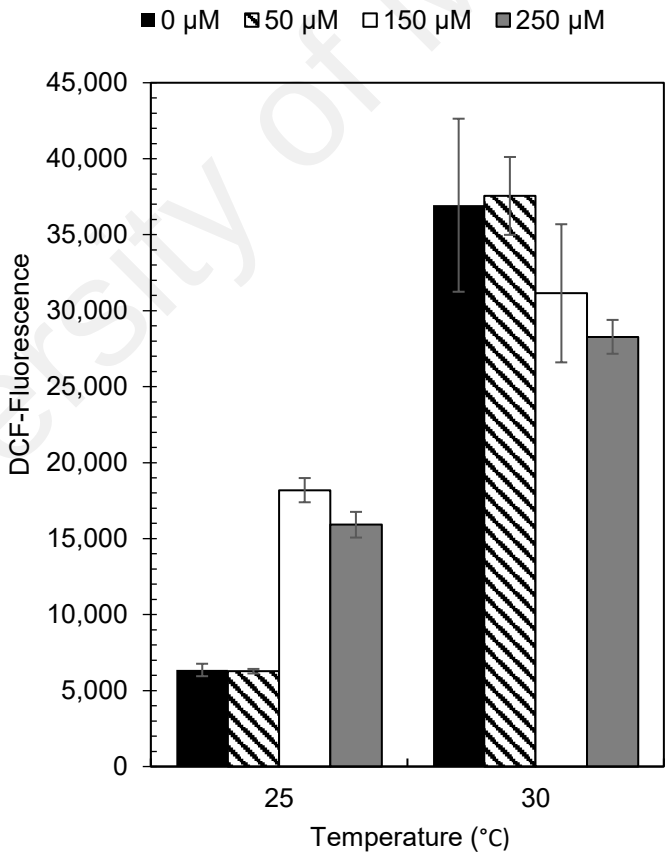

Figure 4.11: Fluorescence of DCF (corresponding to ROS levels) of *C. augustae* (mean ± SD) exposed to various Cu concentrations at 25 and 30°C.

4.2.5 Metal content in biomass

The results showed that the algal biomass was able to absorb substantial amount of Cu, especially in *Chlamy*-250Cu (Figure 4.12). *Chlamy*-250Cu was able to accumulate up to 0.02 – 0.04 pg cell^{-1} Cu in their biomass at 25 and 30°C. The data showed that the cells accumulated slightly higher Cu at 30°C. Based on the results from univariate analysis, the effects of temperature and combined factors on Cu uptake in algal biomass were not statistically significant ($p < 0.05$).

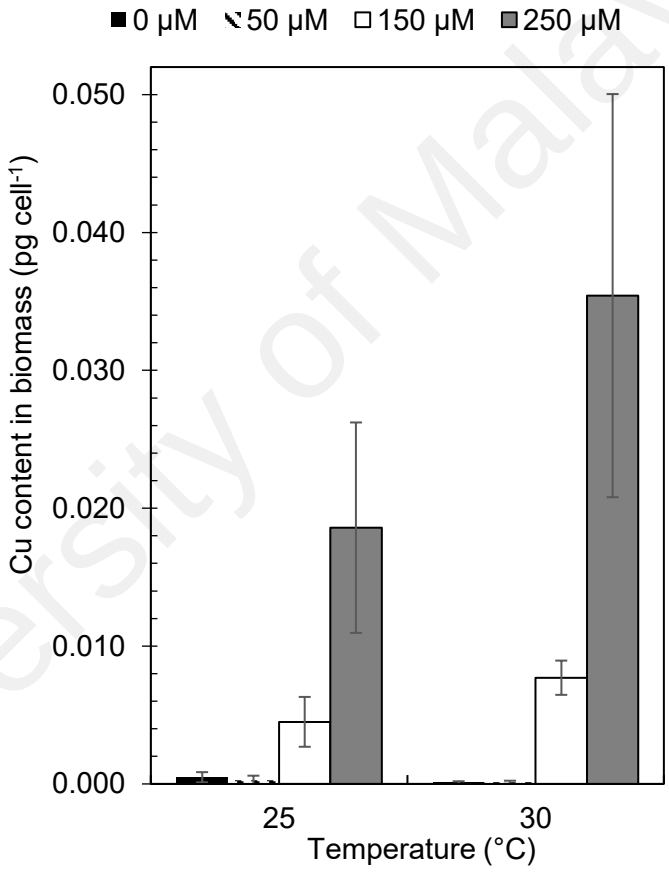

Figure 4.12: Copper content in the biomass of *C. augustae* (mean ± SD) exposed to various Cu concentrations at 25 and 30°C.

4.2.6 Metabolic profile

The ANOVA simultaneous component analysis (ASCA) was conducted to identify the major patterns associated with each factor and their interactive effects on the samples (Figure 4.13). Based on the statistical values, temperature contributed to the most significant differentiation among the samples ($p < 0.05$) and accounted for 100% variation across all platforms. Copper accounted for 57.60%, 48.41% and 60.56% variation respectively for data generated by GCMS and LCMS in positive and negative modes. Interaction between the two factors resulted in 44.47% variation for data generated by GCMS, accompanied by 53.75% and 49.96% variation for data generated by both modes in LCMS.

Generally, pathway analysis with MetaboAnalyst demonstrates that the changes of the metabolic expression were mainly involved in the amino acid, energy, and lipid metabolisms (Figure 4.14). Copper treatment on *C. augustae* induced changes in glutathione metabolism, sulfur metabolism, taurine and hypotaurine metabolism, and zeatin biosynthesis. Warming affected pathways in pantothenate and CoA, isoquinoline alkaloid biosynthesis, sulfur metabolism, tyrosine metabolism, glutathione metabolism, and phenylalanine metabolism. The combined factors impacted on the tropane, piperidine and pyridine alkaloid biosynthesis, phenylalanine metabolism, and glycerolipid metabolism. The glutathione metabolism, a critical antioxidative and metal detoxicification mechanism, was observed to be involved in response to the individual and combined factors. Sulfur metabolism was affected by Cu and temperature. Table 4.11 shows the top three important pathways and metabolites corresponding to each factor. The most significant pathway associated with Cu toxicity was glutathione metabolism ($p < 0.05$; impact score of 0.51) where the significant hits included glutathione and amino acids. The second and third most important pathways were methane and sulfur metabolism. The top three most important pathways involved in the

interactive effects were tropane, piperidine and pyridine alkaloid biosynthesis, phenylalanine metabolism, and glycerolipid metabolism. The top three most significant pathways involved in the temperature treatment were pantothenate and CoA biosynthesis ($p = 0.01$; impact score of 0.30), beta-alanine metabolism ($p = 0.04$; impact score of 0.00) and isoquinoline alkaloid biosynthesis ($p = 0.06$; impact score of 0.5).

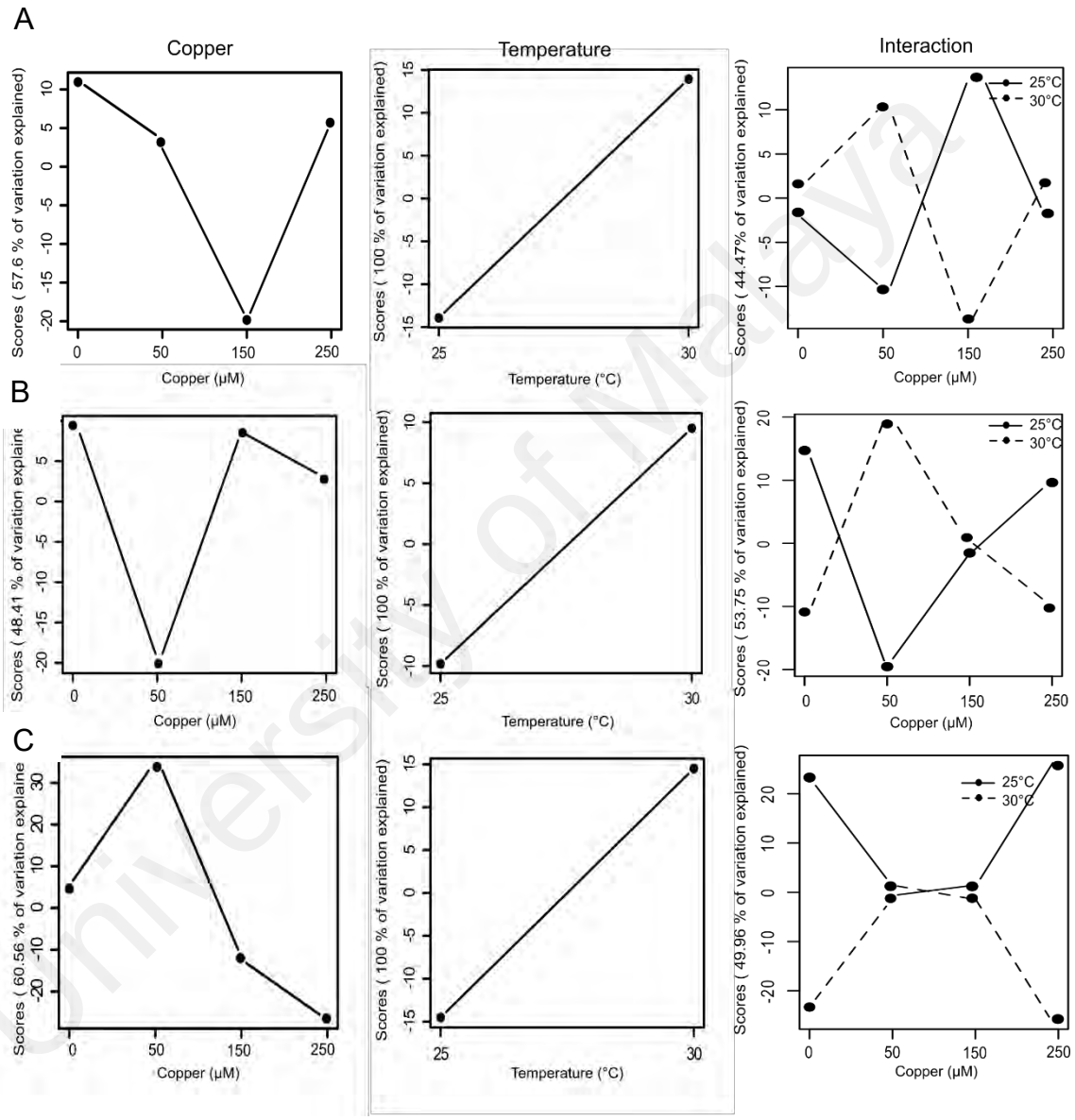

Figure 4.13: Results of ANOVA simultaneous component analysis (ASCA) showing the major patterns associated with temperature, concentration of Cu, and their interaction for (A) GCMS, (B) LC-positive and (C) LC-negative data sets in the response of *C. augustae* to warming and Cu toxicity.

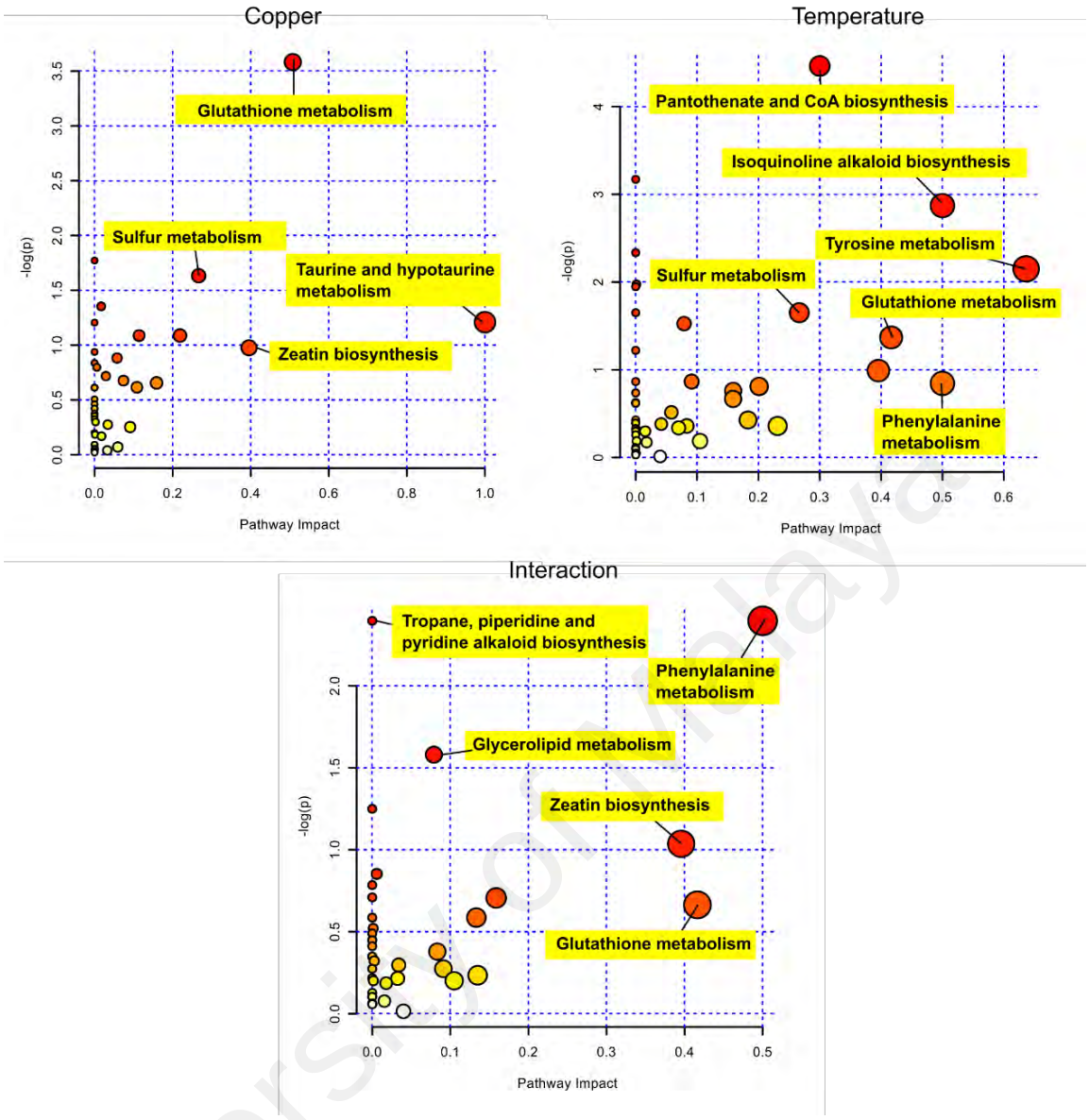

Figure 4.14: Key pathways involved in the stress response of *C. augustae* to Cu, temperature and the interaction between the two factors.

Table 4.11: Significant pathways and compounds involved in the response of *C. augustae* to the Cu toxicity (a), temperature (b) or the interactive effects (ab)

Factor	Pathway	Total	Hits	Raw p	FDR	Impact	Compounds
a	Glutathione metabolism	26	5	0.03	1	0.51	Glutathione; Glycine; Putrescine; Cysteinylglycine; Cysteine
a	Methane metabolism	11	2	0.17	1	0.00	Glycine; Methanol
a	Sulfur metabolism	12	2	0.20	1	0.27	Acetic acid; Cysteine
ab	Tropane, piperidine and pyridine alkaloid biosynthesis	8	2	0.09	1	0.00	Phenylalanine; Tropinone
ab	Phenylalanine metabolism	8	2	0.09	1	0.50	Phenylalanine; Phenylacetaldehyde
ab	Glycerolipid metabolism	13	2	0.21	1	0.08	Glycerol 3-phosphate; Glyceric acid
b	Pantothenate and CoA biosynthesis	14	4	0.01	1	0.30	Dihydrouracil; 2-Acetolactate; Valine; Pantothenic acid
b	beta-Alanine metabolism	12	3	0.04	1	0.00	Aspartic acid; Dihydrouracil; Pantothenic acid
b	Isoquinoline alkaloid biosynthesis	6	2	0.06	1	0.50	Tyrosine; Tyramine

4.3 Experiment 3: Interactive effects of warming and Ni toxicity on *S. quadricauda*

4.3.1 Free Ni^{2+} Concentration

The concentration and activity of free Ni^{2+} ion in the culture media at different temperatures are shown in Table 4.12. The concentrations of Ni^{2+} were higher at 35°C at 0.42 and 4.21 µM nominal concentrations of $NiCl_2 \cdot 6H_2O$, but lower at 42.07 µM compared to 25°C. The estimated chemical activities of Ni^{2+} (pNi = -log Ni^{2+} activity) did not vary considerably between 25 and 35°C.

Table 4.12: Free Ni ion (Ni^{2+}) concentration and the logarithm of Ni^{2+} activity at 25 and 35°C

Nominal [Ni] (µM)	**Nominal [Ni] (ppm)**	**Temperature (°C)**			
		25		**35**	
		[Ni^{2+}] (µM)	**Log Ni^{2+} activity**	**[Ni^{2+}] (µM)**	**Log Ni^{2+} activity**
0	0	0	0	0	0
0.42	0.1	4.82×10^{-4}	-9.59	5.27×10^{-4}	-9.55
4.21	1.0	1.14×10^{-2}	-8.21	1.25×10^{-2}	-8.18
42.07	10.0	18.4	-5.01	18.0	-5.02

4.3.2 Cell density

Table 4.13 shows the Pearson correlation coefficients between factors and responses. Cell density was positively correlated with temperature (p<0.01) and higher at 35°C (Figure 4.15).

Table 4.13: Pearson correlation coefficients between various factors (temperature, Ni concentration, free Ni ions and activity) and responses

Response	**Factor**			
	Temperature	**Nickel**	**[Ni^{2+}]**	**Log Ni^{2+} activity**
Cell density	0.762**	-0.082	-0.069	0.346
F_v/F_m	0.017	-0.489*	-0.474*	-0.027
NPQ	-0.633**	0.353	0.366	0.007
qP	0.781**	-0.156	-0.166	0.006
qN	-0.631**	0.386	0.399	0.012
Alpha (α)	0.161	-0.137	-0.127	-0.051
$rETR_m$	0.766**	-0.532**	-0.533**	-0.014
E_k	0.762**	-0.543**	-0.548**	0.013
ROS	-0.515*	0.505*	0.494*	0.053
Metal content in biomass	0.222	0.478*	0.481*	-0.154

* p<0.05, ** p<0.01

The data shows that *S. quadricauda* was able to thrive at 35°C. Cell densities of *S. quadricauda* remained consistent across all Ni concentrations at 25°C but decreased with increasing Ni concentrations at 35°C, indicating the antagonistic effect of warming on Ni toxicity and increased sensitivity at higher temperature. At 35°C, cell density of cultures grown in 0.42 µM Ni was significantly lower by 35 % compared to control (p < 0.05). Statistical analysis showed that the effect of the individual factors was significant (p =

0.000 for temperature and p = 0.044 for Ni concentrations). However, the combined factors did not affect cell density significantly (p = 0.134). Table 4.14 summarizes data obtained from two-way ANOVA testing the combined effect of Ni concentrations and temperature (25 and 35°C) on the physiological and photosynthetic parameters of *S. quadricauda*.

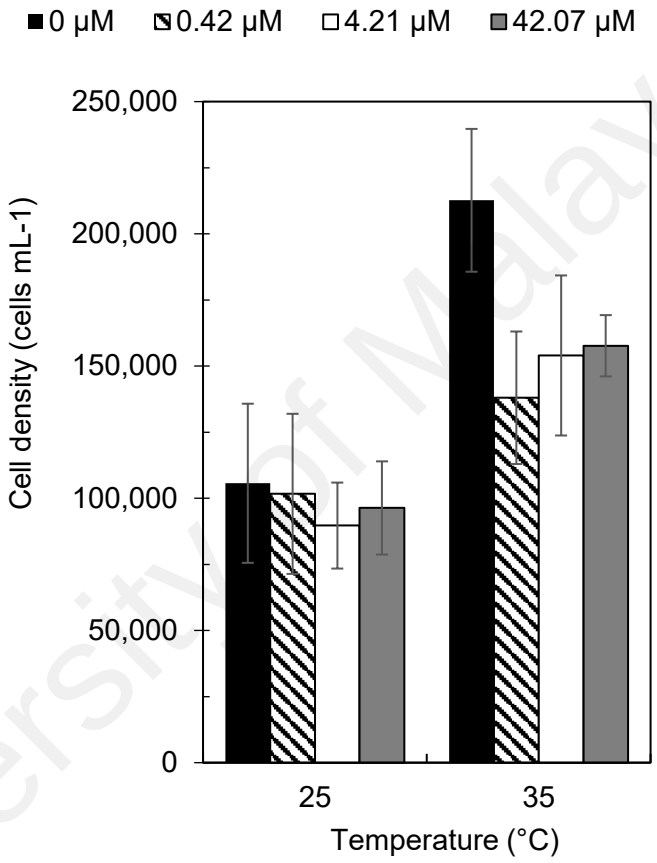

Figure 4.15: Effects of temperature and various Ni concentrations on the cell density (mean ± SD) of *S. quadricauda*.

Table 4.14: Summary of two-way ANOVA testing the combined effect of Ni concentrations and temperature (25 and 35°C) on the physiological and photosynthetic parameters of *S. quadricauda*

Parameter	Source of variation	SS	*df*	F	Sig.
Cell density	Temperature	2.71E+10	1	45.188	0.000
	Ni	6.09E+09	3	3.379	0.044
	Temperature * Ni	3.87E+09	3	2.148	0.134
	Error	9.61E+09	16		
F_v/F_m	Temperature	1.838E-05	1	0.007	0.932
	Ni	0.017	3	2.334	0.113
	Temperature * Ni	0.008	3	1.081	0.385
	Error	0.039	16		
NPQ	Temperature	0.344	1	23.066	0.000
	Ni	0.036	3	0.804	0.510
	Temperature * Ni	0.164	3	3.673	0.035
	Error	0.239	16		
qP	Temperature	0.065	1	91.622	0.000
	Ni	0.012	3	5.622	0.008
	Temperature * Ni	0.002	3	1.092	0.381
	Error	0.011	16		
qN	Temperature	0.040	1	29.563	0.000
	Ni	0.006	3	1.569	0.236
	Temperature * Ni	0.022	3	5.507	0.009
	Error	0.021	16		
Alpha (α)	Temperature	0.000	1	0.694	0.417
	Ni	0.001	3	0.470	0.707
	Temperature * Ni	0.004	3	2.836	0.071
	Error	0.008	16		
$rETR_m$	Temperature	2.88E+04	1	82.257	0.000
	Ni	1.39E+04	3	13.232	0.000
	Temperature * Ni	7.53E+02	3	0.717	0.556
	Error	5.60E+03	16		
E_k	Temperature	3.58E+05	1	84.699	0.000
	Ni	1.84E+05	3	14.539	0.000
	Temperature * Ni	5.90E+03	3	0.466	0.710
	Error	6.75E+04	16		
ROS	Temperature	0.003	1	0.082	0.779
	Ni	0.639	3	6.724	0.004
	Temperature * Ni	0.191	3	2.009	0.153
	Error	0.506	16		
Metal content in biomass	Temperature	2.445E-05	1	22.320	0.000
	Ni	0.001	3	292.554	0.000
	Temperature * Ni	1.292E-05	3	3.930	0.034
	Error	1.424E-05	13		

SS = sum of squares; *df* = degree of freedom

4.3.3 Photosynthetic performance

According to the Pearson correlation coefficients in Table 4.13, F_v/F_m was positively correlated with Ni concentration and free Ni^{2+} concentration. The NPQ and qN were negatively correlated with temperature while a positive correlation was observed for qP. The $rETR_m$ and E_k values were positively correlated with temperature and negatively correlated with Ni concentration and free Ni^{2+} concentration.

Table 4.15 and Figure 4.16 show that the photosynthetic efficiency of *S. quadricauda* was sensitive to warming and excess Ni in the media. The maximum quantum yield of PSII (F_v/F_m) remained highly efficient with the values ranging from 0.68 to 0.76 under all conditions. The individual and combined factors did not affect the F_v/F_m values significantly ($p > 0.05$) (Figure 4.16A).

An increase in NPQ value was observed in *Scene*-42Ni at 25°C, indicating that the cells mitigated the stress effect of excess Ni through heat dissipation (Figure 4.16B). The value increased from 0.85 ± 0.13 at *Scene*-0Ni to 1.11 ± 0.09 in *Scene*-42Ni. At 35°C, the NPQ remained similar across all Ni concentrations. Based on the results from univariate analysis, temperature and the interaction of combined factors induced a significant impact on NPQ ($p < 0.05$). All NPQ values of the samples were lower at 35°C. Warming and high Ni concentrations significantly increased qP values across all treatment samples ($p < 0.01$). At 25°C, the qP value was 0.48 ± 0.01 in *Scene*-0Ni and increased to 0.40 ± 0.02 in *Scene*-42Ni. At 35°C, the qP value remained consistent in the range of 0.53 - 0.57. The qN value of Scene-42Ni was slightly higher than that of the other conditions.

The light harvesting efficiency (alpha, α), $rETR_m$ and E_k values were also demonstrated in Table 4.15. At 25°C, the α values slightly decreased from 0.282 ± 0.10 in control to 0.246 ± 0.005 in *Scene*-42Ni. A 35°C, the α values increased from 0.253 ± 0.013 in *Scene*-0Ni to 0.276 ± 0.009 in *Scene*-42Ni. Neither temperature, excess Ni or the

combined factor had significant impact on alpha across all treatment. Increased doses of Ni had remarkably impacted on the efficiency of the electron transport rate (Figure 4.16C). The $rETR_m$ decreased nearly 42% in *Scene*-42Ni. Warming increased the $rETR_m$ by approximately 30% in *Scene*-0Ni exposed to 35°C. The saturation irradiance for electron transport, E_k was significantly impacted by warming and excess Ni in the culture medium ($p < 0.05$) (Figure 4.16D). Interestingly, the E_k values were generally higher at 35°C. At 25°C, the value was 620.22 ± 38.99 in *Scene*-0Ni and lowered to 413.91 ± 33.58 in *Scene*-42Ni. At 35°C, the value was 895.25 ± 54.45 in *Scene*-0Ni and lowered to 664.05 ± 76.96 in *Scene*-42Ni.

Table 4.15: Effects of temperature and various Ni concentrations on the photosynthetic performance of *S. quadricauda*

Temperature (°C)	**[Ni] (µM)**	**F_v/F_m**	**NPQ**	**qP**	**qN**	**$rETR_m$**	**alpha**	**E_k**
25	0	0.74	0.85	0.48	0.55	174.61	0.28	620.22
	0.42	0.76	0.89	0.46	0.56	166.60	0.28	599.14
	4.21	0.68	0.78	0.46	0.53	153.41	0.24	636.30
	42.07	0.66	1.11	0.40	0.65	101.98	0.25	413.91
35	0	0.71	0.67	0.55	0.50	227.59	0.25	895.25
	0.42	0.72	0.67	0.57	0.50	231.51	0.27	858.35
	4.21	0.74	0.73	0.56	0.51	231.62	0.28	828.35
	42.07	0.68	0.60	0.53	0.47	182.97	0.28	664.05

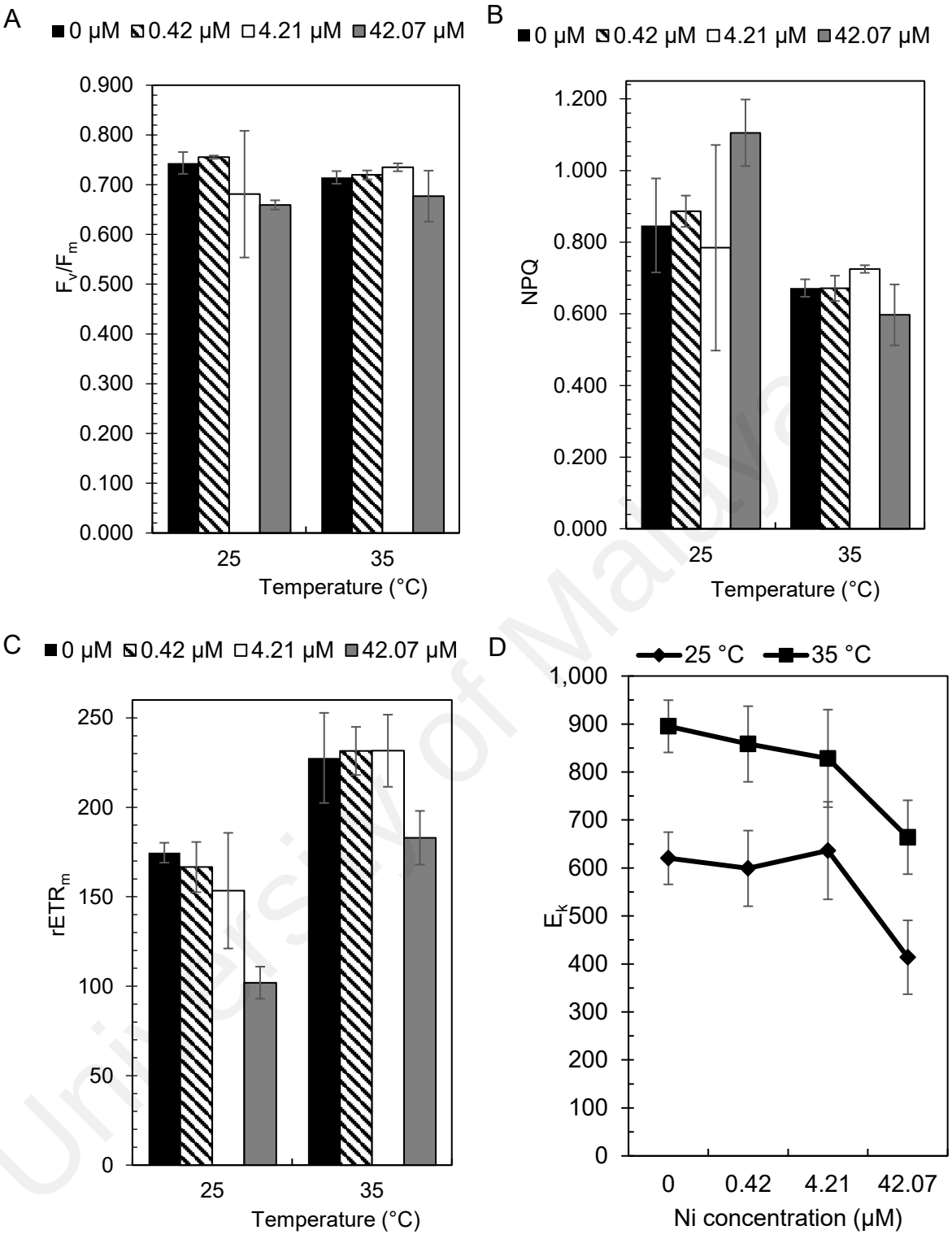

Figure 4.16: Photosynthetic performance (F_v/F_m, NPQ, $rETR_m$, and E_k) of *S. quadricauda* (mean ± SD) exposed to various Ni concentrations at 25 and 35°C.

4.3.4 ROS levels

The induction of intracellular ROS production following the exposure of *S. quadricauda* cells to Ni was probed by fluorescence emission (Figure 4.17). The results showed an increase in ROS production in treated algal cells compared to control, and this change corresponded to the concentration of Ni. The representative histograms generated from the flow cytometer are shown in Appendix B. When *S. quadricauda* were exposed to 42.07 µM of Ni at 35°C, the ROS level increased significantly by 40% ($p < 0.01$). Overall, Ni treatment induced significant changes in the ROS levels ($p = 0.004$) whereas the effects of temperature and the combined factors were not significant ($p > 0.05$). Based on the Pearson correlation coefficients in Table 4.13, the ROS levels were positively correlated with temperature and negatively correlated with Ni concentration and free Ni^{2+} concentration.

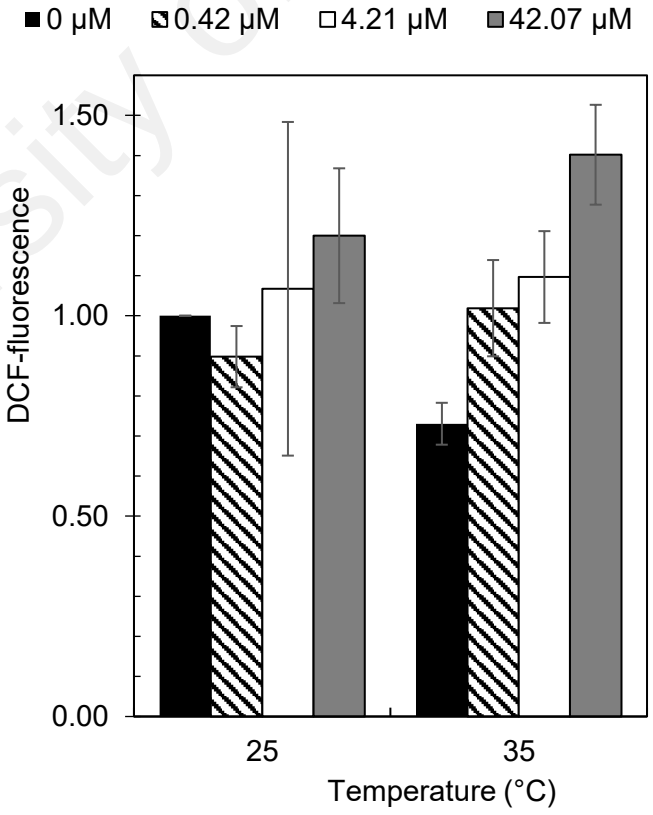

Figure 4.17: Fluorescence of DCF (corresponding to ROS levels) of *S. quadricauda* (mean ± SD) exposed to various Cu concentrations at 25 and 35°C.

4.3.5 Metal content in biomass

According to the Pearson correlation coefficients in Table 4.13, the Ni content in the biomass was positively correlated with Ni concentration and free Ni^{2+} concentration. The results showed that the algal biomass was able to absorb substantial amount of Ni, especially at 42.07 µM (Figure 4.18). The amount of Ni accumulated in the biomass were significant ($p < 0.01$) at both temperatures, with the amount accumulated at 25°C (0.0199 pg $cell^{-1}$) higher than that of 35°C (0.0154 pg $cell^{-1}$). Based on the results from univariate analysis, the effects of individual and combined factors on Ni uptake in algal biomass were statistically significant ($p < 0.05$).

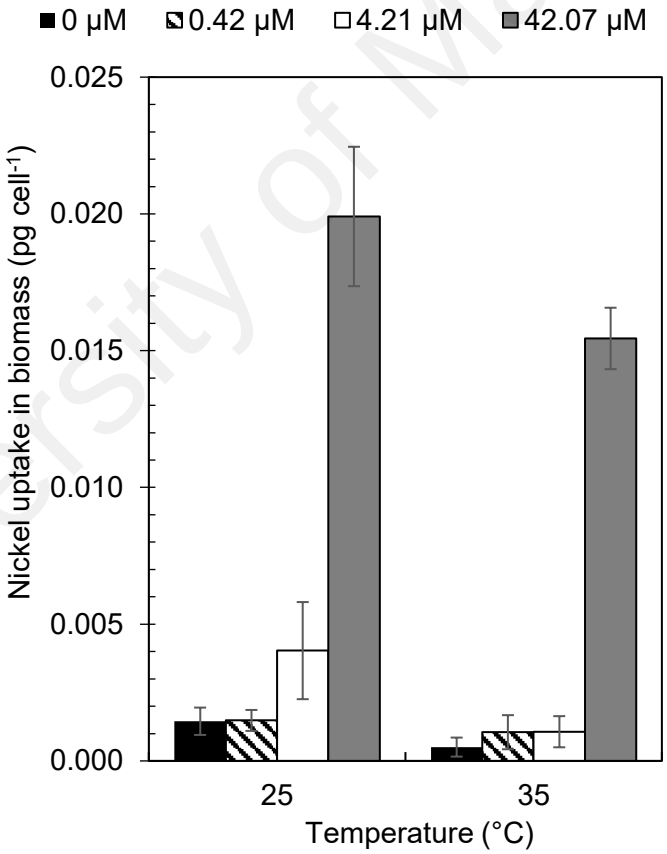

Figure 4.18: Nickel content in the biomass of *S. quadricauda* (mean ± SD) exposed to various Ni concentrations at 25 and 35°C.

4.3.6 Metabolic responses

The ANOVA simultaneous component analysis (ASCA) was conducted to identify the major patterns associated with each factor and their interactive effects on the samples (Figure 4.19). Based on the statistical values, temperature contributed to the most significant differentiation among the samples ($p < 0.05$) and accounted for 100% variation across all platforms. Nickel accounted for 76.72%, 56.73% and 50.36% variation respectively for data generated by GCMS and LCMS in positive and negative modes. Interaction between the two factors resulted in 92.38% variation for data generated by GCMS, accompanied by 47.26% and 48.31% variation for data generated by both modes in LCMS.

Generally, pathway analysis with MetaboAnalyst demonstrates that the changes of the metabolic expression were mainly involved in the amino acid, energy, and lipid metabolisms (Figure 4.20). Pathways classified under amino acid metabolism include cysteine and methionine metabolism; arginine and proline metabolism; alanine, aspartate and glutamate metabolism; and taurine and hypotaurine metabolism. Sulfur and nitrogen metabolisms were significantly affected by the combined factors. Nickel treatment on *S. quadricauda* induced changes in the lipid metabolism-related pathways such as sphingolipid and glycerophospholipid metabolisms.

Table 4.16 shows the top three significant pathways and metabolites corresponding to each factor. The most significant pathway associated with the interactive effects of temperature and Ni toxicity was sulfur metabolism ($p < 0.01$; impact score of 0.933). The second most significant pathway was cysteine and methionine metabolism ($p < 0.01$; impact score of 0.526), followed by nitrogen metabolism ($p < 0.05$; impact score of 0.138). The top three most significant pathways involved in the Ni treatment were cysteine and methionine metabolism ($p < 0.01$; impact score of 0.369), sulfur metabolism

($p < 0.01$; impact score of 0.500) and nitrogen metabolism ($p < 0.05$; impact score of 0.138). The top three most significant pathways involved in the temperature treatment were sulfur metabolism ($p < 0.01$; impact score of 0.933,) cysteine and methionine metabolism ($p < 0.05$; impact score of 0.526), and nitrogen metabolism ($p < 0.05$; impact score of 0.138). The expression levels of annotated metabolites such as sulfur-containing compounds, amino acids, and nitrogenous metabolites were significantly affected.

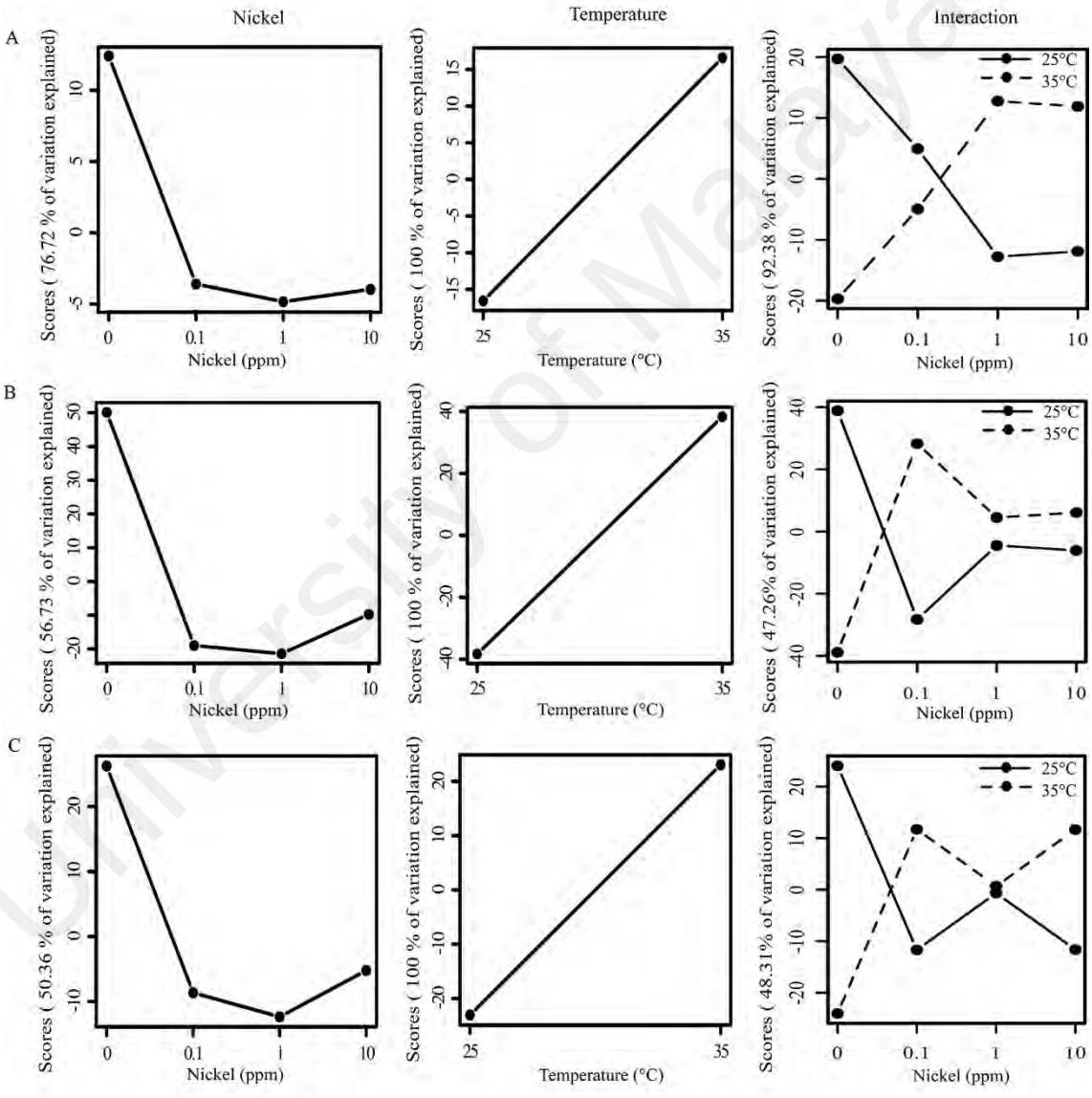

Figure 4.19: Results of ANOVA simultaneous component analysis (ASCA) showing the major patterns associated with temperature, concentration of Ni, and their interaction on *S. quadricauda* for (A) GCMS, (B) LC-positive and (C) LC-negative data sets.

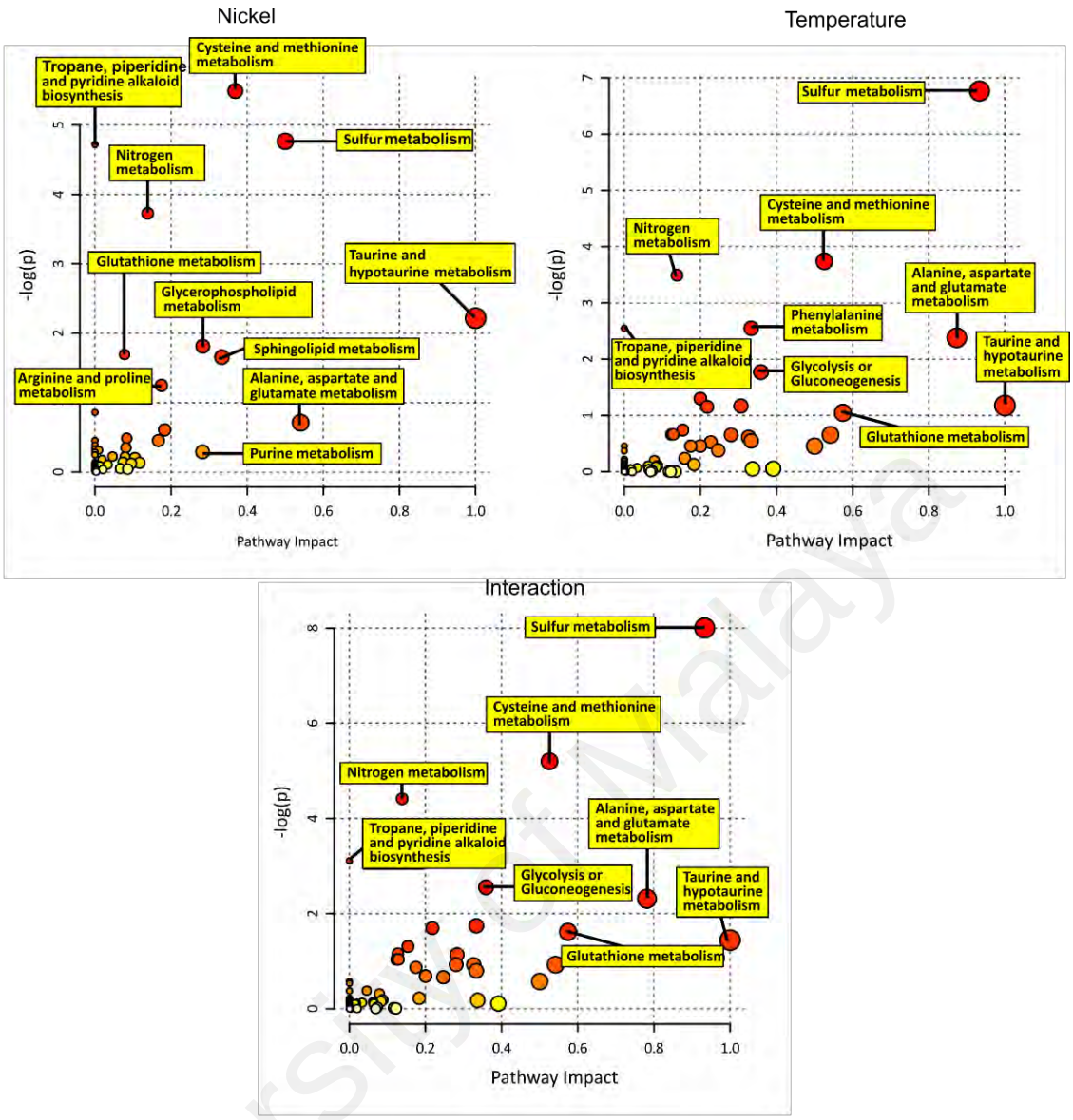

Figure 4.20: Key pathways involved in the stress response of *S. quadricauda* to Ni, temperature and the interaction between the two factors.

Table 4.16: Significant pathways and compounds involved in the response of *S. quadricauda* to the Ni toxicity (a), temperature (b) or the interactive effects (ab)

Factor	Pathway	Total	Hits	Raw p	FDR	Impact	Compound
a	Cysteine and methionine metabolism	34	10	0.004	0.259	0.369	S-Adenosylmethionine; 5'-Methylthioadenosine; S-Adenosylmethioninamine; Cystathionine; O-Succinyl-homoserine; O-Acetylserine; 3-Sulfinoalanine; Cysteine; Aspartic acid; Thiocysteine
a	Sulfur metabolism	12	5	0.009	0.259	0.500	O-Succinyl-homoserine; Sulfate; O-Acetylserine; Allocystathionine; Cysteine
a	Nitrogen metabolism	15	5	0.024	0.523	0.138	Nitrate; Nitrite; Glutamic acid; Allocystathionine; Carbamic acid
b	Sulfur metabolism	12	8	0.001	0.100	0.933	O-Succinyl-homoserine; Sulfate; O-Acetylserine; Hydrogen sulfide; Allocystathionine; Acetic acid; Cysteine; Homocysteine
b	Cysteine and methionine metabolism	34	13	0.024	0.883	0.526	S-Adenosylmethionine; 5'-Methylthioadenosine; S-Adenosylmethioninamine; Cystathionine; Homocysteine; O-Succinyl-homoserine; O-Acetylserine; Hydrogen sulfide; 3-Sulfinoalanine; Cysteine; Aspartic acid; Thiocysteine; Pyruvic acid
b	Nitrogen metabolism	15	7	0.030	0.883	0.138	Nitrate; Nitrite; Glutamic acid; Glutamine; Allocystathionine; Carbamic acid; Carbonic acid
ab	Sulfur metabolism	12	8	0.000	0.029	0.933	O-Succinyl-homoserine; Sulfate; O-Acetylserine; Hydrogen sulfide; Allocystathionine; Acetic acid; Cysteine; Homocysteine

4.4 Experiment 4: Interactive effects of warming and Ni toxicity on *C. augustae*

4.4.1 Free Ni^{2+} Concentration

The concentration and activity of free Ni^{2+} ion in the culture media at different temperatures are shown in Table 4.17. The concentrations of Ni^{2+} were higher at 30°C at 0.42 and 4.21 µM nominal concentrations of $NiCl_2 \cdot 6H_2O$, but lower at 42.07 µM compared to 25°C. The estimated chemical activities of Ni^{2+} (pNi = -log Ni^{2+} activity) did not vary considerably between 25 and 30°C.

Table 4.17: Free Ni ion (Ni^{2+}) concentration and the logarithm of Ni^{2+} activity at 25 and 30°C

Nominal [Ni] (µM)	**Nominal [Ni] (ppm)**	**Temperature (°C)**			
		25		**30**	
		[Ni^{2+}] (µM)	**Log Ni^{2+} activity**	**[Ni^{2+}] (µM)**	**Log Ni^{2+} activity**
0	0	N/A	0	0	0
0.42	0.1	4.82×10^{-4}	-9.59	5.05×10^{-4}	-9.57
4.21	1.0	1.14×10^{-2}	-8.21	1.20×10^{-2}	-8.194
42.07	10.0	18.4	-5.01	18.2	-5.013

4.4.2 Cell density

Table 4.18 shows the Pearson correlation coefficients between factors and responses. Temperature was positively correlated with qP and ROS levels, and negatively correlated with cell density, F_v/F_m, NPQ, qN, $rETR_m$ and E_k. Nickel concentration and free ion concentration were negatively correlated with cell density and positively correlated with metal content in the biomass. Free Ni^{2+} activity was shown to be correlated with F_v/F_m, NPQ, qP, qN, $rETR_m$, and E_k.

Table 4.18: Pearson correlation coefficients between various factors (temperature, Ni concentration, free Ni ions and activity) and responses

Response	Factor			
	Temperature	**Nickel**	**[Ni^{2+}]**	**Log Ni^{2+} activity**
Cell density	-0.405*	-0.800**	-0.771**	-0.293
F_v/F_m	-0.801**	0.212	0.187	-0.622**
NPQ	-0.835**	0.158	0.145	-0.787**
qP	0.868**	-0.134	-0.119	0.808**
qN	-0.446*	-0.059	-0.071	-0.407*
Alpha (α)	-0.127	0.143	0.151	-0.019
$rETR_m$	-0.892**	0.112	0.101	-0.790**
E_k	-0.862**	0.080	0.067	-0.780**
ROS	0.724**	-0.402	-0.416*	0.457*
Metal content in biomass	0.145	0.937**	0.928**	0.104

* $p<0.05$, ** $p<0.01$

In general, the cell density of *C. augustae* decreased with increasing Ni concentrations (Figure 4.21). At 25°C, the cell density of *Chlamy*-0Ni was 2.60 x 10^5 cells mL^{-1} and decreased nearly 28% to 1.86 x 10^5 cells mL^{-1} in *Chlamy*-42Ni. At 30°C, the cell density of *Chlamy*-0Ni was 2.36 x 10^5 cells mL^{-1} and decreased nearly 20% to 1.88 x 10^5 cells mL^{-1} in *Chlamy*-42Ni.

Table 4.19 summarizes data obtained from two-way ANOVA testing the combined effect of Ni concentrations and temperature (25 and 30°C) on the physiological and photosynthetic parameters of *C. augustae*. Statistical analysis showed that the effect of

the individual and combined factors on cell density was significant ($p < 0.05$) (Table 4.19).

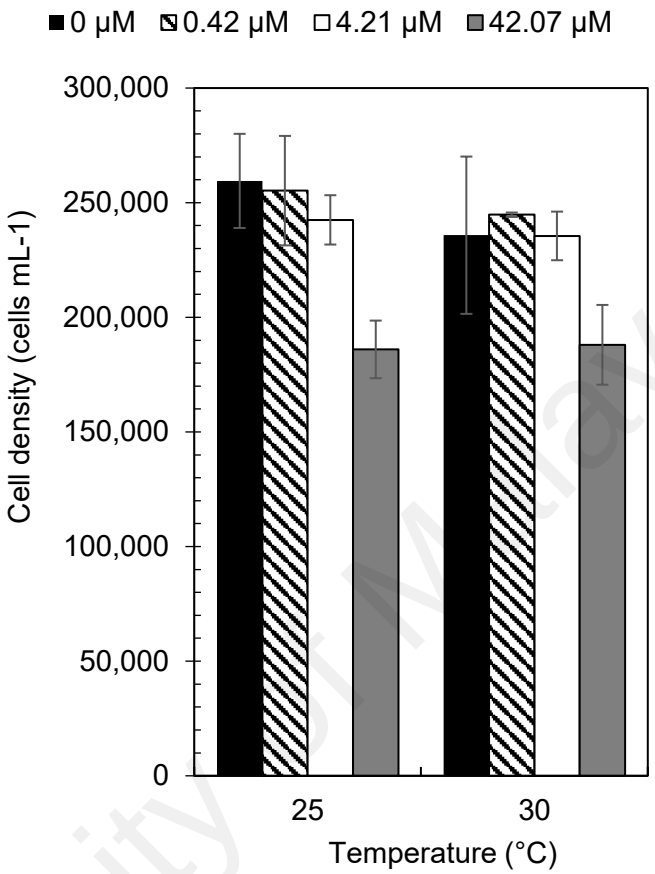

Figure 4.21: Effects of temperature and various Ni concentrations on the cell density (mean ±SD) of *C. augustae*.

Table 4.19: Summary of two-way ANOVA testing the combined effect of Ni concentrations and temperature (25 and 30°C) on the physiological and photosynthetic parameters of *C. augustae*

Parameter	Source of variation	SS	*df*	F	Sig.
Cell density	Temperature	9.77×10^{9}	1	43.166	0.000
	Ni	4.17×10^{10}	3	61.450	0.000
	Temperature * Ni	2.54×10^{9}	3	3.745	0.024
	Error	5.43×10^{9}	24		
F_v/F_m	Temperature	0.072	1	1552.596	0.000
	Ni	0.015	3	108.633	0.000
	Temperature * Ni	0.012	3	86.667	0.000
	Error	0.013	280		
NPQ	Temperature	0.046	1	131.526	0.000
	Ni	0.005	3	4.581	0.011
	Temperature * Ni	0.003	3	2.587	0.077
	Error	0.008	24		
qP	Temperature	0.110	1	168.971	0.000
	Ni	0.011	3	5.808	0.004
	Temperature * Ni	0.005	3	2.767	0.064
	Error	0.016	24		
qN	Temperature	0.003	1	24.586	0.000
	Ni	0.000	3	1.145	0.351
	Temperature * Ni	4.313×10^{-5}	3	0.127	0.943
	Error	0.003	24		
Alpha (α)	Temperature	0.000	1	0.425	0.521
	Ni	0.002	3	0.567	0.642
	Temperature * Ni	0.000	3	0.104	0.957
	Error	0.027	24		
$rETR_m$	Temperature	1.97×10^{-4}	1	169.884	0.000
	Ni	1.64×10^{3}	3	4.691	0.010
	Temperature * Ni	6.63×10^{2}	3	1.900	0.157
	Error	2.79×10^{3}	24		
E_k	Temperature	4.60×10^{4}	1	115.990	0.000
	Ni	4.67×10^{3}	3	3.929	0.021
	Temperature * Ni	1.67×10^{3}	3	1.408	0.265
	Error	9.51×10^{3}	24		
ROS	Temperature	9.57×10^{8}	1	34.232	0.000
	Ni	3.44×10^{8}	3	4.097	0.025
	Temperature * Ni	7.81×10^{7}	3	0.932	0.448
	Error	4.47×10^{8}	16		
Metal content in biomass	Temperature	1.29×10^{-6}	1	5.485	0.032
	Ni	5.44×10^{-5}	3	77.389	0.000
	Temperature * Ni	1.97×10^{-6}	3	2.795	0.074
	Error	0.073	16		

SS = sum of squares; *df* = degree of freedom

4.4.3 Photosynthetic performance

Photosynthetic performance was negatively correlated with temperature. Table 4.20 and Figure 4.22 show the photosynthetic efficiency of *C. augustae* in response to warming and excess Ni in the media. According to the summary of two-way ANOVA in Table 4.19, temperature induced a significant impact on all parameters except light harvesting efficiency (alpha, α). The maximum quantum yield of PSII (F_v/F_m) remained fairly consistent under all conditions (Figure 4.22A). Overall, the cells remained photosynthetically active after 24 h exposure as the F_v/F_m remained above 0.6.

Figure 4.22B shows that the NPQ was altered in response to warming and excess Ni. An increase in NPQ value was observed in Ni-supplemented cultures at 25 and 30°C, indicating that the cells mitigated the stress effect of excess Ni through heat dissipation. The NPQ values were generally higher at 25°C than at 30°C. At 25°C, the NPQ value increased from 0.39 ± 0.03 in *Chlamy*-0Ni to 0.43 ± 0.02 in *Chlamy*-0.42Ni, 0.44 ± 0.01 in *Chlamy*-4.21Ni and 0.42 ± 0.01 in *Chlamy*-42.07Ni. At 30°C, the NPQ value increased from 0.33 ± 0.01 in *Chlamy*-0Ni to 0.37 ± 0.02 in *Chlamy*-42Ni. Based on the results from univariate analysis, temperature and the excess Ni induced a significant impact on NPQ ($p < 0.05$). Overall, the qP values were higher at 30°C than 25°C. At 30°C, the qP values slightly decreased with increasing concentration of Ni. The qN values of cultures supplemented with Ni were higher than *Chlamy*-0Ni.

The light harvesting efficiency (alpha, α), $rETR_m$ and E_k values were also demonstrated in Table 4.20. The α values did not vary considerably across all conditions. Increased doses of Ni had remarkably impacted on the $rETR_m$ (Figure 4.22C). Overall, the $rETR_m$ values were lower at 30°C. The $rETR_m$ of *Chlamy*-0Ni at 30°C was nearly 40 % lower than that of 25°C. At 30°C, the value increased from 75.43 ± 2.30 in *Chlamy*-0Ni to 100.68 ± 12.87 in *Chlamy*-42Ni. The saturation irradiance for electron transport,

E_k was also impacted by warming and excess Ni in the culture medium ($p < 0.05$) (Figure 4.22D). Interestingly, the E_k values were generally higher at 30°C. At 25°C, the value was 197.41 ± 38.47 in *Chlamy*-0Ni and increased to 231.72 ± 4.18 in *Chlamy*-0.42Ni, 225.77 ± 9.99 in *Chlamy*-4.21Ni, and 209.76 ± 9.66 in *Chlamy*-42Ni. At 30°C, the value was 117.56 ± 7.01 in *Chlamy*-0Ni and increased to 138.51 ± 16.80 in *Chlamy*-0.42Ni, 148.72 ± 27.62 in *Chlamy*-4.21Ni, and 156.67 ± 19.65 in *Chlamy*-42Ni.

Table 4.20: Effects of temperature and various Ni concentrations on the photosynthetic performance of *C. augustae*

Temperature (°C)	**[Cu] (µM)**	**F_v/F_m**	**NPQ**	**qP**	**qN**	**$rETR_m$**	**alpha**	**E_k**
25	0	0.68	0.40	0.69	0.12	126.71	0.65	197.41
	50	0.68	0.43	0.63	0.13	146.00	0.63	231.72
	150	0.69	0.44	0.63	0.12	144.60	0.64	225.77
	250	0.68	0.42	0.65	0.12	135.55	0.65	209.76
30	0	0.63	0.33	0.79	0.10	75.43	0.64	117.56
	50	0.65	0.33	0.78	0.11	86.38	0.62	138.51
	150	0.66	0.35	0.76	0.10	91.65	0.62	148.72
	250	0.67	0.37	0.73	0.11	100.68	0.64	156.67

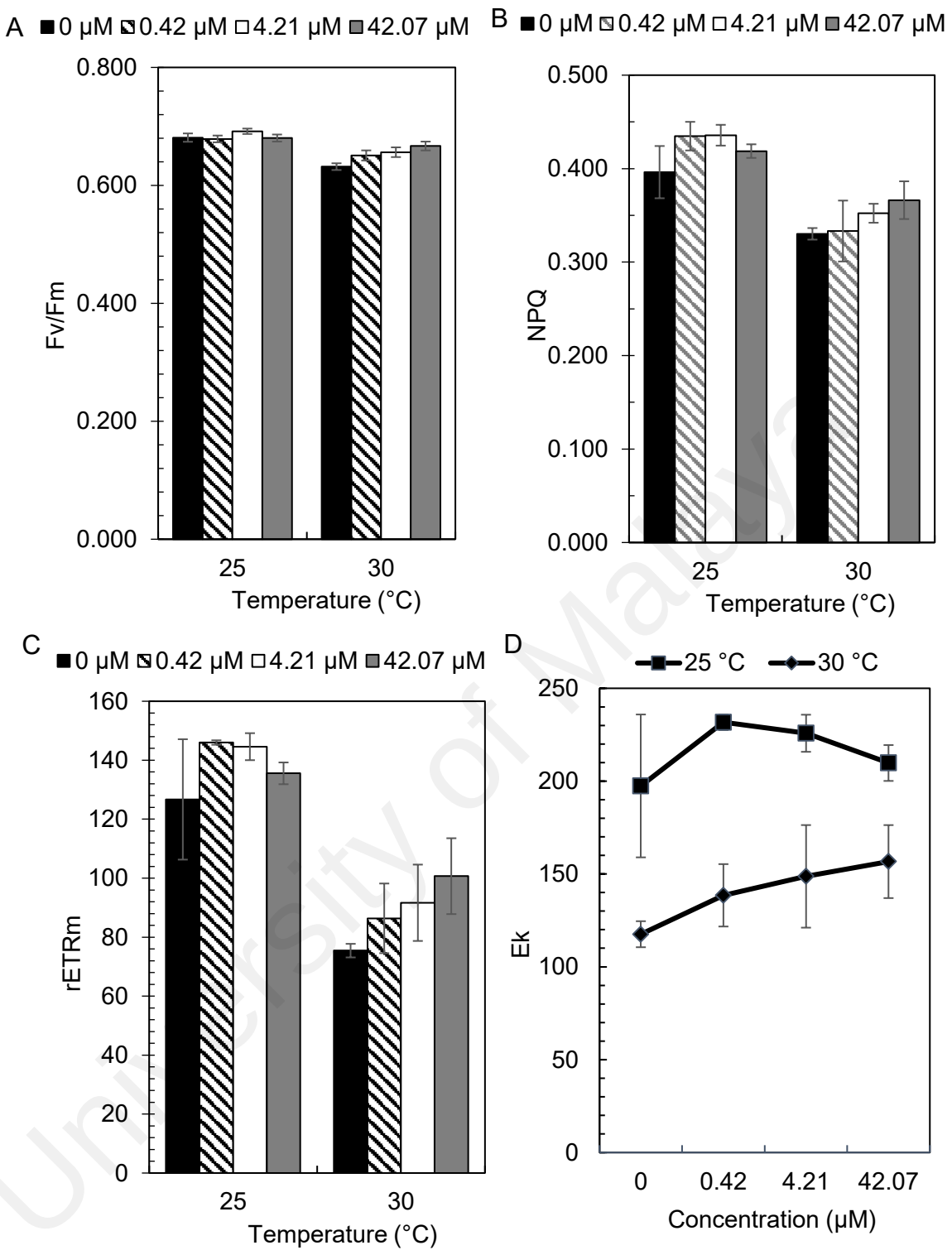

Figure 4.22: Photosynthetic performance (F_v/F_m, NPQ, $rETR_m$, and E_k) of *C. augustae* (mean ± SD) exposed to various Ni concentrations at 25 and 30°C.

4.4.4 ROS levels

The results showed that the levels of DCF-Fluorescence were higher at 30°C than at 25°C (Figure 4.23). Overall, temperature and excess Ni induced significant changes in the ROS levels ($p = 0.000$ and $p = 0.025$ respectively) whereas the effects of the combined factors were not significant ($p > 0.05$). The representative histograms generated from the flow cytometer are shown in Appendix C.

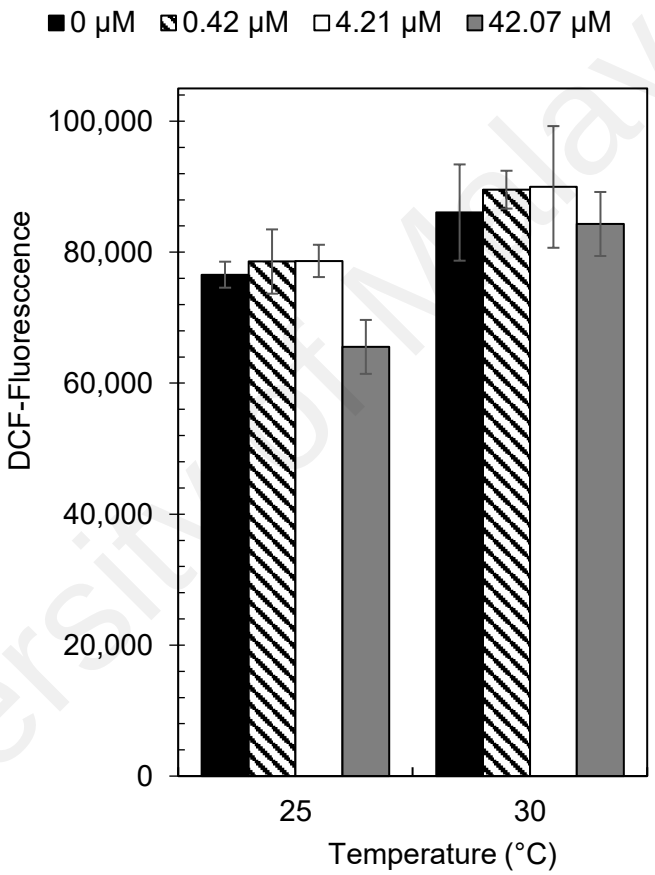

Figure 4.23: Fluorescence of DCF (corresponding to ROS levels) of *C. augustae* (mean ± SD) exposed to various Cu concentrations at 25 and 30°C.

4.4.5 Metal content in biomass

The results showed that the algal biomass was able to absorb substantial amount of Ni, especially at 42.07 µM (Figure 4.24). *Chlamy*-42Ni was able to accumulate around 0.4 – 0.005 pg cell^{-1} Ni in their biomass.

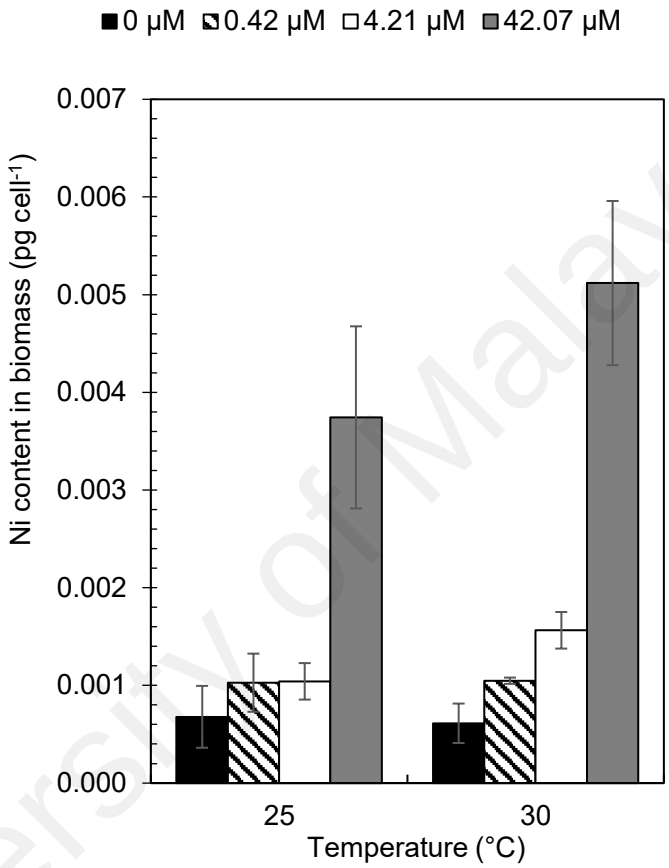

Figure 4.24: Nickel content in the biomass of *C. augustae* (mean ± SD) exposed to various Ni concentrations at 25 and 30°C.

4.4.6 Metabolic profile

Figure 4.25 showed the results from the ANOVA simultaneous component analysis (ASCA). Based on the statistical values, temperature contributed to the most differentiation among the samples and accounted for 100% variation across all platforms. Nickel accounted for 46.48%, 46.64% and 49.42% variation respectively for data generated by GCMS and LCMS in positive and negative modes. Interaction between the

two factors resulted in 78.28% variation for data generated by GCMS, accompanied by 76.39% and 47.57% variation for data generated by both modes in LCMS.

Generally, pathway analysis with MetaboAnalyst demonstrates that the changes of the metabolic expression were mainly involved in the amino acid, energy, and lipid metabolisms (Figure 4.26). Nickel treatment on *C. augustae* affected pathways such as lysine biosynthesis, phenylalanine, tyrosine and tryptophan biosynthesis, phenylalanine metabolism, ascorbate and aldarate metabolism, tyrosine metabolism, glutathione metabolism and glycine, serine and threonine metabolism. Temperature affected metabolites involved in the phenylalanine pathway, tropane, piperidine and pyridine alkaloid biosynthesis, pantothenate and CoA biosynthesis, glyoxylate and dicarboxylate metabolism, and glutathione metabolism. The combined factors affected tropane, piperidine and pyridine alkaloid biosynthesis, phenylalanine metabolism, pantothenate and CoA biosynthesis, phenylalanine, tyrosine, and tryptophan biosynthesis, flavone and flavonol biosynthesis and glutathione metabolism.

Table 4.21 shows the top key pathways and metabolites corresponding to each factor. The most significant pathway associated with the interactive effects of temperature and Ni toxicity was tropane, piperidine and pyridine alkaloid biosynthesis (p = 0.01; impact score of 0.00). The second most significant pathway was phenylalanine metabolism (p = 0.01; impact score of 0.50), followed by pantothenate and CoA biosynthesis (p = 0.04; impact score of 0.15). The top most significant pathways involved in the Ni treatment were lysine biosynthesis (p = 0.02; impact score of 0.24), and phenylalanine, tyrosine and tryptophan biosynthesis (p = 0.03; impact score of 0.10). The top most significant pathways involved in the temperature treatment were tropane, piperidine and pyridine alkaloid biosynthesis (p = 0.04; impact score of 0.00), and phenylalanine metabolism (p = 0.04; impact score of 0.50). The expression levels of annotated metabolites such as

sulfur-containing compounds, amino acids, and nitrogenous metabolites were significantly affected.

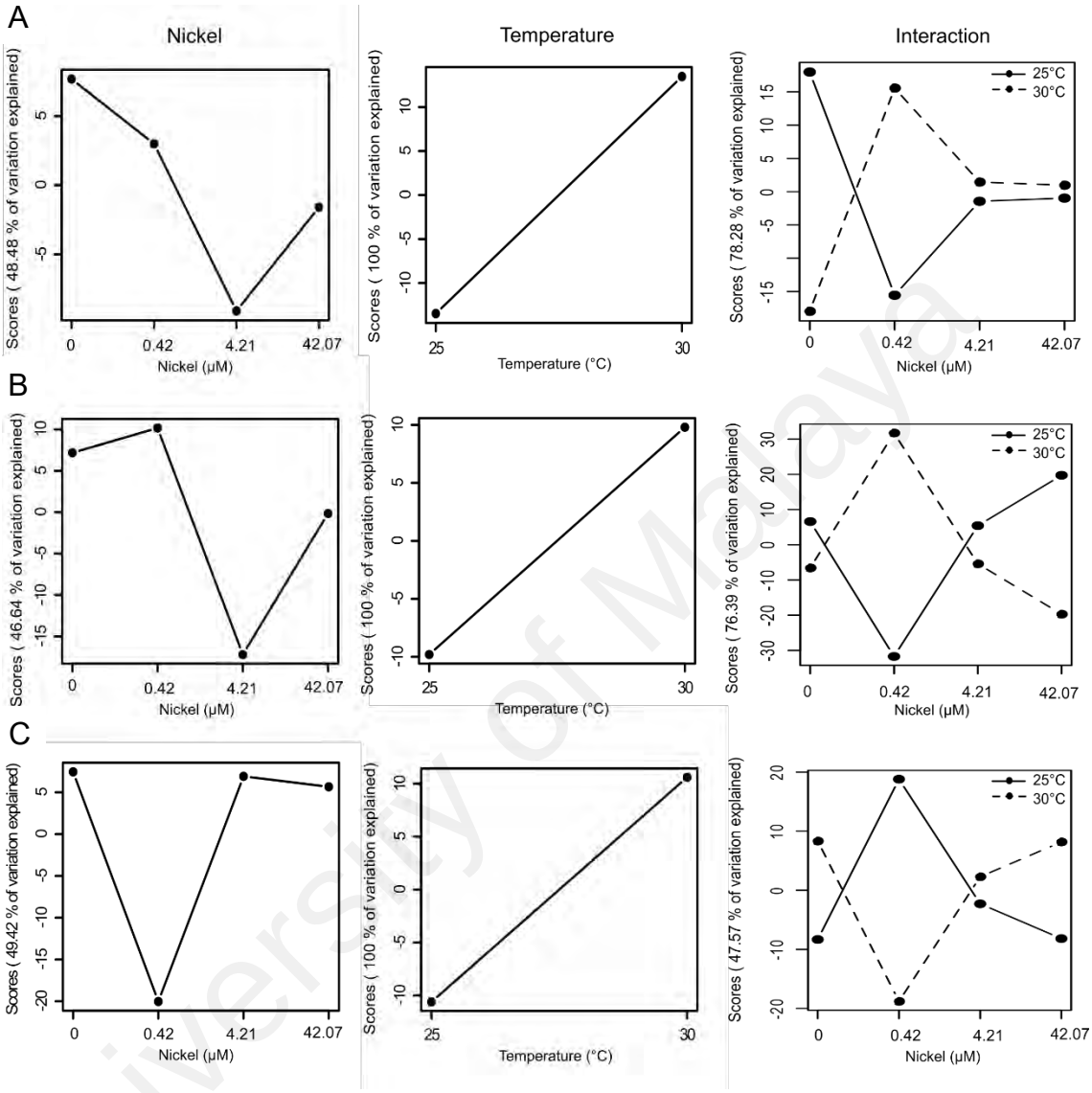

Figure 4.25: Results of ANOVA simultaneous component analysis (ASCA) showing the major patterns associated with temperature, concentration of Ni, and their interaction on *C. augustae* for (A) GCMS, (B) LC-positive and (C) LC-negative data sets.

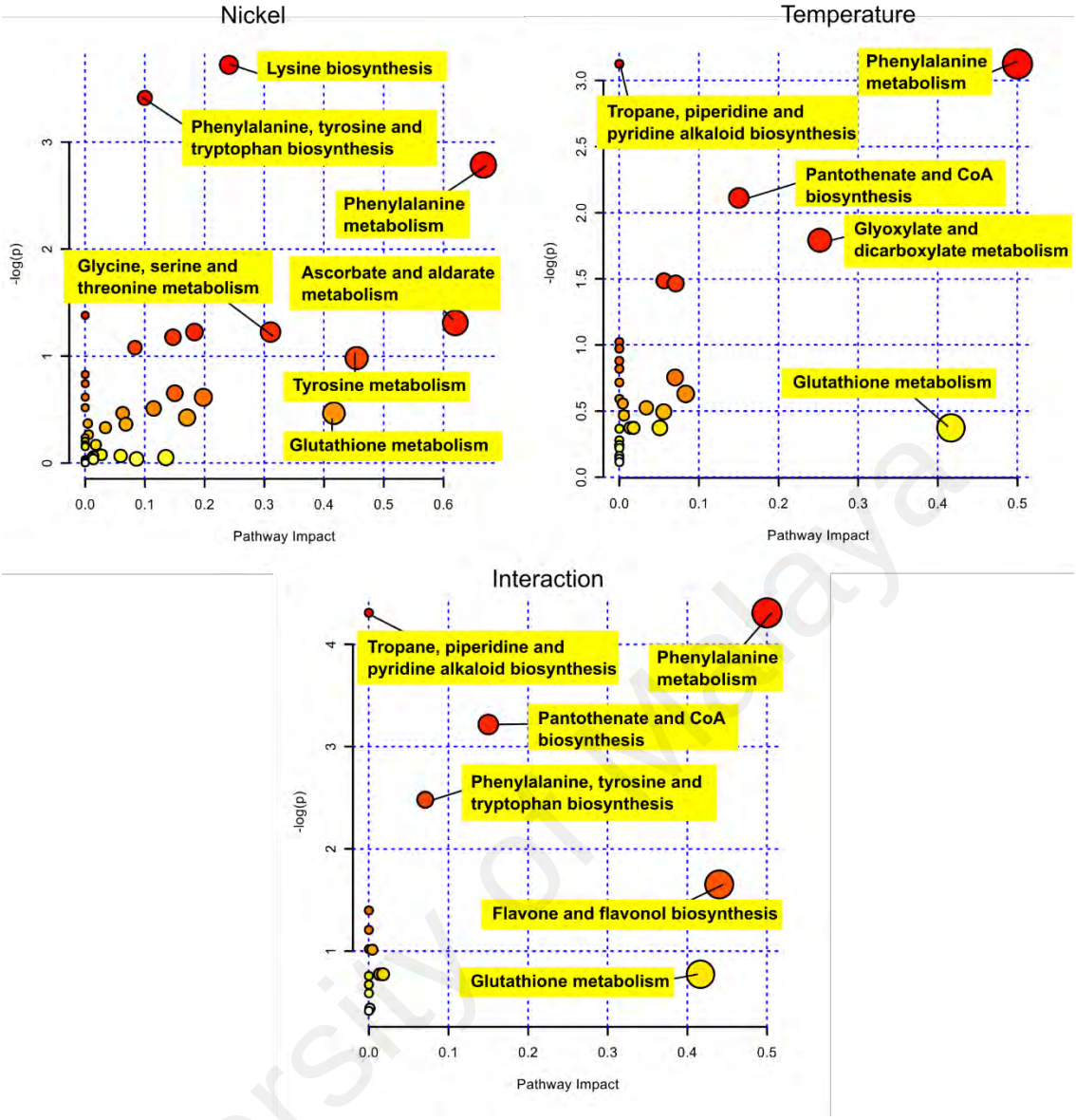

Figure 4.26: Key pathways involved in the stress response of *C. augustae* to Ni, temperature and the interaction between the two factors.

Table 4.21: Significant pathways and compounds involved in the response of *C. augustae* to Ni toxicity (a), temperature (b) or the interactive effects (ab)

Factor	Pathway	Total	Hits	Raw p	FDR	Impact	Hits
a	Lysine biosynthesis	10	4	0.02	1	0.24	Diaminopimelic acid; Homoserine; Saccharopine; Lysine
a	Phenylalanine, tyrosine and tryptophan biosynthesis	21	6	0.03	1	0.10	Phenylpyruvic acid; Shikimic acid; Phosphoenolpyruvic acid; Tryptophan; Phenylalanine; 4-Hydroxyphenylpyruvic acid
ab	Tropane, piperidine and pyridine alkaloid biosynthesis	8	2	0.01	0.59	0.00	Phenylalanine; Tropinone
ab	Phenylalanine metabolism	8	2	0.01	0.59	0.50	Phenylalanine; Phenylacetaldehyde
ab	Pantothenate and CoA biosynthesis	14	2	0.04	1	0.15	Valine; Pantothenic acid
b	Tropane, piperidine and pyridine alkaloid biosynthesis	8	2	0.04	1	0.00	Phenylalanine; Tropinone
b	Phenylalanine metabolism	8	2	0.04	1	0.50	Phenylalanine; Phenylacetaldehyde

CHAPTER 5: DISCUSSION

5.1 Interactive effects of Cu toxicity and temperature on green microalgae

Based on the calculation from the Visual Minteq equilibrium software, metal speciation and free ion activities were temperature-dependent (Byrne et al., 1988). Table 4.1 shows that the free Cu^{2+} concentrations at 25°C were higher than the concentrations at 35°C. Table 4.7 shows that the Cu^{2+} concentrations of BBM supplemented with 150 and 250 µM Cu were lower at 30°C compared to 25°C. The estimated chemical activities of Cu^{2+} were higher at 30 and 35°C compared to 25 °C in media supplemented with Cu concentrations higher than 150 µM.

Warming and Cu toxicity did not significantly decrease the cell density of *S. quadricauda* after the exposure for 6 days. Microalgae are generally adaptive to a wide range of Cu concentrations. For example, cell growth was not altered in *P. subcapitata* and *C. vulgaris* over the wide range of 10^{-9} to 10^{-3} M total Cu (Knauert & Knauer, 2008). *Scenedesmus subspicatus* was reported to exhibit optimal growth rate over a broad range of Cu^{2+} (10^{-15} to 10^{-7} M) (Knauer et al., 1997). On the contrary, the range of Cu concentrations used in this study induced a concentration-dependent decrease in the cell density of *C. augustae*. The species demonstrated higher sensitivity to Cu as the cell density decreased significantly with increasing concentrations of Cu. At 30°C, the cell density in *Chlamy*-250Cu was 39% lower than that of *Chlamy*-0Cu.

Heavy metals such as Cu, Pb, and Ni have been shown to substitute the magnesium ions in chlorophyll molecules. The substituted pigment molecules are inefficient for photosynthesis due to the changes in both absorption spectra and fluorescence quantum yields (Küpper et al., 2003). In this study, the *in vivo* absorption spectra were affected by temperature and Cu concentrations. Treatment of *S. quadricauda* cells with Cu resulted in a shift of the red absorbance maximum from 678 nm to 685 nm due to the formation

of Cu-chlorophylls (Küpper et al., 1998). The *in vivo* absorption spectra of a dinoflagellate, *Alexandrium tamarense* showed changes in the blue absorption peak when exposed to different levels of iron, indicating a change in pigment content and composition (He et al., 2010).

Excess Cu^{2+} levels in the culture was reported to impair photosynthesis sooner than cell division (Küpper et al., 2003). Various photosynthetic parameters in this study (such as F_v/F_m, NPQ, qP, qN, alpha, $rETR_m$ and E_k) showed that the photosynthetic activities were markedly affected by temperature and Cu toxicity.

Freshwater green algae were reported to adapt to a wide range of temperature by executing efficient light energy partitioning between non-photochemical quenching, alternative electron pathways and growth (Fanesi et al., 2016). The site of Cu inhibitory effect on PSII photochemistry is associated with the function of PSII water splitting system. Inhibition of PSII photochemistry resulted in excess excitation energy de-excited by thermal dissipation processes, known as NPQ. Based on the results, the F_v/F_m ratio of *S. quadricauda* and *C. augustae* remained above the value of 0.6, indicating that the cells were still photosynthetically active and viable.

According to the results on NPQ and qN, *S. quadricauda* might be dissipating excess energy as heat to combat the interactive effects of warming and Cu toxicity. High qN values in the Cu-treated cultures on day 3 might be attributed to increased self-protection against photoinhibition under Cu stress, as observed in *C. reinhardtii* exposed to different concentrations of Cu (Jiang et al., 2016). The NPQ values increased as the concentrations of Cu^{2+} increased in the culture medium of *S. incrassatululus* (Perales-Vela et al., 2007). The qN value was also reported as the indicative photosynthetic biomarkers for Cu effect in *S. obliquus* (Dewez et al., 2005). Based on the study by Oukarroum et al. (2012b), increased temperature induced more significant changes to PSII quantum yield, primary

electron transport and decrease in total photosynthetic performance compared to the Cu effect alone. The same study also reported that the interactive effects of high temperature and Cu toxicity increased energy dissipation via non-photochemical pathway in *C. vulgaris*. The NPQ values in *C. augustae* did not increase as anticipated. This indicates that the cells might utilize other mechanism to dissipate excess energy. The decline in E_k at both high temperature and Cu concentration were observed in *C. augustae*. This phenomenon is often regarded as a mechanism to mitigate the consequence of over-saturation and the damaging effect on the photosynthetic apparatus (Malapascua et al., 2014). The $rETR_m$ of *C. augustae* was also markedly decreased in response to warming and Cu toxicity, indicating a damage in the PSII.

Increased ROS levels observed in this study were consistent with other studies on the abiotic stress response of microalgae. Previous studies highlighted that ROS or oxidative stress were primarily involved in Cu toxicity to *P. subcapitata* and *C. vulgaris* (Knauert & Knauer, 2008), *Cylindrotheca closterium*, *Phaeodactylum tricornutum*, and *Rhodomonas salina* (Lozano et al., 2014). Similar findings were also observed in *C. ehrenbergii* where Cu reduced the F_v/F_m ratio, increased production of ROS, and induced severe physiological damage within the cells (Wang et al., 2017). Increased levels of ROS might trigger a series of antioxidant systems for survival and adaptation. Genes and antioxidant enzymes involved in the oxidative stress defence mechanisms were differentially expressed to acclimatize to heavy-metal stress in *C. reinhardtii* (Jamers et al., 2006; Nowicka et al., 2016). Copper toxicity in *S. bijugatus* activated the glutathione metabolism and increased the activities of antioxidant enzymes (Nagalakshmi & Prasad, 2001).

This study implied that sub-optimal temperature and Cu toxicity induced remarkable metabolic perturbations in *S. quadricauda*. Overall, it was observed that high temperature

and excess Cu interfered with the levels of amino acids, fatty acids and sugars in *S. quadricauda* and *C. augustae*. This finding is consistent with other metabolomics studies where primary metabolites (sugars, amino acids, organic acids, and inorganic acids) are involved in the survival and adaptation to metal toxicity (Jamers et al., 2013b; Kováčik et al., 2016; Zhang et al., 2015). The general mechanisms in the metabolic network restructuring involve galactose metabolism, starch and sucrose metabolism, biosynthesis of fatty acids, and biosynthesis of amino acids (Wang et al., 2015).

In *S. quadricauda*, the decreased levels of carbohydrates might be attributed to reduced energy supply from photosynthesis and activation of catabolic processes for energy supply (Kluender et al., 2008). Proline was reported to be involved in photosynthetic organisms in response to a wide range of abiotic and biotic stresses (Hamed et al., 2017). Proline accumulation in the cells was reported to be an important strategy to overcome oxidative threat imposed by 7-day exposure of *Scenedesmus* sp. to elevated levels of Cu^{2+} (Tripathi et al., 2006). Exogenous supply of proline decreased the inhibitory effects of metal-induced toxicity by protecting cells from oxidative stress, counteracting lipid peroxidation, reducing adsorption of Cu in algal cells and potassium ion efflux (Oukarroum, 2016). *Scenedesmus quadricauda* was able to develop a reversible high resistance towards Cu^{2+} by intricate regulation of cell cycle, thylakoid ultrastructure and metal transporter proteins (Küpper et al., 2003). Changes in carbohydrate and amino acid metabolism observed in this study are consistent with findings from Zhang et al. (2015), where metabolic profile of *Chlorella* sp. exposed to Cu showed a decrease in sucrose and amino acids such as alanine, glutamate, lysine and arginine. The change of monosaccharide levels in this study is in agreement with the metabolite profile of *Acutodesmus obliquus* exposed to lead, where the reduced monosaccharide content might be due to degradation of photosynthesis pigments and sugar accumulation (Piotrowska-Niczyporuk et al., 2015). Fatty acids were differentially regulated by both temperature

and Cu treatment. Transcripts related to fatty acid synthesis pathway has been found to be affected by Cu toxicity on *C. acidophila* (Olsson et al., 2015). Other metabolites such as polyphosphate bodies, reduced glutathione (GSH) and phytochelatins also played vital roles in the detoxification of Cu in microalgae (Zhang et al., 2015; Adams et al., 2016). High Cu concentration induced redox imbalance by decreasing organic osmolytes such as glycerophosphocholine and betaine in *C. vulgaris* (Zhang et al., 2014). When metal ions are present at high concentrations, organisms may produce organic acids to enhance the formation of metal-organic complexes to lower bioavailability and toxicity of metal ions (Prapaipong et al., 1999).

Warming and excess Cu interfered with the levels of amino acids and polyamines in *C. augustae*. Glutathione metabolism was involved in the response to excess Cu, warming and the interaction of the two factors. Glutathione (GSH) is a sulfur-containing tripeptide that protects cells from HMs by quenching ROS and involves in phytochelatin synthesis. Sulfur metabolism was also identified as one of the most significant pathways. Excess Cu ions might bind to protein-SH group, modify protein structure, and subsequently inhibit enzymes with sulfhydryl groups in their activity centres (Seregin and Kozhevnikova, 2006). In response, microalgae might regulate the synthesis and catabolism of protein-SH (e.g. glutathione and phytochelatin) to resist Cu toxicity (Huang et al. 2018). Taurines were involved in osmoregulation in the response of microalgae to increased salinity and pollutants (Tevatia et al. 2015; Wang et al. 2019). Amino acid and protein metabolisms were also involved in the microalgal response. These pathways include the tropane, piperidine and pyridine alkaloid biosynthesis, phenylalanine metabolism, and isoquinoline alkaloid biosynthesis pathways. In general, amino acids are the key organic osmolytes and metal chelators in plants (Singh et al. 2016). Other amino acid derivatives, organic acids and peptides are also involved in reducing the formation of free radicals and maintaining homeostasis (Jamers et al., 2013; Wang et al., 2015; Zhang et al., 2015).

Zeatins are phytohormones involved in the growth of photosynthetic organisms and was reported to be enhanced in response to HMs (Miazek et al., 2015). The pantothenate and CoA biosynthesis involved in the response of *C. augustae* to Cu was associated with the synthesis of coenzyme A and the acyl carrier proteins. This finding was consistent with other studies where the pathway was significantly regulated in the response to calcium stress in yeasts and heat stress in corals (Hillyer et al., 2016; Jenkins et al., 2013).

5.2 Interactive effects of Ni toxicity and temperature on green microalgae

The South East Asian Melanesian (SEAM) region has the largest Ni lateritic ore deposits in the world (Gissi et al., 2016). The increasing demand of Ni in the electronic, chemical and manufacturing industries will contribute to the increasing Ni contamination in the surrounding areas. Nickel is required by microalgae as a micronutrient for metalloprotein and enzyme activity in minute (picomolar to micromolar) concentrations (Muyssen et al., 2004). For example, Ni^{2+} concentrations in the range of 0.1 – 1 µM was required by marine diatom *Cyclotella cryptica* to synthesize urease and utilize urea as the nitrogenous source (Oliveira & Antia, 1984). Concentrations in micromolar were shown to be toxic to microalgae and initiated stress response (Deleebeeck et al., 2009).

The Ni concentrations used in this study (0.42, 4.21, 42.07 µM, or expressed as 0.1, 1.0, 10.0 ppm) represented a wide range of Ni content found in the natural unpolluted freshwaters and polluted industrial wastewater (Binet et al., 2018). The amount of Ni in unpolluted freshwaters usually ranged from 0.0005 – 0.02 ppm. Nickel concentrations in the range of 0.1 to 2 ppm were sufficient to be toxic to marine diatoms (Panneerselvam et al., 2018). The same study also reported that the total dissolved Ni concentration in the water should not exceed 13 ppb to protect 95% of the plankton species in the ecosystem. The viability of *C. vulgaris* decreased by 97% upon exposure to 10 and 100 mg L^{-1} of Ni oxide nanoparticles (Oukarroum et al., 2017). The IC_{10} values (Ni concentration required

to induce 10% inhibition in population growth rate) ranged from 340 to 6100 µg L^{-1} (estimated to be 0.34 – 6.1 ppm Ni) in microalgae and cyanobacterium over 72 h exposures (Gissi et al., 2016).

Heavy metal uptake and toxicity on the biological system are influenced by many factors such as temperature, pH, and duration of exposure. Temperature affects metal toxicity by altering metal speciation, activity, ion biosorption capacity and formation of ligand complexes (Suresh Kumar et al., 2015). In this study, the bioavailability of Ni^{2+} to algal cells was higher at 35°C based on the calculation from the chemical equilibrium software. The results indicate that the estimated chemical activities of Ni^{2+} (pNi = -log Ni^{2+} activity) did not vary considerably between 25, 30, and 35°C.

The ability of *S. quadricauda* to thrive at 35°C was in agreement with the temperature study by Hanagata et al. (1992), where the growth rate of *Scenedesmus* was higher at 35°C compared to 25°C. In this study, the cell density of *S. quadricauda* remained fairly consistent at 25°C. The cell densities were generally higher at 35°C compared to 25°C, despite the reduced cell density with the increasing concentration of Ni at 35°C. the cell density of *C. augustae* decreased with increasing Ni concentrations. The inhibition of cell division due to Ni toxicity had been reported in *C. vulgaris* and *C. miniate* after 24 h exposure to Ni (Wong et al., 2000). The decrease in cell density observed in the present study might be associated with the decrease in photosynthetic efficiency and increased ROS production (Dao & Beardall, 2016a).

Overall, the results from PAM fluorometry suggested that the photosynthetic parameters of *S. quadricauda* were affected by Ni at 42.07 µM. This observation is consistent with other previous studies which reported that Ni in high doses significantly interfered with the photosynthetic process by affecting PSII, active sites of the oxygen-evolving complex and electron transport chain proteins (Koppel et al., 2017). The $rETR_m$

values were higher at 35°C, indicating increased electron flow in the electron transport chain to maximize photosynthetic efficiency (Barati et al., 2018). The $rETR_m$ of *S. quadricauda* decreased with increasing Ni concentrations, indicating a damage in the PSII. Nickel concentrations ranging between 2.25 – 180 mg/L (estimated to be 9.5 – 757 µM) greatly decreased the values of ETR and photosynthetic yields in *Euglena gracilis*, a common freshwater alga (Ahmed & Häder, 2010). In this study, the value for NPQ increased in cells exposed to 42.07 µM Ni at 25°C and 4.21 µM Ni at 35°C. Similar results were also reported by Yong et al. (2018) where the increase in NPQ values were observed in *S. quadricauda* exposed to Cu and warming. This indicates that the cells utilized the thermal dissipation process to mitigate over-saturation and the damaging effects of abiotic stresses on the photosynthetic apparatus. The exposure of algal cells to concentrations up to 42 µM Ni did not affect the F_v/F_m which indicates that the light harvesting efficiency of PSII remains undamaged. Freshwater green algae can adapt to a wide range of temperature through efficient light energy partitioning between NPQ, alternative electron pathways, and growth (Fanesi et al., 2016). The impact of Ni on photosynthesis can also occur via displacement of essential ions from molecules, reduction of chlorophyll pigments and disruption of photosynthetic apparatus (Yusuf et al., 2011). Nickel oxide nanoparticles in the range of 0.01 – 100 mg L^{-1} decreased the total chlorophyll content by 75 – 97% and changed the morphological structures of *C. vulgaris* (Oukarroum et al., 2017). Ultrastructural studies of the chloroplast of *C. vulgaris* revealed that the grana lamella in the thylakoids were disorganized after being exposed to nanoparticles of nickel oxide (Gong et al., 2011). On the other hand, the $rETR_m$ values of *C. augustae* were lower at 30 and markedly increased in response to high Ni concentrations in the media. The E_k values at 30°C were also lower than that of 25°C. Overall, the results show that *C. augustae* was more sensitive to warming than Ni toxicity. Freshwater green algae can adapt to a wide range of temperature through efficient light

energy partitioning between NPQ, alternative electron pathways, and growth (Fanesi et al., 2016).

The relative ROS level was the highest in *S. quadricauda* exposed to 42.07 μM Ni at 35°C, suggesting that the combination of temperature and Ni toxicity induced a strong oxidative stress response in the cells. Nickel is an essential cofactor for superoxide dismutase to regulate cellular ROS levels and protect nitrogenase which are involved in carbon and nitrogen fixation (Rodriguez & Ho, 2014). However, when present in excess, transition metals like Ni produced free radicals through Fenton or Haber-Weiss reaction, induced ROS generation and increased the activity of antioxidant enzymes (Sun et al., 2017). For instance, the enzyme activities of catalase, glutathione peroxidase, and superoxide dismutase were affected by sub-lethal concentrations of Ni (Martínez-Ruiz & Martínez-Jerónimo, 2015). Excess metals also induced generation of free radicals and ROS through direct transfer of electron in inactivation and down-regulation of the enzymes of the antioxidative defence system such as glutathione reductase in other photosynthetic organisms (Nagajyoti et al., 2010). The ROS levels in *C. augustae* were higher at 30°C than at 25°C, indicating that the species is more sensitive to warming than Ni toxicity. Overproduction of ROS due to interruption of redox homeostasis may lead to cell death and reduced viable cell population (Oukarroum et al., 2017).

Microalgae are potential candidates for phycoremediation due to their high efficiency in sequestering various metal ions such as Ni, Cd, Cu and Pb from industrial wastewater (Suresh Kumar et al., 2015). In this study, *S. quadricauda* accumulated higher amount of Ni at 25°C compared to 35°C. No significant difference was observed in the Ni content in the biomass of *C. augustae* at 25 and 30°C. High metal uptake capability of microalgae is attributed to their large surface area and complex cell wall structure. The *S. quadricauda* culture isolated from wastewater could take up around 0.04 mg Ni per gram

of biomass possibly because each colony consists of two, four or eight cells attached together and four long spines that are extended from the cell envelope which enhance the metal binding surface area (Chong et al., 2000). The binding capacity of silver nanoparticles on the biomass of *C. vulgaris* was shown as a function of temperature and initial Ni^{2+} concentration (Aksu, 2002).

In general, the biochemical adaptation and tolerance strategies of photosynthetic organisms can be divided into six main categories: (i) protection by physical barriers; (ii) synthesis of phytochelatins and metallothiones; (iii) differential expression levels of N-containing compounds such as proline, arginine, and polyamines; (iv) regulation of growth regulators; (v) increased activities of antioxidant enzymes; and (vi) differential expression levels of S-containing compounds (Sachan & Lal, 2017).

The metabolomic analysis provides a valuable insight into the complex adaptation mechanisms to interactive effects of temperature and heavy metals. In this study, sulfur metabolism was identified as one of the most significant pathways and sulfur-containing metabolites were significantly involved in the response to Ni toxicity under different temperatures. Heavy metal toxicity is highly dependent on their binding to various ligands primarily sulfhydryl groups (R-SH) and the levels of thiols. Excess Ni can bind to protein-SH group, modify protein structure, and inhibit enzymes containing sulfhydryl groups in their activity centres (Seregin & Kozhevnikova, 2006). In response, microalgae might regulate the synthesis and catabolism of protein-SH (e.g. glutathione and phytochelatin) to resist Ni toxicity (Huang et al., 2018). Previous studies reported that the macromolecules content in microalgae varied greatly after they were exposed to Ni (Martínez-Ruiz & Martínez-Jerónimo, 2015). Organic osmolytes such as amino acids, soluble sugars, and soluble proteins are crucially involved in the biochemical responses of photosynthetic organisms under stress conditions. In this study, pathways related to

amino acid metabolism (cysteine and methionine metabolism, alanine, aspartate and glutamate metabolism, and phenylalanine metabolism) were significantly affected. Amino acids including cysteine, acetylserine, aspartic acid, and glutamic acid were also dysregulated in response to the combined stresses. These findings are consistent with other studies in which proteins were reported to chelate metal ions and reduce free heavy metals in plants (Singh et al., 2016). For example, time-course changes in soluble proteins were associated with the maximum ratios of Ni reduced by *C. vulgaris* (Gong et al., 2011). Nickel also induced free amino acids accumulation in plants, particularly alanine, aspartic acid, cysteine and proline (Yusuf et al., 2011). The cellular lipid concentrations of a polar microalga, *Cryothecomonas armigera* decreased by 40% after being exposed to 1.95 ppm Ni (Koppel et al., 2017). Based on the metabolomics data, changes in metabolites related to glycolysis and gluconeogenesis metabolism suggested that the combined factors influenced the carbohydrate and energy metabolism pathways, suggesting an increased energy expenditure and metabolization of glucose via glycolysis. Carbohydrates including polysaccharides and organic acids such as malic and citric acid were highly involved in the response to excess Ni through binding to metal ions (Kaplan, 2013). The concentrations of carbohydrates were significantly different in *Ankistrodesmus falcatus* exposed to Ni (Martínez-Ruiz & Martínez-Jerónimo, 2015). Dissolved organic carbons (DOC) released by microalgae can also complex with heavy metals to reduce cellular toxicity (Huang et al., 2018). In this study, nitrogen metabolism was identified as one of the key pathways involved in the stress response. This observation is consistent with findings reviewed by Yusuf et al. (2011) in which the nitrogen metabolism and nitrate-related enzymes were sensitive to Ni. Rizwan et al. (2017) reported that Ni stress triggered proline accumulation and decreased the levels of soluble proteins and sugars in *Oryza sativa*. The same study also reported that the changes in osmolyte accumulation was accompanied by increased levels of H_2O_2, malondialdehyde, ascorbic acid, glutathione,

and elevated activities of catalase and peroxidase. In general, the results suggest that Ni toxicity under different temperatures affect key primary metabolisms of *S. quadricauda* and *C. augustae* such as sulfur, amino acid and energy metabolism. The application of metabolomics analysis is crucial to identify biomarkers in detoxification mechanisms (Singh & Verma, 2018).

Overall, results of this study supported the notion that Ni toxicity can act synergistically with warming to induce multitudes of stress response in microalgae. In addition to temperature, Ni toxicity in the ecosystem is influenced by other factors such as salinity, anionic complexation, and water hardness. Organisms in the freshwater ecosystems are generally more sensitive to Ni compared to the organisms in the marine ecosystems because salinity and the anions present in the seawater (such as SO_4^{2-} and Cl^-) can complex with Ni and reduce Ni bioavailability, toxicity and uptake (Blewett & Leonard, 2017). Interaction of Ni^{2+} and other metal ions present in the water bodies also have a significant impact on the toxicity effects. For example, Ni and Cu have a synergistic interaction and reduced Chl-*a* content in *S. quadricauda* (Fargašová, 2001). Nickel also interacts and competes with Ca^{2+} and Mg^{2+} transport systems, which will affect metal bioavailability and homeostasis in the cells (Brix et al., 2017). Studies on the interactive effects of multiple abiotic stresses and metal toxicity are necessary to construct projections on the future of microalgae and the aquatic ecosystems.

5.3 Implications of the data on the environment

This study shows that warming and metal toxicity affect microalgae at the biochemical and cellular level. The response of primary producers to climate change have garnered attention due to their roles in primary productivity and nutrient cycling. Rise in global water surface temperature has resulted in stronger stratification in the water column which reduced the depth of the upper mixing layer. This phenomenon brings more

photosynthetic microalgae closer to the surface of the sea, where they could be exposed to stresses such as drastic light, pollutants and ultraviolet (UV) fluctuations (Steinacher et al., 2009). Weaker mixing and stronger stratification also limit nutrient flux in the water bodies which will affect phytoplankton growth (Winder & Sommer, 2012). Therefore, changes in water temperature might influence the biomass and nutritional values of microalgae in the long run. Wagner et al. (2016) described the relationship between global warming and its impact on the biomass quality of phytoplankton and implied that temperature might affect the efficiency of energy transfer across the trophic levels. This will eventually lead to a change in species distribution. A study conducted by Jensen et al. (2017) showed that the changes in environmental conditions such as temperature and nutrients can affect distributions of two important abundant and cosmopolitan species, the diatom *Chaetoceros diadema* and the coccolithophore *Emiliania huxleyi*.

At the species level, organisms are changing morphologically, physiologically, phenologically and genetically. The disruption at the species levels will eventually result in disruption at the dynamics, distribution, interspecific relationships and productivity of the whole community (Scheffers et al., 2016). Various studies have shown that anthropogenic climate change has direct impact on terrestrial, freshwater and marine ecosystems. A microcosm study using phototrophic and heterotrophic periphytic communities showed that warming and chronic Cu exposure would modify microbial community structure (Pesce et al., 2018). Waga et al. (2017) built a model using phytoplankton size structure and data from sea surface temperature to predict distributional shifts of marine species, which can subsequently provide information to global or regional ecosystem projections. Nickel toxicity and elevated temperature severely reduced the growth of an important reef-building coral, *Acropora muricata* (Biscéré et al., 2017). Combined exposure to Cu and warming induced species selection among the diatom communities in a mesocosm study conducted by Morin et al. (2017).

Another study by Lambert et al. (2017) reported that high temperature and metal toxicity acted antagonistically on the tolerance acquisition of freshwater phototrophic periphyton, where the communities exhibited lower tolerance to metal ions at warmer temperature. Various studies also reported that the abundance and distribution of diatoms were highly related to global environmental changes (Rühland et al., 2015; Saros & Anderson, 2015). Taken together, ecological change in ecosystems is likely to change the competitive, trophic and symbiotic relationships of the organisms (Harley et al., 2012).

5.4 Microalgae for phytotoxicity testing and phycoremediation

Microalgae are potential candidates for phycoremediation due to their high efficiency to sequester metal ions (Suresh Kumar et al., 2015). In this study, *S. quadricauda* showed higher tolerance and resistance to heat and metal toxicity than *C. augustae.* A preliminary screening shows that *S. quadricauda* was able to thrive up to 35°C whereas the growth rate of *C. augustae* declined at temperature beyond 30°C. *Chlamydomonas augustae* showed a higher sensitivity to warming than Ni toxicity. In the context of Cu toxicity, *S. quadricauda* was able to survive at higher Cu concentrations (300, 600 and 1000 μM) compared to *C. augustae* (50, 150 and 250 μM), suggesting that *S. quadricauda* might be a better candidate for phycoremediation. This finding is in consistent with other reports where species from the *Scenedesmus* genus are versatile and ideal for bioremediation and biotechnological applications (von Alvensleben et al., 2016). Zhou et al. (2012) reported that *S. obliquus* efficiently removed 75.9-91.4% of Cu from modified BG11 medium after 8 days of cultivation. Species-dependent metal uptake capacity was also observed in other studies (Khan et al., 2017; Suresh Kumar et al., 2015). A study by Wang & Wood (1984) showed that *Scenedesmus* was more tolerant than *Synechococcus*, and *Chlamydomonas*, *Oscillatoria* and *Euglena* to Ni toxicity. This is largely caused by the different cell size, growth rate and metal binding ability of algal cell wall. For example, *S. quadricauda*'s

ability to remove up to 99% of Ni from wastewater was attributed to their thick cell wall and large surface area upon their unique coenobium formation (Chong et al., 2000).

Both *S. quadricauda* and *C. augustae* accumulated high amount of Cu and Ni in their biomass. *Scenedesmus quadricauda* accumulated higher amount of Ni at 25°C compared to 35°C. *Chlamydomonas augustae* was able to absorb up to 4.0 ppm Cu and 0.7 ppm Ni per 10^4 cells at 25 and 30°C, respectively. Warming did affect the metal uptake capacity of *S. quadricauda* significantly but not on *C. augustae*. Sorption of metals by microalgae is dependent by several parameters such as temperature, pH, metal concentration, speciation and biomass concentration. Temperature must be considered when using microalgae for bio-remediation of metal-polluted water because it affects the chemical and biological reactions of aquatic organisms. Temperature also influences the physicochemical composition of toxicants and pollutants (Rawat et al., 2011).

Microalgae are effective in removing nitrates, phosphates, xenobiotic compounds, gaseous effluents and heavy metals from wastewaters as summarized by Pacheco et al. (2015). Various studies were conducted to integrate wastewater treatment as a medium for microalgal cultivation. Khan et al. (2017) reported that freshwater algae (*Cladophora glomerata*, *Oedogonium westii*, *Vaucheria debaryana*, and *Zygnema insigne*) substantially decreased the biological oxygen demand, chemical oxygen demand, total dissolved solids, and toxic metals in wastewater derived from an industrial area.

Some papers proposed to integrate the cultivation of microalgae in municipal wastewaters and biofuel production (Cheah et al., 2016; Eladel et al., 2019; Nath et al., 2019). Anthropogenic wastewaters are generally loaded with organics and nutrients which could be assimilated for microalgal cultivation (Rawat et al., 2011). For example, palm oil mill effluent (POME) is rich with nitrogenous compounds, phosphates, and macromolecules such as carbohydrates, proteins and lipids. Similarly, sewage and landfill

leachate contain organic substances and nitrogenous compounds that can contribute to algal growth. Microalgae are able to absorb and transform the pollutants while accumulating a substantial amount of biomass. Following the cultivation in wastewaters, the algal biomass loaded with high lipid and carbohydrate contents can be used as feedstocks to produce biodiesel, bioethanol, biobutanol, biohydrogen or biomethane (Cheah et al., 2016). This approach is economically-feasible and contributes to carbon sequestration.

CHAPTER 6: CONCLUSION

6.1 Conclusion

This study provides a comprehensive physiological and metabolomic insights on the interactive effects of warming on Cu or Ni toxicity on green microalgae. In Experiment 1, the effects of Cu toxicity on the physiology and biochemistry of *S. quadricauda* were highly dependent on water temperature. The interactive effects of both stressors induced significant impact on the photosynthetic parameters such as F_v/F_m, E_k, NPQ. Temperature induced significant impact on cell density, E_k and NPQ; while the Cu toxicity significantly affected the F_v/F_m and NPQ. Changes in the *in vivo* absorption spectra and high levels of ROS were observed across different treatments. Overall, *S. quadricauda* adapted to the Cu toxicity and warming via NPQ and metabolic restructuring. Key metabolites including glycine, proline, hexadecanoic acid, propanoic acid, octadecanoic acid, galactose, lactose and sucrose were involved in the microalgal response.

In Experiment 2, *C. augustae* exhibited a Cu concentration-dependent decrease in the cell density. Copper greatly impacted the photosynthetic efficiency of *C. augustae* by reducing the $rETR_m$ and E_k. Warming increased the ROS production significantly. Overall, the data showed that warming enhanced Cu toxicity in the cultures. Copper treatment on *C. augustae* induced changes in glutathione metabolism, sulfur metabolism, taurine and hypotaurine metabolism, and zeatin biosynthesis. Warming affected pathways in pantothenate and CoA, isoquinoline alkaloid biosynthesis, sulfur metabolism, tyrosine metabolism, glutathione metabolism, and phenylalanine metabolism. The combined factors impacted on the tropane, piperidine and pyridine alkaloid biosynthesis.

In Experiment 3, the results showed that warming did not decrease the photosynthetic efficiency of *S. quadricauda* in response to Ni. Nickel concentration at 42.07 μM affected $rETR_m$ and E_k. At 25°C, the increase of NPQ values might indicate the onset of thermal

dissipation process as a self-protection mechanism against Ni toxicity. The level of ROS increased significantly by Ni exposure. The amount of Ni accumulated in the biomass was higher at 25°C compared to 35°C. Based on the metabolic profile, amino acids, sugars and organic acids were significantly regulated by the combined factors to restore homeostasis. The most affected pathways include sulfur, amino acids, and nitrogen metabolisms. Overall, the results suggest that the inhibitory effect of Ni was lower at 35°C compared to 25°C probably due to lower metal uptake and primary metabolism restructuring.

In Experiment 4, the cell density of *C. augustae* decreased especially at the highest Ni concentration (42.07 μM). The $rETR_m$ values of the cells were reduced by warming. The overall E_k values were lower at 30°C than at 25°C. As for the metal uptake in biomass, *C. augustae* accumulated high amount of Ni at 30°C. Nickel treatment on *C. augustae* affected pathways such as lysine biosynthesis, phenylalanine, tyrosine and tryptophan biosynthesis, phenylalanine metabolism, ascorbate and aldarate metabolism, tyrosine metabolism, glutathione metabolism and glycine, serine and threonine metabolism. Temperature affected metabolites involved in the phenylalanine pathway, tropane, piperidine and pyridine alkaloid biosynthesis, pantothenate and CoA biosynthesis, glyoxylate and dicarboxylate metabolism, and glutathione metabolism. The combined factors affected tropane, piperidine and pyridine alkaloid biosynthesis, phenylalanine metabolism, pantothenate and CoA biosynthesis, phenylalanine, tyrosine, and tryptophan biosynthesis, flavone and flavonol biosynthesis and glutathione metabolism.

In summary, the microalgal photosynthetic machinery and efficiency were highly sensitive to both abiotic stressors. The $rETR_m$ values decreased in response to warming and metal toxicity. The decline of E_k at high temperature and metal concentrations were regarded as an adaptive strategy to mitigate over-saturation on the photosynthetic

apparatus. The increase of NPQ values might indicate the onset of thermal dissipation process as a self-protection mechanism against photoinhibition. Overall, the values of F_v/F_m generated from Chl-*a* fluorescence were generally above 0.6. This implied that the algal cells remained photosynthetically active upon exposure to warming and high concentrations of Cu or Ni.

The increased level of ROS corresponded to the increasing concentrations of Cu and Ni. This observation is in consistent with other studies which reported that oxidative stress is one of the main mechanisms involved in metal-mediated toxicity. Heavy metal ions catalyse the formation of free radicals and disrupt the metabolic equilibrium in the cells. Based on the results, warming did not induce a significant increase in the level of ROS.

The metabolomics analysis provides a valuable insight into the complex adaptation mechanisms to the interactive effects of temperature and heavy metals. In general, the two species underwent primary metabolism restructuring for adaptation and restoration of homeostasis. The results show that amino acids, fatty acids and sugars were the key primary metabolites involved in the microalgal adaptation. Amino acids and proteins were involved in chelating metal ions and reducing free metal ions in the cells. Pathways related to the carbohydrate and energy metabolism were also involved in the response, suggesting a change in energy expenditure. Sulfur-containing metabolites and sulfur metabolism were also significantly dysregulated because excess metal ions would bind to various ligands, primarily molecules with sulfhydryl groups and thiols such as glutathione and phytochelatins.

Increased temperature and metal toxicity due to anthropogenic activities and global warming will pose numerous threats to biodiversity of the aquatic systems. These environmental stresses might alter growth patterns and physiology of microalgae, the primary producer in the aquatic food web. This phenomenon could further impact on the

distributional shift of aquatic organisms. Understanding bioaccumulation of metals in the primary producer is important to study the effects of metal toxicity across the trophic levels.

Comparing between the two species, the results show that *S. quadricauda* was more resistant to heat and metal toxicity than *C. augustae.* The former species was able to thrive at 35°C whereas the latter showed a rapid decline in growth rate beyond 30°C. In the context of Cu toxicity, *S. quadricauda* was able to survive at higher Cu concentrations (300, 600 and 1000 µM) compared to *C. augustae* (50, 150 and 250 µM), suggesting that *S. quadricauda* is a better candidate for phycoremediation.

6.2 Appraisal of study

Microalgae are primary producers that form the basis of aquatic food webs. Therefore, any changes in primary productivity, size, growth and composition of microalgal communities will bring profound impact to the ecosystems. Many reports drew inferences from a single environmental variable in understanding the response of microalgae to abiotic stresses. It has become increasingly evident that the natural environment is multivariate and the interaction of biotic and abiotic variables plays remarkable effects on microalgae and their distribution in the ecosystem. This study discussed the interactive effects of two abiotic stresses and provided valuable information into how different variables can interplay on the biochemical network of microalgae.

Understanding the adaptive mechanisms of microalgae under the combined stress conditions is important to make projections about future ecological effects and species distribution. This study assessed the stress responses from the physiological (growth, photosynthesis, ROS, metal uptake) and biochemical (metabolite) aspects. This integrated approach combines observations from different parameters and provide an overview into the underlying mechanisms of the stress response. The metabolic pathways reported in

this study could well benefit future studies on the metabolomics of microalgae in response to other abiotic stresses.

Two genera reported in this study, *Scenedesmus* and *Chlamydomonas*, are ecologically-important microalgae and regarded as the model organisms for phytotoxicity tests. Based on the data on photosynthetic efficiency and metal uptake by algal biomass, this study confirmed the sensitivity and metal removal efficacy of these species. Their ability to tolerate high metal concentration in the culture media supports their application for phycoremediation.

6.3 Limitation of this study

Comparing the results obtained in this study and other published studies is challenging because not only does metal toxicity vary at the species and strain level, but also due to variations in culture conditions. The concentrations might vary by an order of magnitude. The data obtained in this study indicate a complex and somewhat inconsistent relationship between metal and temperature. Similar observations were reported and summarized by Suresh Kumar et al. (2015) and Zeraatkar et al. (2016), where the influence of temperature on metal toxicity is often different for each algal species and metal ion. Hence, interpretation of biological responses to multiple stressors must be evaluated with care.

The metabolomics in this study used the untargeted approach to understand the mechanisms underlying the physiological and biochemical changes inside the cells. The data compared the relative intensity of features between different samples, instead of the absolute amount. This is due to the lack of metabolite standards to generate standard curves to quantify and identify the metabolites. Nevertheless, this untargeted approach has been widely reported in the literature and used in different research fields.

Metabolite identification has always been the biggest challenge in metabolomics. In this study, the significant metabolites were annotated using the mummichog algorithm which identifies the m/z features based on biological activities and networks. Future work might utilize targeted metabolomics and multiple reaction monitoring (MRM) as a more reliable and accurate identification approach.

6.4 Future research direction

This study is laboratory-based and only involved a single species of microalgae in each set of experiment. A mesocosm study involving multiple species of microalgae can be carried out to investigate the competitive ability of different microalgae. Studies on algal-grazer interaction should also be initiated to provide better understanding on community tolerance to the combined effects of warming and metal toxicity.

Microalgae are potential candidates for phycoremediation to remove pollutants from the environment based on their ability to tolerate high metal concentration, harvest carbon dioxide and low maintenance cost. In this study, microalgae were cultivated in artificial culture medium supplemented with metal ions. The objective of using culture media with known composition was to ensure the reproducibility between replicates. Future studies should utilize industrial wastewater to cultivate microalgae at various temperature. Despite the challenges to profile metal content and physicochemical properties in the wastewaters, this approach should provide a more realistic insight into the application of microalgae for phycoremediation.

REFERENCES

Abdel-Tawwab, M., & Wafeek, M. (2014). Influence of water temperature and waterborne cadmium toxicity on growth performance and metallothionein – cadmium distribution in different organs of Nile tilapia, *Oreochromis niloticus* L.). *Journal of Thermal Biology*, *45*, 157–162. http://doi.org/10.1016/j.jtherbio.2014.09.002

Adams, M. S., Dillon, C. T., Vogt, S., Lai, B., Stauber, J., & Jolley, D. F. (2016). Copper uptake, intracellular localization, and speciation in marine microalgae measured by synchrotron radiation X-ray fluorescence and absorption microspectroscopy. *Environmental Science and Technology*, *50*, 8827–8839. http://doi.org/10.1021/acs.est.6b00861

Adrees, M., Ali, S., Rizwan, M., Ibrahim, M., Abbas, F., Farid, M., … Bharwana, S. A. (2015). The effect of excess copper on growth and physiology of important food crops: a review. *Environmental Science and Pollution Research*, *22*, 8148–8162. http://doi.org/10.1007/s11356-015-4496-5

Ahmed, H., & Häder, D. P. (2010). Rapid ecotoxicological bioassay of nickel and cadmium using motility and photosynthetic parameters of *Euglena gracilis*. *Environmental and Experimental Botany*, *69*(1), 68–75. http://doi.org/10.1016/j.envexpbot.2010.02.009

Aksu, Z. (2002). Determination of the equilibrium, kinetic and thermodynamic parameters of the batch biosorption of nickel (II) ions onto *Chlorella vulgaris*. *Process Biochemistry*, *38*(1), 89–99. http://doi.org/10.1016/S0032-9592(02)00051-1

Allen, O. P. Dube, W. Solecki, F. Aragón–Durand, W. Cramer, S. Humphreys, M. Kainuma, J. Kala, N. Mahowald, Y. Mulugetta, R. Perez, M. Wairiu, K. Z. (2018). Framing and Context. In T. W. V. Masson-Delmotte, P. Zhai, H. O. Pörtner, D. Roberts, J. Skea, P.R. Shukla, A. Pirani, W. Moufouma-Okia, C. Péan, R. Pidcock, S. Connors, J. B. R. Matthews, Y. Chen, X. Zhou, M. I. Gomis, E. Lonnoy, T. Maycock, M. Tignor (Ed.), *Global warming of 1.5°C. An IPCC Special Report on the impacts of global warming of 1.5°C above pre-industrial levels and related global greenhouse gas emission pathways, in the context of strengthening the global response to the threat of climate change.* Intergovernmental Panel on Climate Change.

An, M., Mou, S., Zhang, X., Ye, N., Cao, S., Xu, D., … Miao, J. (2013). Temperature regulates fatty acid desaturases at a transcriptional level and modulates the fatty acid profile in the Antarctic microalga *Chlamydomonas* sp. ICE-L. *Bioresource Technology*, *134*, 151–157. http://doi.org/10.1016/j.biortech.2013.01.142

André, C., Auclair, J., & Gagné, J. F. (2017). Urban pollution increases sensitivity to temperature changes in *Elliptio complanata* mussels exposed to municipal wastewaters. *Environment Pollution and Climate Change*, *1*(2), 1–8.

Ansari, F. A., Singh, P., Guldhe, A., & Bux, F. (2017). Microalgal cultivation using aquaculture wastewater: Integrated biomass generation and nutrient remediation. *Algal Research*, *21*, 169–177. http://doi.org/10.1016/j.algal.2016.11.015

Appenroth, K. (2010). What are "heavy metals" in plant sciences? *Acta Physiologiae Plantarum*, *32*, 615–619. http://doi.org/10.1007/s11738-009-0455-4

Arbona, V., Manzi, M., Ollas, C. De, & Gómez-Cadenas, A. (2013). Metabolomics as a tool to investigate abiotic stress tolerance in plants. *International Journal of Molecular Sciences*, *14*(3), 4885–911. http://doi.org/10.3390/ijms14034885

Aust, S. D., Morehouse, L. A., & Thomas, C. E. (1985). Role of metals in oxygen radical reactions. *Journal of Free Radicals in Biology & Medicine*, *1*, 3–25. http://doi.org/10.1016/0748-5514(85)90025-x

Baglieri, A., Sidella, S., Barone, V., Fragala, F., Silkina, A., Negre, M., & Gennari, M. (2016). Cultivating *Chlorella vulgaris* and *Scenedesmus quadricauda* microalgae to degrade inorganic compounds and pesticides. *Environmental Science and Pollution Research*, *23*(18). http://doi.org/10.1007/s11356-016-6996-3

Barati, B., Lim, P.-E., Gan, S.-Y., Poong, S.-W., Phang, S.-M., & Beardall, J. (2018). Effect of elevated temperature on the physiological responses of marine *Chlorella* strains from different latitudes. *Journal of Applied Phycology*. http://doi.org/10.1007/s10811-017-1198-z

Batley, G. E., Apte, S. C., & Stauber, J. L. (2004). Speciation and bioavailability of trace metals in water: Progress Since 1982. *Australian Journal of Chemistry*, *57*(10), 903–919. http://doi.org/10.1071/CH04095

Behrenfeld, M. J., O'Malley, R. T., Boss, E. S., Westberry, T. K., Graff, J. R., Halsey, K. H., … Brown, M. B. (2016). Revaluating ocean warming impacts on global phytoplankton. *Nature Climate Change*, *6*, 323–330. http://doi.org/10.1038/nclimate2838

Binet, M. T., Adams, M. S., Gissi, F., Golding, L. A., Schlekat, C. E., Garman, E. R., … Stauber, J. L. (2018). Toxicity of nickel to tropical freshwater and sediment biota: A critical literature review and gap analysis. *Environmental Toxicology and Chemistry*, *37*(2), 293–317. http://doi.org/10.1002/etc.3988

Biscéré, T., Lorrain, A., Rodolfo-Metalpa, R., Gilbert, A., Wright, A., Devissi, C., … Houlbrèque, F. (2017). Nickel and ocean warming affect scleractinian coral growth. *Marine Pollution Bulletin*, *120*(1–2), 250–258. http://doi.org/10.1016/j.marpolbul.2017.05.025

Blewett, T. A., & Leonard, E. M. (2017). Mechanisms of nickel toxicity to fish and invertebrates in marine and estuarine waters. *Environmental Pollution*, *223*, 311–322. http://doi.org/10.1016/j.envpol.2017.01.028

Boivin, M. E. Y., Massieux, B., Breure, A. M., Van Den Ende, F. P., Greve, G. D., Rutgers, M., & Admiraal, W. (2005). Effects of copper and temperature on aquatic bacterial communities. *Aquatic Toxicology*, *71*, 345–356. http://doi.org/10.1016/j.aquatox.2004.12.004

Booth, S. C., Workentine, M. L., Weljie, A. M., & Turner, R. J. (2011). Metabolomics and its application to studying metal toxicity. *Metallomics*, *3*, 1142–1152. http://doi.org/10.1039/c1mt00070e

Boyce, D. G., Lewis, M. R., & Worm, B. (2010). Global phytoplankton decline over the past century. *Nature*, *466*, 591–596. http://doi.org/10.1038/nature09268

Bradl, H. B. (2005). Sources and origins of heavy metals. In H. B. Bradl (Ed.), *Heavy metals in the environment* (pp. 1–27). Elsevier Ltd.

Brierley, A. S., & Kingsford, M. J. (2009). Impacts of climate change on marine organisms and ecosystems. *Current Biology*, *19*(14), R602–R614. http://doi.org/10.1016/j.cub.2009.05.046

Brix, K. V., Schlekat, C. E., & Garman, E. R. (2017). The mechanisms of nickel toxicity in aquatic environments: An adverse outcome pathway analysis. *Environmental Toxicology and Chemistry*, *36*(5), 1128–1137. http://doi.org/10.1002/etc.3706

Burkhead, J. L., Reynolds, K. A. G., Abdel-ghany, S. E., Cohu, C. M., & Pilon, M. (2009). Copper homeostasis. *New Phytologist*, *182*, 799–816. http://doi.org/10.1111/j.1469-8137.2009.02846.x

Byrne, R. H., Kump, L. R., & Cantrell, K. J. (1988). The influence of temperature and pH on trace metal speciation in seawater. *Marine Chemistry*, *25*, 163–181. https://doi.org/10.1016/0304-4203(88)90062-X

Cairns, J., Heath, A. G., & Parker, B. C. (1975). The effects of temperature upon the toxicity of chemicals to aquatic organisms. *Hydrobiologia*, *47*(1), 135–171. http://doi.org/10.1007/BF00036747

Cao, K., He, M., Yang, W., Chen, B., Luo, W., Zou, S., & Wang, C. (2016). The eurythermal adaptivity and temperature tolerance of a newly isolated psychrotolerant Arctic *Chlorella* sp. *Journal of Applied Phycology*, *28*(2), 877–888. http://doi.org/10.1007/s10811-015-0627-0

Castruita, M., Casero, D., Karpowicz, S. J., Kropat, J., Vieler, A., Hsieh, S. I., … Merchant, S. S. (2011). Systems biology approach in *Chlamydomonas* reveals connections between copper nutrition and multiple metabolic steps. *The Plant Cell*, *23*(4), 1273–1292. http://doi.org/10.1105/tpc.111.084400

Cempel, M., & Nikel, G. (2006). Nickel: A review of its sources and environmental toxicology. *Polish Journal of Environmental Studies*, *15*(3), 375–382. http://doi.org/10.1109/TUFFC.2008.827

Chankova, S., Mitrovska, Z., Miteva, D., Oleskina, Y. P., & Yurina, N. P. (2013). Heat shock protein HSP70B as a marker for genotype resistance to environmental stress in *Chlorella* species from contrasting habitats. *Gene*, *516*(1), 184–189. http://doi.org/10.1016/j.gene.2012.11.052

Cheah, W. Y., Ling, T. C., Show, P. L., Juan, J. C., Chang, J.-S., & Lee, D.-J. (2016). Cultivation in wastewaters for energy: A microalgae platform. *Applied Energy*, *179*, 609–625. http://doi.org/10.1016/j.apenergy.2016.07.015

Chen, Y., Jiang, X., Wang, Y., & Zhuang, D. (2018). Spatial characteristics of heavy metal pollution and the potential ecological risk of a typical mining area: A case study in China. *Process Safety and Environmental Protection*, *113*, 204–219. http://doi.org/10.1016/j.psep.2017.10.008

Chong, A. M., Wong, Y., & Tam, N. F. (2000). Performance of different microalgal species in removing nickel and zinc from industrial wastewater. *Chemosphere*, *41*, 251–257. http://doi.org/10.1016/S0045-6535(99)00418-X

Chong, J., Soufan, O., Li, C., Caraus, I., Li, S., Bourque, G., … Xia, J. (2018). MetaboAnalyst 4.0: Towards more transparent and integrative metabolomics analysis. *Nucleic Acids Research*, *46*. http://doi.org/10.1093/nar/gky310

Cid, A., Torres, E., & Abalde, J. (1995). Copper toxicity on the marine microalga *Phaeodactylum tricornutum*: Effects on photosynthesis related parameters. *Aquatic Toxicology*, *31*, 165–174. https://doi.org/10.1016/0166-445X(94)00071-W

Dai, D., Gao, Y., Chen, J., Huang, Y., Zhang, Z., & Xu, F. (2016). Time-resolved metabolomics analysis of individual differences during the early stage of lipopolysaccharide-treated rats. *Scientific Reports*, *6*, 34136. http://doi.org/10.1038/srep34136

Dao, L. H. T., & Beardall, J. (2016a). Effects of lead on growth, photosynthetic characteristics and production of reactive oxygen species of two freshwater green algae. *Chemosphere*, *147*, 420–429. http://doi.org/10.1016/j.chemosphere.2015.12.117

Dao, L. H. T., & Beardall, J. (2016b). Effects of lead on two green microalgae *Chlorella* and *Scenedesmus*: Photosystem II activity and heterogeneity. *Algal Research*, *16*, 150–159. http://doi.org/10.1016/j.algal.2016.03.006

Davey, M. P., Norman, L., Sterk, P., Huete-ortega, M., Bunbury, F., Kin, B., … Davey, M. P. (2019). Snow algae communities in Antarctica: Metabolic and taxonomic composition. *New Phytologist*, *222*, 1242–1255. http://doi.org/10.1111/nph.15701

De Laender, F., Melian, C. J., Bindler, R., Van den Brink, P. J., Daam, M., Roussel, H., … Janssen, C. R. (2013). The contribution of intra- and interspecific tolerance variability to biodiversity changes along toxicity gradients. *Ecology Letters*, *17*, 72–81. http://doi.org/10.1111/ele.12210

Debelius, B., Forja, J. M., & Lubián, L. M. (2011). Toxicity of copper, nickel and zinc to *Synechococcus* populations from the Strait of Gibraltar. *Journal of Marine Systems*, *88*, 113–119. http://doi.org/10.1016/j.jmarsys.2011.02.009

Deleebeeck, N. M. E., De Laender, F., Chepurnov, V. A., Vyverman, W., Janssen, C. R., & De Schamphelaere, K. A. C. (2009). A single bioavailability model can accurately predict Ni toxicity to green microalgae in soft and hard surface waters. *Water Research*, *43*(7), 1935–1947. http://doi.org/10.1016/j.watres.2009.01.019

Dewez, D., Geoffroy, L., Vernet, G., & Popovic, R. (2005). Determination of photosynthetic and enzymatic biomarkers sensitivity used to evaluate toxic effects of copper and fludioxonil in alga *Scenedesmus obliquus*. *Aquatic Toxicology*, *74*, 150–159. http://doi.org/10.1016/j.aquatox.2005.05.007

Döll, P., Trautmann, T., Gerten, D., Schmied, H. M., Ostberg, S., Saaed, F., & Schleussner, C.-F. (2018). Risks for the global freshwater system at 1.5°C and 2°C global warming. *Environmental Research Letters*, *13*(4), 044038. http://doi.org/10.1088/1748-9326/aab792

Domingos, R. F., Gélabert, A., Carreira, S., Cordeiro, A., Sivry, Y., & Benedetti, M. F. (2014). Metals in the aquatic environment — Interactions and implications for the speciation and bioavailability: A critical overview. *Aquatic Geochemistry*, *21*(2–4), 231–257. http://doi.org/10.1007/s10498-014-9251-x

Duffus, J. H. (2002). "Heavy metals" - A meaningless term? *Pure and Applied Chemistry*, *74*, 793–807. http://doi.org/10.1351/pac200274050793

Echeveste, P., Silva, J. C., & Lombardi, A. T. (2017). Cu and Cd affect distinctly the physiology of a cosmopolitan tropical freshwater phytoplankton. *Ecotoxicology and Environmental Safety*, *143*, 228–235. http://doi.org/10.1016/j.ecoenv.2017.05.030

Egleston, E. S., & Morel, F. M. M. (2008). Nickel limitation and zinc toxicity in a urea-grown diatom. *Limnology and Oceanography*, *53*(6), 2462–2471. http://doi.org/10.4319/lo.2008.53.6.2462

Eladel, H., Esakkimuthu, S., & Abomohra, A. E. (2019). Dual role of microalgae in wastewater treatment and biodiesel production. In G. S. & B. F. (Eds.), *Application of Microalgae in Wastewater Treatment* (pp. 85–121). Cham: Springer. http://doi.org/10.1007/978-3-030-13909-4

El-Sheekh, M., Abomohra, A. E.-F., & El-Azim, M. A. (2017). Effect of temperature on growth and fatty acids profile of the biodiesel producing microalga *Scenedesmus acutus*. *Biotechnology, Agronomy, Society and Environment*, *21*(4), 233–239. http://doi.org/10.25518/1780-4507.15291

Elshkaki, A., Graedel, T. E., Ciacci, L., & Reck, B. (2016). Copper demand, supply, and associated energy use to 2050. *Global Environmental Change*, *39*, 305–315. http://doi.org/10.1016/j.gloenvcha.2016.06.006

Fanesi, A., Wagner, H., Becker, A., & Wilhelm, C. (2016). Temperature affects the partitioning of absorbed light energy in freshwater phytoplankton. *Freshwater Biology*, *61*, 1365–1378. http://doi.org/10.1111/fwb.12777

FAO and UN-Water. (2018). Progress on level of water stress. Global baseline for SDG 6 Indicator 6.4.2: Level of water stress: freshwater withdrawal as a proportion of available freshwater resources.

Fargašová, A. (2001). Interactive effect of manganese, molybdenum, nickel, copper I and II, and vanadium on the freshwater alga *Scenedesmus quadricauda*. *Bulletin of*

Environmental Contamination and Toxicology, *67*, 688–695. http://doi.org/10.1007/s00128-001-0178-8

Fargašová, A., Bumbálová, A., & Havránek, E. (1999). Ecotoxicological effects and uptake of metals (Cu^{+}, Cu^{2+}, Mn^{2+}, Mo^{6+}, Ni^{2+}, V^{5+}) in freshwater alga *Scenedesmus quadricauda*. *Chemosphere*, *38*(5), 1165–1173. http://doi.org/10.1016/S0045-6535(98)00346-4

Fawaz, E. G., Salam, D. A., & Kamareddine, L. (2018). Evaluation of copper toxicity using site specific algae and water chemistry: Field validation of laboratory bioassays. *Ecotoxicology and Environmental Safety*, *155*(November 2017), 59–65. http://doi.org/10.1016/j.ecoenv.2018.02.054

Festa, R. A., & Thiele, D. J. (2011). Copper: An essential metal in biology. *Current Biology*, *21*(21), R877–R883. http://doi.org/10.1016/j.cub.2011.09.040

Fiehn, O., Kopka, J., Trethewey, R. N., & Willmitzer, L. (2000). Identification of uncommon plant metabolites based on calculation of elemental compositions using gas chromatography and quadrupole mass spectrometry. *Analytical Chemistry*, *72*(15), 3573–3580. http://doi.org/10.1021/ac991142i

Frölicher, T. L., Fischer, E. M., & Gruber, N. (2018). Marine heatwaves under global warming. *Nature*, *560*(360–364). http://doi.org/10.1038/s41586-018-0383-9

Gavis, J., Chamberlim, C., & Lystad, L. D. (1979). Coenobial cell number in *Scenedesmus quadricauda* (Chlorophyceae) as a function of growth rate in nitrate-limited chemostats. *Journal of Phycology*, *15*, 273–275. https://doi.org/10.1111/j.0022-3646.1979.00273.x

Giraldo-Zuluaga, J. H., Díez, G., Gómez, A., Martínez, T., Vasquez, M. P., Bonilla, J. V., & Jimenez, A. E. S. (2016). Automatic identification and counting of *Scenedesmus* polymorphic microalgae from microscopic images. *IEEE Journal of Selected Topics in Signal Processing*, *9*, 1–9. https://doi.org/10.1007/s10044-017-0662-3

Gissi, F., Stauber, J. L., Binet, M. T., Golding, L. A., Adams, M. S., Schlekat, C. E., … Jolley, D. F. (2016). A review of nickel toxicity to marine and estuarine tropical biota with particular reference to the South East Asian and Melanesian region. *Environmental Pollution*, *218*, 1308–1323. http://doi.org/10.1016/j.envpol.2016.08.089

Gong, N., Shao, K., Feng, W., Lin, Z., Liang, C., & Sun, Y. (2011). Biotoxicity of nickel oxide nanoparticles and bio-remediation by microalgae *Chlorella vulgaris*. *Chemosphere*, *83*(4), 510–516. http://doi.org/10.1016/J.CHEMOSPHERE.2010.12.059

Gowda, H., Ivanisevic, J., Johnson, C. H., Kurczy, M. E., Benton, H. P., Rinehart, D., … Siuzdak, G. (2014). Interactive XCMS Online: Simplifying advanced metabolomic data processing and subsequent statistical analyses. *Analytical Chemistry*, *86*, 6931–6939. https://doi.org/10.1021/ac500734c

Gruner, D. S., Bracken, M. E. S., Berger, S. A., Eriksson, B. K., Gamfeldt, L., Matthiessen, B., … Hillebrand, H. (2017). Effects of experimental warming on biodiversity depend on ecosystem type and local species composition. *Oikos*, *126*(1), 8–17. http://doi.org/10.1111/oik.03688

Guo, R., Lim, W. A., & Ki, J. S. (2016). Genome-wide analysis of transcription and photosynthesis inhibition in the harmful dinoflagellate *Prorocentrum minimum* in response to the biocide copper sulfate. *Harmful Algae*, *57*, 27–38. http://doi.org/10.1016/j.hal.2016.05.004

Häder, D.-P., & Gao, K. (2015). Interactions of anthropogenic stress factors on marine phytoplankton. *Frontiers in Environmental Science*, *3*, 14. http://doi.org/10.3389/fenvs.2015.00014

Hamed, S. M., Selim, S., Klöck, G., & AbdElgawad, H. (2017). Sensitivity of two green microalgae to copper stress: Growth, oxidative and antioxidants analyses. *Ecotoxicology and Environmental Safety*, *144*, 19–25. http://doi.org/10.1016/j.ecoenv.2017.05.048

Hanagata, N., Takeuchia, T., Fukuju, Y., Barnesa, D. J., & Karube, I. (1992). Tolerance of microalgae to high CO_2 and high temperature. *Phytochemistry*, *31*(10), 3345–3348.

Harley, C. D. G., Anderson, K. M., Demes, K. W., Jorve, J. P., Kordas, R. L., Coyle, T. A., & Graham, M. H. (2012). Effects of climate change on global seaweed communities. *Journal of Phycology*, *48*, 1064–1078. http://doi.org/10.1111/j.1529-8817.2012.01224.x

Harris, E. H. (2001). *Chlamydomonas* as a model organism. *Annual Review of Plant Physiology and Plant Molecular Biology*, *52*, 363–406. https://doi.org/10.1146/annurev.arplant.52.1.363

Harvey, P. J., Handley, H. K., & Taylor, M. P. (2016). Widespread copper and lead contamination of household drinking water, New South Wales, Australia. *Environmental Research*, *151*, 275–285. http://doi.org/10.1016/j.envres.2016.07.041

Hasanuzzaman, M., Nahar, K., Alam, M., Roychowdhury, R., & Fujita, M. (2013). Physiological, biochemical, and molecular mechanisms of heat stress tolerance in plants. *International Journal of Molecular Sciences*, *14*, 9643–9684. http://doi.org/10.3390/ijms14059643

He, H., Chen, F., Li, H., Xiang, W., Li, Y., & Jiang, Y. (2010). Effect of iron on growth, biochemical composition and paralytic shellfish poisoning toxins production of *Alexandrium tamarense*. *Harmful Algae*, *9*(1), 98–104. http://doi.org/10.1016/j.hal.2009.08.006

Hillyer, K. E., Dias, D. A., Lutz, A., Wilkinson, S. P., Roessner, U., & Davy, S. K. (2016). Metabolite profiling of symbiont and host during thermal stress and bleaching in the coral *Acropora aspera*. *Coral Reefs*, *219*, 516–527. http://doi.org/10.1007/s00338-016-1508-y

Ho, T. Y. (2013). Nickel limitation of nitrogen fixation in *Trichodesmium*. *Limnology and Oceanography*, *58*(1), 112–120. http://doi.org/10.4319/lo.2013.58.1.0112

Hoffmann, L. J., Breitbarth, E., Boyd, P. W., & Hunter, K. A. (2012). Influence of ocean warming and acidification on trace metal biogeochemistry. *Marine Ecology Progress Series*, *470*, 191–205. http://doi.org/10.3354/meps10082

Huang, X.-G., Li, S.-X., Liu, F.-J., & Lan, W.-R. (2018). Regulated effects of *Prorocentrum donghaiense* Lu exudate on nickel bioavailability when cultured with different nitrogen sources. *Chemosphere*, *197*, 57–64. http://doi.org/10.1016/j.chemosphere.2018.01.014

Husak, V. (2015). Copper and copper-containing pesticides: metabolism, toxicity and oxidative stress. *Journal of Vasyl Stefanyk Precarpathian National University*, *2*(1), 39–51. http://doi.org/10.15330/jpnu.2.1.39-51

Hutchins, D. A., Teyssii, J., Boisson, F., Fowle, S. W., & Fisher, N. S. (1996). Temperature effects on uptake and retention of contaminant radionuclides and trace metals by the brittle star *Ophiothrix fragilis*. *Marine Environmental Research*, *41*(4), 363–378.

IPCC. (2013). Climate Change 2013: The Physical Science Basis. In Stocker, T.F., D. Qin, G.-K. Plattner, M. Tignor, S.K. Allen, J. Boschung, A. Nauels, Y. Xia, V. Bex and P.M. Midgley (Eds.), *Contribution of working group I to the fifth assessment report of the intergovernmental panel on climate change*, (p. 1535). Cambridge University Press, Cambridge, United Kingdom and New York, NY, USA.

IPCC. (2018). Summary for Policymakers. In M. I. G. V. Masson-Delmotte, P. Zhai, H. O. Pörtner, D. Roberts, J. Skea, P. R. Shukla, A. Pirani, W. Moufouma-Okia, C. Péan, R. Pidcock, S. Connors, J. B. R. Matthews, Y. Chen, X. Zhou & T. W. E. Lonnoy, T. Maycock, M. Tignor (Eds.), *Global warming of 1.5°C. An IPCC Special Report on the impacts of global warming of 1.5°C above pre-industrial levels and related global greenhouse gas emission pathways, in the context of strengthening the global response to the threat of climate change,* (p. 32). World Meteorological Organization.

Islam, M. S., Ahmed, M. K., Raknuzzaman, M., Habibullah -Al- Mamun, M., & Islam, M. K. (2015). Heavy metal pollution in surface water and sediment: A preliminary assessment of an urban river in a developing country. *Ecological Indicators*, *48*, 282–291. http://doi.org/10.1016/j.ecolind.2014.08.016

Ismail, A., Toriman, M. E., Juahir, H., Zain, S. M., Habir, N. L. A., Retnam, A., … Azid, A. (2016). Spatial assessment and source identification of heavy metals pollution in surface water using several chemometric techniques. *Marine Pollution Bulletin*, *106*, 292–300. http://doi.org/10.1016/j.marpolbul.2015.10.019

Jakimska, A., Konieczka, P., Skóra, K., & Namieśnik, J. (2011). Bioaccumulation of metals in tissues of marine animals, part I: The role and impact of heavy metals on organisms. *Polish Journal of Environmental Studies*, *20*(5), 1117–1125.

Jamers, A., Blust, R., De Coen, W., Griffin, J. L., & Jones, O. A. H. (2013a). Copper toxicity in the microalga *Chlamydomonas reinhardtii*: An integrated approach. *Biometals*, *26*, 731–740. http://doi.org/10.1007/s10534-013-9648-9

Jamers, A., Blust, R., De Coen, W., Griffin, J. L., & Jones, O. A. H. (2013b). An omics based assessment of cadmium toxicity in the green alga *Chlamydomonas reinhardtii. Aquatic Toxicology*, *126*, 355–364. http://doi.org/10.1016/j.aquatox.2012.09.007

Jamers, A., Van der Ven, K., Moens, L., Robbens, J., Potters, G., Guisez, Y., … De Coen, W. (2006). Effect of copper exposure on gene expression profiles in *Chlamydomonas reinhardtii* based on microarray analysis. *Aquatic Toxicology*, *80*(3), 249–260. http://doi.org/10.1016/j.aquatox.2006.09.002

Järup, L. (2003). Hazards of heavy metal contamination. *British Medical Bulletin*, *68*, 167–182. http://doi.org/10.1093/bmb/ldg032

Jenkins, S., Fischer, S. M., Chen, L., & Sana, T. R. (2013). Global LC/MS metabolomics profiling of calcium stressed and immunosuppressant drug treated *Saccharomyces cerevisiae*. *Metabolites*, *3*(4), 1102–17. http://doi.org/10.3390/metabo3041102

Jensen, L. Ø., Mousing, E. A., & Richardson, K. (2017). Using species distribution modelling to predict future distributions of phytoplankton: Case study using species important for the biological pump. *Marine Ecology*, *38*(3), 1–12. http://doi.org/10.1111/maec.12427

Jiang, Y., Zhu, Y., Hu, Z., Lei, A., & Wang, J. (2016). Towards elucidation of the toxic mechanism of copper on the model green alga *Chlamydomonas reinhardtii*. *Ecotoxicology*, *25*, 1417–1425. http://doi.org/10.1007/s10646-016-1692-0

Johnson, C. H., Ivanisevic, J., & Siuzdak, G. (2016). Metabolomics: beyond biomarkers and towards mechanisms. *Nature Reviews Molecular Cell Biology*, *17*(7), 451-9. http://doi.org/10.1038/nrm.2016.25

Kaplan, D. (2013). Absorption and adsorption of heavy metals by microalgae. In A. Richmond & Q. Hu (Eds.), *Handbook of Microalgal Culture: Applied Phycology and Biotechnology, Second Edition* (pp. 602–611). Oxford, UK: John Wiley & Sons, Ltd.

Khan, S., Shamshad, I., Waqas, M., Nawab, J., & Ming, L. (2017). Remediating industrial wastewater containing potentially toxic elements with four freshwater algae. *Ecological Engineering*, *102*(3), 536–541. http://doi.org/10.1016/j.ecoleng.2017.02.038

Khodami, S., Surif, M., W.O., W. M., & Daryanabard, R. (2017). Assessment of heavy metal pollution in surface sediments of the Bayan Lepas area, Penang, Malaysia. *Marine Pollution Bulletin*, *114*(1), 615–622. http://doi.org/10.1016/j.marpolbul.2016.09.038

Kinouchi, T., Yagi, H., & Miyamoto, M. (2007). Increase in stream temperature related to anthropogenic heat input from urban wastewater. *Journal of Hydrology*, *335*, 78–88. http://doi.org/10.1016/j.jhydrol.2006.11.002

Kluender, C., Sans-Piché, F., Riedl, J., Altenburger, R., Härtig, C., Laue, G., & Schmitt-Jansen, M. (2009). A metabolomics approach to assessing phytotoxic effects on the green alga *Scenedesmus vacuolatus*. *Metabolomics*, *5*, 59–71. http://doi.org/10.1007/s11306-008-0139-x

Knauer, K., Behra, R., & Sigg, L. (1997). Effects of free Cu^{2+} and Zn^{2+} ions on growth and metal accumulation in freshwater algae. *Environmental Toxicology and Chemistry*, *16*(2), 220–229. https://doi.org/10.1002/etc.5620160218

Knauert, S., & Knauer, K. (2008). The role of reactive oxygen species in copper toxicity to two freshwater green algae. *Journal of Phycology*, *44*, 311–319. http://doi.org/10.1111/j.1529-8817.2008.00471.x

Koppel, D. J., Gissi, F., Adams, M. S., King, C. K., & Jolley, D. F. (2017). Chronic toxicity of five metals to the polar marine microalga *Cryothecomonas armigera* – Application of a new bioassay. *Environmental Pollution*, *228*, 211–221. http://doi.org/10.1016/j.envpol.2017.05.034

Kováčik, J., Babula, P., Peterková, V., & Hedbavny, J. (2017). Long-term impact of cadmium shows little damage in *Scenedesmus acutiformis* cultures. *Algal Research*, *25*, 184–190. http://doi.org/10.1016/j.algal.2017.04.029

Kováčik, J., Dresler, S., & Babula, P. (2018). Metabolic responses of terrestrial macrolichens to nickel. *Plant Physiology and Biochemistry*, *127*, 32–38. http://doi.org/10.1016/j.plaphy.2018.03.006

Kováčik, J., Klejdus, B., & Bačkor, M. (2010). Physiological Responses of *Scenedesmus quadricauda* (Chlorophyceae) to UV-A and UV-C Light. *Photochemistry and Photobiology*, *20*, 612–616.

Kováčik, J., Klejdus, B., Babula, P., & Hedbavny, J. (2016). Age affects not only metabolome but also metal toxicity in *Scenedesmus quadricauda* cultures. *Journal of Hazardous Materials*, *306*, 58–66. http://doi.org/10.1016/j.jhazmat.2015.11.056

Kropat, J., Gallaher, S. D., Urzica, E. I., Nakamoto, S. S., Strenkert, D., Tottey, S., … Merchant, S. S. (2015). Copper economy in *Chlamydomonas*: prioritized allocation and reallocation of copper to respiration vs. photosynthesis. *Proceedings of the National Academy of Sciences of the United States of America*, *112*(9), 2644–51. http://doi.org/10.1073/pnas.1422492112

Küpper, H., Küpper, F., & Spiller, M. (1998). *In situ* detection of heavy metal substituted chlorophylls in water plants. *Photosynthesis Research*, *58*(2), 123–133. http://doi.org/10.1023/A:1006132608181

Küpper, H., Šetlík, I., Šetliková, E., Ferimazova, N., Spiller, M., & Küpper, F. C. (2003). Copper-induced inhibition of photosynthesis: Limiting steps of *in vivo* copper chlorophyll formation in *Scenedesmus quadricauda*. *Functional Plant Biology*, *30*(12), 1187–1196. http://doi.org/10.1071/FP03129

Küpper, H., Šetlík, I., Spiller, M., Küpper, F. C., & Prášil, O. (2002). Heavy-metal induced inhibition of photosynthesis: Targets of *in vivo* heavy metal chlorophyll formation. *Journal of Phycology*, *38*, 429–441. https://doi.org/10.1046/j.1529-8817.2002.01148.x

Kyewalyanga, M. (2015). Phytoplankton Primary Production. In J. Paula (Ed.), *The Regional State of the Coast Report: Western Indian Ocean* (pp. 207–226). Nairobi, Kenya: UNEP and WIOMSA.

Lambert, A. S., Dabrin, A., Foulquier, A., Morin, S., Rosy, C., Coquery, M., & Pesce, S. (2017). Influence of temperature in pollution-induced community tolerance approaches used to assess effects of copper on freshwater phototrophic periphyton. *Science of the Total Environment*, *607–608*, 1018–1025. http://doi.org/10.1016/j.scitotenv.2017.07.035

Leal, P. P., Hurd, C. L., Sander, S. G., Armstrong, E., Leal, P. P., Hurd, C. L., … Armstrong, E. (2016). Copper ecotoxicology of marine algae: a methodological appraisal. *Chemistry and Ecology*, *32*(8), 786–800. http://doi.org/10.1080/02757540.2016.1177520

Lee, K.-K., Lim, P.-E., Poong, S.-W., Wong, C.-Y., Phang, S.-M., & Beardall, J. (2017). Growth and photosynthesis of *Chlorella* strains from polar, temperate and tropical freshwater environments under temperature stress. *Chinese Journal of Oceanology and Limnology*, 1–14. http://doi.org/10.1007/s00343-018-7093-x

Lehmann, J., Coumou, D., & Frieler, K. (2015). Increased record-breaking precipitation events under global warming. *Climatic Change, 132*(4), 501-515. http://doi.org/10.1007/s10584-015-1434-y

Leung, P. T. Y., Yi, A. X., Ip, J. C. H., Mak, S. S. T., & Leung, K. M. Y. (2017). Photosynthetic and transcriptional responses of the marine diatom *Thalassiosira pseudonana* to the combined effect of temperature stress and copper exposure. *Marine Pollution Bulletin*, *124*(2), 938–945. http://doi.org/10.1016/j.marpolbul.2017.03.038

Li, S., Park, Y., Duraisingham, S., Strobel, F. H., Khan, N., Soltow, Q. A., … Pulendran, B. (2013). Predicting network activity from high throughput metabolomics. *PLoS Computational Biology*, *9*(7). http://doi.org/10.1371/journal.pcbi.1003123

Li, W., Xu, X., Fujibayashi, M., Niu, Q., Tanaka, N., & Nishimura, O. (2016). Response of microalgae to elevated CO_2 and temperature: impact of climate change on freshwater ecosystems. *Environmental Science and Pollution Research*, *23*(19), 19847–19860. http://doi.org/10.1007/s11356-016-7180-5

Li, W., Xu, X., Yao, J., Tanaka, N., Nishimura, O., & Ma, H. (2019). Combined effects of elevated carbon dioxide and temperature on phytoplankton-zooplankton link: A multi-in fluence of climate change on freshwater planktonic communities. *Science of the Total Environment*, *658*, 1175–1185. http://doi.org/10.1016/j.scitotenv.2018.12.180

Liu, Y., Zhan, J., & Hong, Y. (2017). Effects of metal ions on the cultivation of an oleaginous microalga *Chlorella* sp. *Environmental Science and Pollution Research*. http://doi.org/10.1007/s11356-017-0258-x

Lombardi, A. T., & Maldonado, M. T. (2011). The effects of copper on the photosynthetic response of *Phaeocystis cordata*. *Photosynthesis Research*, *108*, 77–87. http://doi.org/10.1007/s11120-011-9655-z

Lozano, P., Trombini, C., Crespo, E., Blasco, J., & Moreno-Garrido, I. (2014). ROI-scavenging enzyme activities as toxicity biomarkers in three species of marine microalgae exposed to model contaminants (copper, Irgarol and atrazine). *Ecotoxicology and Environmental Safety*, *104*, 294–301. http://doi.org/10.1016/j.ecoenv.2014.03.021

Lukeš, M., Procházková, L., Shmidt, V., Nedbalová, L., & Kaftan, D. (2014). Temperature dependence of photosynthesis and thylakoid lipid composition in the red snow alga *Chlamydomonas* cf. *nivalis* (Chlorophyceae). *FEMS Microbiology Ecology*, *89*(2), 303–15. http://doi.org/10.1111/1574-6941.12299

Lürling, M., Eshetu, F., Faassen, E. J., Kosten, S., & Huszar, V. L. M. (2013). Comparison of cyanobacterial and green algal growth rates at different temperatures. *Freshwater Biology*, *58*(3), 552–559. http://doi.org/10.1111/j.1365-2427.2012.02866.x

Lutz, S., Anesio, A. M., Field, K., & Benning, L. G. (2015). Integrated "Omics", targeted metabolite and single-cell analyses of arctic snow algae functionality and adaptability. *Frontiers in Microbiology*, *6*, 1–17. http://doi.org/10.3389/fmicb.2015.01323

Machado, M. D., Lopes, A. R., & Soares, E. V. (2015). Responses of the alga *Pseudokirchneriella subcapitata* to long-term exposure to metal stress. *Journal of Hazardous Materials*, *296*, 82–92. http://doi.org/10.1016/j.jhazmat.2015.04.022

Malapascua, J. R. F., Jerez, C. G., Sergejevová, M., Figueroa, F., & Masojídek, J. (2014). Photosynthesis monitoring to optimize growth of microalgal mass cultures: Application of chlorophyll fluorescence techniques. *Aquatic Biology*, *22*, 123–140. http://doi.org/10.3354/ab00597

Martínez-Ruiz, E. B., & Martínez-Jerónimo, F. (2015). Nickel has biochemical, physiological, and structural effects on the green microalga *Ankistrodesmus falcatus*: An integrative study. *Aquatic Toxicology*, *169*, 27–36. http://doi.org/10.1016/j.aquatox.2015.10.007

Maxwell, K., & Johnson, G. N. (2000). Chlorophyll fluorescence--a practical guide. *Journal of Experimental Botany*, *51*(345), 659–668. http://doi.org/10.1093/jexbot/51.345.659

Merchant, S. S., Allen, M. D., Kropat, J., Moseley, J. L., Long, J. C., Tottey, S., & Terauchi, A. M. (2006). Between a rock and a hard place: Trace element nutrition in *Chlamydomonas*. *Biochimica et Biophysica Acta*, *1763*, 578–594. http://doi.org/10.1016/j.bbamcr.2006.04.007

Miazek, K., Iwanek, W., Remacle, C., Richel, A., & Goffin, D. (2015). Effect of metals, metalloids and metallic nanoparticles on microalgae growth and industrial product biosynthesis: A review. *International Journal of Molecular Sciences*, *16*, 23929–23969. http://doi.org/10.3390/ijms161023929

Monteiro, C. M., Castro, P. M. L., & Malcata, F. X. (2012). Metal uptake by microalgae: Underlying mechanisms and practical applications. *Biotechnology Progress*, *28*(2), 299–311. http://doi.org/10.1002/btpr.1504

Morin, S., Lambert, A. S., Rodriguez, E. P., Dabrin, A., Coquery, M., & Pesce, S. (2017). Changes in copper toxicity towards diatom communities with experimental warming. *Journal of Hazardous Materials*, *334*, 223–232. http://doi.org/10.1016/j.jhazmat.2017.04.016

Mudd, G., & Jowitt, S. (2014). A detailed assessment of global Ni resource trends and endowments. *Economic Geology*, *109*, 1813–1841. http://doi.org/10.2113/econgeo.108.5.1163

Muyssen, B. T., Brix, K. V, DeForest, D. K., & Janssen, C. R. (2004). Nickel essentiality and homeostasis in aquatic organisms. *Environmental Reviews*, *12*(2), 113–131. http://doi.org/10.1139/a04-004

Nagajyoti, P. C., Lee, K. D., & Sreekanth, T. V. M. (2010). Heavy metals, occurrence and toxicity for plants: A review. *Environmental Chemistry Letters*, *8*, 199–216. http://doi.org/10.1007/s10311-010-0297-8

Nagalakshmi, N., & Prasad, M. N. V. (2001). Responses of glutathione cycle enzymes and glutathione metabolism to copper stress in *Scenedesmus bijugatus*. *Plant Science*, *160*(2), 291–299. http://doi.org/10.1016/S0168-9452(00)00392-7

Nalewajko, C., Colman, B., & Olaveson, M. (1997). Effects of pH on growth, photosynthesis, respiration, and copper tolerance of three *Scenedesmus* strains. *Environmental and Experimental Botany*, *37*, 153–160. http://doi.org/10.1016/S0098-8472(96)01029-5

Nath, A., Dixit, K., & Sundaram, S. (2019). Developing designer microalgae consortia: A suitable approach to sustainable wastewater treatment. In G. S. & B. F. (Eds.), *Application of Microalgae in Wastewater Treatment* (pp. 57–80). Cham: Springer Nature. http://doi.org/10.1007/978-3-030-13913-1_4

Ng, F.-L., Phang, S.-M., Periasamy, V., Yunus, K., & Fisher, A. C. (2014). Evaluation of algal biofilms on indium tin oxide (ITO) for use in biophotovoltaic platforms based on photosynthetic performance. *PloS One*, *9*(5), e97643. http://doi.org/10.1371/journal.pone.0097643

Nowicka, B., Pluciński, B., Kuczyńska, P., & Kruk, J. (2016). Physiological characterization of *Chlamydomonas reinhardtii* acclimated to chronic stress induced by Ag, Cd, Cr, Cu and Hg ions. *Ecotoxicology and Environmental Safety*, *130*, 133–145. http://doi.org/10.1016/j.ecoenv.2016.04.010

Obata, T., & Fernie, A. R. (2012). The use of metabolomics to dissect plant responses to abiotic stresses. *Cellular and Molecular Life Sciences*, *69*(19), 3225–43. http://doi.org/10.1007/s00018-012-1091-5

OECD. (2002). OECD guidelines for the testing of chemicals.

OECD. (2011). OECD guidelines for the testing of chemicals.

Oliveira, L., & Antia, N. J. (1984). Evidence of nickel ion requirement for autotrophic growth of a marine diatom with urea serving as nitrogen source. *British Phycological Journal*, *19*(2), 125–134. http://doi.org/10.1080/00071618400650131

Olsson, S., Puente-Sánchez, F., Gómez, M. J., & Aguilera, A. (2015). Transcriptional response to copper excess and identification of genes involved in heavy metal tolerance in the extremophilic microalga *Chlamydomonas acidophila*. *Extremophiles*, *19*, 657–672. http://doi.org/10.1007/s00792-015-0746-1

Oukarroum, A. (2016). Alleviation of metal-induced toxicity in aquatic plants by exogenous compounds: A mini-review. *Water, Air, and Soil Pollution*, *227*, 204. http://doi.org/10.1007/s11270-016-2907-y

Oukarroum, A., Perreault, F., & Popovic, R. (2012b). Interactive effects of temperature and copper on photosystem II photochemistry in *Chlorella vulgaris*. *Journal of Photochemistry & Photobiology, B: Biology*, *110*, 9–14. http://doi.org/10.1016/j.jphotobiol.2012.02.003

Oukarroum, A., Polchtchikov, S., Perreault, F., & Popovic, R. (2012a). Temperature influence on silver nanoparticles inhibitory effect on photosystem II photochemistry in two green algae, *Chlorella vulgaris* and *Dunaliella tertiolecta*. *Environmental Science and Pollution Research*, *19*(5), 1755–1762. http://doi.org/10.1007/s11356-011-0689-8

Oukarroum, A., Zaidi, W., Samadani, M., & Dewez, D. (2017). Toxicity of nickel oxide nanoparticles on a freshwater green algal strain of *Chlorella vulgaris*. *BioMed Research International*, *2017*, 8. http://doi.org/10.1155/2017/9528180

Pacheco, M. M., Hoeltz, M., Moraes, M. S. A., & Schneider, R. C. S. (2015). Microalgae: Cultivation techniques and wastewater phycoremediation. *Journal of Environmental Science and Health*, *50*, 573–589. http://doi.org/10.1080/10934529.2015.994951

Pacyna, J. M., Scholtz, M. T., & Li, A. Y. F. (1995). Global budget of trace metal sources. *Environment Reviews*, *3*, 145–159.

Palmer, C., & Guerinot, M. Lou. (2009). A question of balance: Facing the challenges of Cu, Fe and Zn homeostasis. *Nature Chemical Biology*, *5*(5), 333–340. http://doi.org/10.1038/nchembio.166.A

Panneerselvam, K., Marigoudar, S. R., & Dhandapani, M. (2018). Toxicity of nickel on the selected species of marine diatoms and copepods. *Bulletin of Environmental Contamination and Toxicology*, *100*(3), 331–337. http://doi.org/10.1007/s00128-018-2279-7

Papiol, G. G. (2017). Climate conditions, and changes, affect microalgae communities… should we worry? *Integrated Environmental Assessment and Management*, *14*(2), 181–184. http://doi.org/10.1002/ieam.2009

Pathammavong, P. (2016). *Chronic nickel and copper toxicity in the Hyalella azteca Cryptic species complex*. University of Waterloo.

Perales-Vela, H. V., González-Moreno, S., Montes-Horcasitas, C., & Cañizares-Villanueva, R. O. (2007). Growth, photosynthetic and respiratory responses to sub-lethal copper concentrations in *Scenedesmus incrassatulus* (Chlorophyceae). *Chemosphere*, *67*, 2274–2281. http://doi.org/10.1016/j.chemosphere.2006.11.036

Pesce, S., Lambert, A., Morin, S., Foulquier, A., Coquery, M., & Dabrin, A. (2018). Experimental warming differentially influences the vulnerability of phototrophic and heterotrophic periphytic communities to copper toxicity. *Frontiers in Microbiology*, *9*, 1424. http://doi.org/10.3389/fmicb.2018.01424

Phang, S.-M., & Chu, W.-L. (1999). *University of Malaya Algae Culture Collection (UMACC). Catalogue of Strains.* Kuala Lumpur: Institute of Postgraduate Studies and Research, University of Malaya.

Phinyo, K. (2017). Distribution and ecological habitat of *Scenedesmus* and related genera in some freshwater resources of Northern and North-Eastern Thailand. *Biodiversitas, Journal of Biological Diversity*, *18*(3), 1092–1099. http://doi.org/10.13057/biodiv/d180329

Piggott, J. J., Townsend, C. R., & Matthaei, C. D. (2015). Reconceptualizing synergism and antagonism among multiple stressors. http://doi.org/10.1002/ece3.1465

Pillai, S., Behra, R., Nestler, H., Suter, M. J.-F., Sigg, L., & Schirmer, K. (2014). Linking toxicity and adaptive responses across the transcriptome, proteome, and phenotype of *Chlamydomonas reinhardtii* exposed to silver. *Proceedings of the National Academy of Sciences of the United States of America*, *111*(9), 3490–5. http://doi.org/10.1073/pnas.1319388111

Piotrowska-Niczyporuk, A., Bajguz, A., Talarek, M., Bralska, M., & Zambrzycka, E. (2015). The effect of lead on the growth, content of primary metabolites, and antioxidant response of green alga *Acutodesmus obliquus* (Chlorophyceae). *Environmental Science and Pollution Research*, *22*, 19112–19123. http://doi.org/10.1007/s11356-015-5118-y

Prapaipong, P., Shock, E. L., & Koretsky, C. M. (1999). Metal-organic complexes in geochemical processes: Temperature dependence of the standard thermodynamic properties of aqueous complexes between metal cations and dicarboxylate ligands. *Geochimica et Cosmochimica Acta*, *63*(17), 2547–2577. http://doi.org/10.1016/S0016-7037(99)00146-5

Praveena, S. M., Pradhan, B., & Aris, A. Z. (2018). Assessment of bioavailability and human health exposure risk to heavy metals in surface soils (Klang district, Malaysia). *Toxin Reviews*, *37*(3), 196–205. http://doi.org/10.1080/15569543.2017.1350193

Raptis, C. E., Vliet, M. T. H. van, & Pfister, S. (2016). Global thermal pollution of rivers from thermoelectric power plants. *Environmental Research Letters*, *11*, 104011. https://doi.org/10.1088/1748-9326/11/10/104011

Rawat, I., Kumar, R. R., Mutanda, T., & Bux, F. (2011). Dual role of microalgae: Phycoremediation of domestic wastewater and biomass production for sustainable biofuels production. *Applied Energy*, *88*, 3411–3424. http://doi.org/10.1016/j.apenergy.2010.11.025

Razali, A., Syed Ismail, N. S., Awang, S., Praveena, S. M., & Zainal Abidin, E. (2018). Heavy metals contamination and potential health risk in highland river watershed (Malaysia). *Malaysian Journal of Medicine and Health Sciences*, *14*, 45–55.

Reynolds, W. W., & Casterlin, M. E. (1980). The role of temperature in the environmental physiology of fishes. In A. M.A. (Ed.), *Environmental Physiology of Fishes* (35th ed.). NATO Advanced Study Institutes Series (Series A: Life Science), vol 35. Boston: Springer.

Rizwan, M., Imtiaz, M., Dai, Z., Mehmood, S., Adeel, M., Liu, J., & Tu, S. (2017). Nickel stressed responses of rice in Ni subcellular distribution, antioxidant production, and osmolyte accumulation. *Environmental Science and Pollution Research*, *24*(25), 20587–20598. http://doi.org/10.1007/s11356-017-9665-2

Rodriguez, I. B., & Ho, T.-Y. (2014). Diel nitrogen fixation pattern of *Trichodesmium*: The interactive control of light and Ni. *Scientific Reports*, *4*(4445), 1–5. http://doi.org/10.1038/srep04445

Rose, J. M., Feng, Y., Ditullio, G. R., Dunbar, R. B., Hare, C. E., Lee, P. A., … Hutchins, D. A. (2009). Synergistic effects of iron and temperature on Antarctic phytoplankton and microzooplankton assemblages. *Biogeosciences*, *6*, 3131–3147.

Rühland, K. M., Paterson, A. M., & Smol, J. P. (2015). Lake diatom responses to warming: reviewing the evidence. *Journal of Paleolimnology*, *54*(1), 1–35. http://doi.org/10.1007/s10933-015-9837-3

Sachan, P., & Lal, N. (2017). An overview of nickel (Ni^{2+}) essentiality, toxicity and tolerance strategies in plants. *Asian Journal of Biology*, *2*(4), 1–15. http://doi.org/10.9734/AJOB/2017/33931

Sakai, N., & Yoneda, M. (2018). Potential health risk of heavy metals in Malaysia. In M. Yoneda & M. Mokhtar (Eds.), *Environmental Risk Analysis for Asian-Oriented, Risk-Based Watershed Management* (pp. 19–32). Singapore: Springer Nature.

Sakai, N., Alsaad, Z., Thuong, N. T., Shiota, K., Yoneda, M., & Mohd, M. A. (2017). Source profiling of arsenic and heavy metals in the Selangor River basin and their maternal and cord blood levels in Selangor State, Malaysia. *Chemosphere*, *184*, 857–865. http://doi.org/10.1016/j.chemosphere.2017.06.070

Sampaio, E., & Rosa, R. (2019). Climate change, multiple stressors, and responses of marine biota. In W. L. Filho, A. Azul, L. Brandli, P. Özuyar, & T. Wall (Eds.), *Climate Action*. Cham: Springer. http://doi.org/10.1007/978-3-319-71063-1

Sany, S. B. T., Salleh, A., Sulaiman, A. H., Sasekumar, A., Rezayi, M., & Tehrani, G. M. (2013). Heavy metal contamination in water and sediment of the Port Klang coastal area, Selangor, Malaysia. *Environmental Earth Sciences*, *69*, 2013–2025. http://doi.org/10.1007/s12665-012-2038-8

Saros, J. E., & Anderson, N. J. (2015). The ecology of the planktonic diatom *Cyclotella* and its implications for global environmental change studies. *Biological Reviews*, *90*, 522–541. http://doi.org/10.1111/brv.12120

Scheffers, B. R., De Meester, L., Bridge, T. C. L., Hoffmann, A. A., Pandolfi, J. M., Corlett, R. T., … Watson, J. E. M. (2016). The broad footprint of climate change from genes to biomes to people. *Science*, *354*(6313), aaf7671. http://doi.org/10.1126/science.aaf7671

Schroda, M., Hemme, D., & Mühlhaus, T. (2015). The *Chlamydomonas* heat stress response. *The Plant Journal: For Cell and Molecular Biology*, *82*(3), 466–80. http://doi.org/10.1111/tpj.12816

Seregin, I. V., & Kozhevnikova, A. D. (2006). Physiological role of nickel and its toxic effects on higher plants. *Russian Journal of Plant Physiology*, *53*(2), 257–277. http://doi.org/10.1134/S1021443706020178

Shahid, M., Pourrut, B., Shahid, M., Pourrut, B., Dumat, C., Nadeem, M., … Pinelli, E. (2014). Heavy-metal-induced reactive oxygen species: Phytotoxicity and physicochemical changes in plants. In D. Whitacre (Ed.), *Reviews of environmental contamination and toxicology Volume 232* (Vol. 232, pp. 1–44). Springer, Cham. http://doi.org/10.1007/978-3-319-06746-9_1

Sharma, N. K., & Rai, A. K. (2011). Biodiversity and biogeography of microalgae: progress and pitfalls. *Environmental Reviews*, *19*, 1–15. http://doi.org/10.1139/A10-020

Sibi, G., Anuraag, T. S., & Bafila, G. (2014). Copper stress on cellular contents and fatty acid profiles in *Chlorella* species. *Online Journal of Biological Sciences*, *14*(143), 209–217. http://doi.org/10.3844/ojbssp.2014.209.217

Singh, M., Pant, G., Hossain, K., & Bhatia, A. K. (2016). Green remediation. Tool for safe and sustainable environment: A review. *Applied Water Science*, 1–7. http://doi.org/10.1007/s13201-016-0461-9

Singh, R., Gautam, N., Mishra, A., & Rajiv, G. (2011). Heavy metals and living systems: An overview. *Indian Journal of Pharmacology*, *43*(3), 246–253. http://doi.org/10.4103/0253-7613.81505

Singh, S., Parihar, P., Singh, R., Singh, Vi. P., & Prasad, S. M. (2015). Heavy metal tolerance in plants: Role of transcriptomics, proteomics, metabolomics and ionomics. *Frontiers in Plant Science*, *6*, 1143. http://doi.org/10.3389/fpls.2015.01143

Singh, V., & Verma, K. (2018). Metals from cell to environment: Connecting metallomics with other omics. *Open Journal of Plant Science*, *3*(1), 1–14. http://doi.org/10.13140/RG.2.2.11868.90247

Smirnoff, N. (1995). Metabolic flexibility in relation to the environment. In N. Smirnoff (Ed.), *Environment and Plant Metabolism: Flexibility and Acclimation* (pp. 1–16). Oxford: BIOS Scientific Publishers.

Soldo, D., Hari, R., Sigg, L., & Behra, R. (2005). Tolerance of *Oocystis nephrocytioides* to copper: intracellular distribution and extracellular complexation of copper. *Aquatic Toxicology*, *71*, 307–317. http://doi.org/10.1016/j.aquatox.2004.11.011

Sousa, C. A., Soares, H. M. V. M., & Soares, E. V. (2018). Toxic effects of nickel oxide (NiO) nanoparticles on the freshwater alga *Pseudokirchneriella subcapitata*. *Aquatic Toxicology*, *204*(September), 80–90. http://doi.org/10.1016/J.AQUATOX.2018.08.022

Spolaore, P., Joannis-Cassan, C., Duran, E., & Isambert, A. (2006). Commercial applications of microalgae. *Journal of Bioscience and Bioengineering*, *101*(2), 87–96. http://doi.org/10.1263/jbb.101.87

Stankovic, S., Kalaba, P., & Stankovic, A. R. (2014). Biota as toxic metal indicators. *Environmental Chemistry Letters*, *12*, 63–84. http://doi.org/10.1007/s10311-013-0430-6

Steinacher, M., Joos, F., Frölicher, T. L., Plattner, G.-K., & Doney, S. C. (2009). Imminent ocean acidification in the Arctic projected with the NCAR global coupled carbon cycle-climate model. *Biogeosciences*, *6*, 515–533. https://doi.org/10.5194/bg-6-515-2009

Stewart, T. J., Szlachetko, J., Sigg, L., Behra, R., & Nachtegaal, M. (2015). Tracking the temporal dynamics of intracellular lead speciation in a green alga. *Environmental Science and Technology*, *49*, 11176–11181. http://doi.org/10.1021/acs.est.5b02603

Sun, J., Yang, Q., Wang, D., Wang, S., Chen, F., Zhong, Y., … Zeng, G. (2017). Nickel toxicity to the performance and microbial community of enhanced biological phosphorus removal system. *Chemical Engineering Journal*, *313*, 415–423. http://doi.org/10.1016/j.cej.2016.12.078

Sunda, W. (1975). *The relationship between cupric ion activity and the toxicity of copper to phytoplankton*. Massachusetts Institute of Technology.

Suresh Kumar, K., Dahms, H. U., Won, E. J., Lee, J. S., & Shin, K. H. (2015). Microalgae - A promising tool for heavy metal remediation. *Ecotoxicology and Environmental Safety*, *113*, 329–352. http://doi.org/10.1016/j.ecoenv.2014.12.019

Suresh Kumar, K., Dahms, H.-U., Lee, J.-S., Kim, H. C., Lee, W. C., & Shin, K.-H. (2014). Algal photosynthetic responses to toxic metals and herbicides assessed by chlorophyll *a* fluorescence. *Ecotoxicology and Environmental Safety*, *104*, 51–71. http://doi.org/10.1016/j.ecoenv.2014.01.042

Szivák, I., Behra, R., & Sigg, L. (2009). Metal-induced reactive oxygen species production in *Chlamydomonas reinhardtii* (Chlorophyceae). *Journal of Phycology*, *45*, 427–435. http://doi.org/10.1111/j.1529-8817.2009.00663.x

Teoh, M. L., Phang, S. M., & Chu, W. L. (2013). Response of Antarctic, temperate, and tropical microalgae to temperature stress. *Journal of Applied Phycology*, *25*(1), 285–297. http://doi.org/10.1007/s10811-012-9863-8

Tevatia, R., Allen, J., Rudrappa, D., White, D., Clemente, T. E., Cerutti, H., & Blum, P. (2015). The taurine biosynthetic pathway of microalgae. *Algal Research*, *9*, 21–26. http://doi.org/10.1016/j.algal.2015.02.012

Todgham, A. E., & Stillman, J. H. (2013). Physiological responses to shifts in multiple environmental stressors: Relevance in a changing world. *Integrative and Comparative Biology*, *53*(4), 539–544. http://doi.org/10.1093/icb/ict086

Toseland, A., Daines, S. J., Clark, J. R., Kirkham, A., Strauss, J., Uhlig, C., … Mock, T. (2013). The impact of temperature on marine phytoplankton resource allocation and metabolism. *Nature Climate Change*, *3*, 979–984. http://doi.org/10.1038/nclimate1989

Tripathi, B. N., & Gaur, J. P. (2004). Relationship between copper- and zinc-induced oxidative stress and proline accumulation in *Scenedesmus* sp. *Planta*, *219*, 397–404. http://doi.org/10.1007/s00425-004-1237-2

Tripathi, B. N., Mehta, S. K., Amar, A., & Gaur, J. P. (2006). Oxidative stress in *Scenedesmus* sp. during short- and long-term exposure to Cu^{2+} and Zn^{2+}. *Chemosphere*, *62*, 538–544. http://doi.org/10.1016/j.chemosphere.2005.06.031

Vavilin, D. V, Ducruet, J. M., Matorin, D. N., Venediktov, P. S., & Rubin, A. B. (1998). Membrane lipid peroxidation, cell viability and photosystem II activity in the green alga *Chlorella pyrenoidosa* subjected to various stress conditions. *Journal of Photochemistry and Photobiology B-Biology*, *42*(3), 233–239. http://doi.org/10.1016/S1011-1344(98)00076-1

Velthuis, M., De Senerpont Domis, L. N., Frenken, T., Stephan, S., Kazanjian, G., Aben, R., … Van De Waal, D. B. (2017). Warming advances top-down control and reduces producer biomass in a freshwater plankton community. *Ecosphere*, *8*(1), e01651. http://doi.org/10.1002/ecs2.1651

Vetrivel, S. A., Gaurav, N., Diptanghu, M., Ebhin, M. R., Sydavalli, S., & Tiger, K. P. (2017). Green algae of the genus *Spirogyra*: A potential absorbent for heavy metal from coal mine water. *Remediation*, *27*, 81–90. http://doi.org/10.1002/rem.21522

Veyel, D., Erban, A., Fehrle, I., Kopka, J., & Schroda, M. (2014). Rationales and approaches for studying metabolism in eukaryotic microalgae. *Metabolites, 4*(2), 184-217. http://doi.org/10.3390/metabo4020184

Vliet, M. T. H. Van, Franssen, W. H. P., Yearsley, J. R., Ludwig, F., Haddeland, I., Lettenmaier, D. P., & Kabat, P. (2013). Global river discharge and water temperature under climate change. *Global Environmental Change*, *23*, 450–464. http://doi.org/10.1016/j.gloenvcha.2012.11.002

von Alvensleben, N., Magnusson, M., & Heimann, K. (2016). Salinity tolerance of four freshwater microalgal species and the effects of salinity and nutrient limitation on

biochemical profiles. *Journal of Applied Phycology*, *28*(2), 861–876. http://doi.org/10.1007/s10811-015-0666-6

Waga, H., Hirawake, T., Fujiwara, A., Kikuchi, T., Nishino, S., Suzuki, K., … Saitoh, S. I. (2017). Differences in rate and direction of shifts between phytoplankton size structure and sea surface temperature. *Remote Sensing*, *9*, 222. http://doi.org/10.3390/rs9030222

Wagner, H., Fanesi, A., & Wilhelm, C. (2016). Freshwater phytoplankton responses to global warming. *Journal of Plant Physiology*, *203*, 127–134. http://doi.org/10.1016/j.jplph.2016.05.018

Walz, H. (2000). *WinControl - Windows software for PAM Fluorometers user's manual*. Effeltrich: Heinz Walz GmbH.

Wang, H., & Wood, J. M. (1984). Bioaccumulation of nickel by algae. *Environmental Science & Technology*, *18*(2), 106–109.

Wang, H., Sathasivam, R., & Ki, J. (2017). Physiological effects of copper on the freshwater alga *Closterium ehrenbergii* Meneghini (Conjugatophyceae) and its potential use in toxicity assessments. *Algae*, *32*(2), 131–137. https://doi.org/10.4490/algae.2017.32.5.24

Wang, L., Huang, X., Lim, D. J., Laserna, A. K. C., & Fong, S. Y. L. (2019). Uptake and toxic effects of triphenyl phosphate on freshwater microalgae *Chlorella vulgaris and Scenedesmus obliquus*: Insights from untargeted metabolomics. *Science of the Total Environment*, *650*, 1239–1249. http://doi.org/10.1016/j.scitotenv.2018.09.024

Wang, M.-J., & Wang, W.-X. (2008). Temperature-dependent sensitivity of a marine diatom to cadmium stress explained by subcellular distribution and thiol synthesis. *Environmental Science and Technology*, *42*, 8603–8608. http://doi.org/10.1021/es801470w

Wang, Y., Ho, S. H., Cheng, C. L., Guo, W. Q., Nagarajan, D., Ren, N. Q., … Chang, J. S. (2016). Perspectives on the feasibility of using microalgae for industrial wastewater treatment. *Bioresource Technology*, *222*, 485–497. http://doi.org/10.1016/j.biortech.2016.09.106

Wang, Y., Xu, L., Shen, H., Wang, J., Liu, W., Zhu, X., … Liu, L. (2015). Metabolomic analysis with GC-MS to reveal potential metabolites and biological pathways involved in Pb & Cd stress response of radish roots. *Scientific Reports*, *5*(December), 18296. http://doi.org/10.1038/srep18296

Wettstein, D. Von, Gough, S., & Kannangara, C. G. (1995). Chlorophyll biosynthesis. *The Plant Cell*, *7*, 1039–1057.

Winder, M., & Sommer, U. (2012). Phytoplankton response to a changing climate. *Hydrobiologia*, *698*, 5–16. http://doi.org/10.1007/s10750-012-1149-2

Wong, J. P., Wong, Y., & Tam, N. F. (2000). Nickel biosorption by two *Chlorella* species, *C. vulgaris* (a commercial species) and *C. miniata* (a local isolate).

Bioresource Technology, *73*, 133–137. http://doi.org/10.1016/S0960-8524(99)00175-3

Wong, S. W. Y., & Leung, K. M. Y. (2014). Temperature-dependent toxicities of nano zinc oxide to marine diatom, amphipod and fish in relation to its aggregation size and ion dissolution. *Nanotoxicology*, *8*(S1), 24–35. http://doi.org/10.3109/17435390.2013.848949

Wong, Y. K., Yung, K. K. L., Tsang, Y. F., Xia, Y., Wang, L., & Ho, K. C. (2015). *Scenedesmus quadricauda* for nutrient removal and lipid production in wastewater. *Water Environment Research*, *87*(12), 2037–2044. http://doi.org/10.2175/106143015X14362865227193

Wu, N., Dong, X., Liu, Y., Wang, C., Baattrup-Pedersen, A., & Riis, T. (2017). Using river microalgae as indicators for freshwater biomonitoring: Review of published research and future directions. *Ecological Indicators*, *81*, 124–131. http://doi.org/10.1016/j.ecolind.2017.05.066

WWAP (United Nations World Water Assessment Programme). (2018). *The United Nations World Water Development Report 2018: Nature-based solutions for water*. Paris: UNESCO.

Xia, J., Mandal, R., Sinelnikov, I. V, Broadhurst, D., & Wishart, D. S. (2012). MetaboAnalyst 2.0--A comprehensive server for metabolomic data analysis. *Nucleic Acids Research*, *40*(Web Server issue), W127-33. http://doi.org/10.1093/nar/gks374

Xia, J., Sinelnikov, I. V, Han, B., & Wishart, D. S. (2015). MetaboAnalyst 3.0 — making metabolomics more meaningful. *Nucleic Acids Research*, *43*, W251-257. http://doi.org/10.1093/nar/gkv380

Xia, L., Song, S., & Hu, C. (2016). High temperature enhances lipid accumulation in nitrogen-deprived *Scenedesmus obtusus* XJ-15. *Journal of Applied Phycology*, *28*, 831–837. http://doi.org/10.1007/s10811-015-0636-z

Xue, Z., Duan, L., & Qi, X. (2015). Gas chromatography mass spectrometry coupling techniques. In X. Qi, X. Chen, & Y. Wang (Eds.), *Plant Metabolomics: Methods and Applications* (1st ed., pp. 25–45). Springer Netherlands. http://doi.org/10.1007/978-94-017-9291-2

Xyländer, M., & Wolfram Braune. (1994). Influence of nickel on the green alga *Haematococcus lacustris* Rostafinski in phases of its life cycle. *Journal of Plant Physiology*, *144*(1), 86–93. http://doi.org/10.1016/S0176-1617(11)80998-3

Yan, H., & Pan, G. (2002). Toxicity and bioaccumulation of copper in three green microalgal species. *Chemosphere*, *49*, 471–476. https://doi.org/10.1016/s0045-6535(02)00285-0

Yong, W. K., Sim, K. S., Poong, S. W., Wei, D., Phang, S. M., & Lim, P. E. (2018). Interactive effects of temperature and copper toxicity on photosynthetic efficiency and metabolic plasticity in *Scenedesmus quadricauda* (Chlorophyceae). *Journal of Applied Phycology*, 1–13. http://doi.org/10.1007/s10811-018-1574-3

Yong, W.-K., Tan, Y.-H., Poong, S.-W., & Lim, P.-E. (2016). Response of microalgae in a changing climate and environment. *Malaysian Journal of Science*, *35*(2), 167–187. https://doi.org/10.22452/mjs.vol35no2.7

Yruela, I. (2005). Copper in plants. *Brazilian Journal of Plant Physiology*, *17*(1), 145–156. http:// doi.org/10.1590/S1677-04202005000100012

Yun, J.-H., Smith, V. H., La, H.-J., & Chang, Y. K. (2016). Towards managing food-web structure and algal crop diversity in industrial-scale algal biomass production. *Current Biotechnology*, *5*, 118–129. http://doi.org/10.2174/2211550105666160127002552

Yusuf, M., Fariduddin, Q., Hayat, S., & Ahmad, A. (2011). Nickel: An overview of uptake, essentiality and toxicity in plants. *Bulletin of Environmental Contamination and Toxicology*, *86*, 1–17. http://doi.org/10.1007/s00128-010-0171-1

Zargar, S., Krishnamurthi, K., Saravana Devi, S., Ghosh, T. K., & Chakrabarti, T. (2006). Temperature-induced stress on growth and expression of hsp in freshwater alga *Scenedesmus quadricauda*. *Biomedical and Environmental Sciences*, *19*(6), 414–21.

Zeraatkar, A. K., Ahmadzadeh, H., Talebi, A. F., Moheimani, N. R., & McHenry, M. P. (2016). Potential use of algae for heavy metal bioremediation, a critical review. *Journal of Environmental Management*, *181*, In Press. http://doi.org/10.1016/j.jenvman.2016.06.059

Zhang, B., Zhang, H., Du, C., Xiang, Q., Hu, C., He, Y., & Nam, C. (2017). Metabolic responses of the growing *Daphnia similis* to chronic AgNPs exposure as revealed by GC-Q-TOF/MS and LC-Q-TOF/MS. *Water Research*, *114*, 135–143. http://doi.org/10.1016/j.watres.2017.02.046

Zhang, W., Tan, N. G. J., & Li, S. F. Y. (2014). NMR-based metabolomics and LC-MS/MS quantification reveal metal-specific tolerance and redox homeostasis in *Chlorella vulgaris*. *Molecular BioSystems*, *10*, 149–160. http://doi.org/10.1039/c3mb70425d

Zhang, W., Tan, N. G. J., Fua, B., & Li, S. F. Y. (2015). Metallomics and NMR-based metabolomics of *Chlorella* sp. reveal synergistic role of copper and cadmium in multi-metal toxicity and oxidative stress. *Metallomics*, *7*(3), 426–38. http://doi.org/10.1039/C4MT00253A

Zhou, G., Peng, F., Zhang, L., & Ying, G.-G. (2012). Biosorption of zinc and copper from aqueous solutions by two freshwater green microalgae *Chlorella pyrenoidosa* and *Scenedesmus obliquus*. *Environmental Science and Pollution Research*, *19*, 2918–2929. http://doi.org/10.1007/s11356-012-0800-9

Zidarova, R., & Pouneva, I. (2006). Physiological and biochemical characterization of Antarctic isolate *Choricystis minor* during oxidative stress at different temperatures and light intensities. *General and Applied Plant Physiology*, *Special Is*, 109–115

LIST OF PUBLICATIONS AND PAPERS PRESENTED

List of Publications

1. Yong, W.-K., Sim, K.-S., Poong, S.-W., Wei, D., Phang, S.-M., & Lim, P. E. (2019). Physiological and metabolic responses of *Scenedesmus quadricauda* (Chlorophyceae) to nickel toxicity and warming. *3 Biotech*, *9*(315), 1–11. http://doi.org/10.1007/s13205-019-1848-8 (*ISI-indexed journal*)
2. Yong, W.-K., Sim, K.-S., Poong, S.-W., Wei, D., Phang, S.-M., & Lim, P.-E. (2018). Interactive effects of temperature and copper toxicity on photosynthetic efficiency and metabolic plasticity in *Scenedesmus quadricauda* (Chlorophyceae). *Journal of Applied Phycology, 30*(6), 3029-3041. http://doi.org/10.1007/s10811-018-1574-3 (*ISI-indexed journal*)
3. Yong, W.-K., Lim, P.-E., Vello, V., Sim, K.-S., Abdul Majid, N., Mustafa, E. M., Nik Sulaiman, N. M., Liew, K.-E., Chen, B.J-T., & Phang, S.-M., (2019). Metabolic and physiological regulation of *Chlorella* sp. (Trebouxiophyceae, Chlorophyta) under nitrogen deprivation. *Journal of Oceanology and Limnology, 37*(1), 186-198. http://doi.org/ 10.1007/s00343-019-7263-5 (*ISI-indexed journal*)
4. Yong, W.-K., Tan, Y.-H., Poong, S.-W., & Lim, P.-E. (2016). Response of microalgae in a changing climate and environment. Malaysian Journal of Science, 35(2), 167–187. https://doi.org/10.22452/mjs.vol35no2.7 (*SCOPUS-indexed journal*)

Conference and Seminar Presentation

1. Yong, W.-K., Sim, K.-S., & Lim, P.-E. (2017). Integrative effects of temperature and copper stresses on *Scenedesmus quadricauda*. Asian Pacific Phycological Forum, 8-13 October 2017, Kuala Lumpur, Malaysia
2. Yong, W.-K., Sim, K.-S., & Lim, P.-E. (2017). Copper tolerance of green microalgae *Scenedesmus quadricauda*, IOES HICoE Seminar, 12 September 2017, University of Malaya, Kuala Lumpur, Malaysia